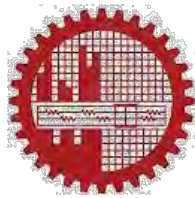**Seismic Assessment of RC Frame Building Designed Using Gross and Cracked Sections**

Md. Zahidul Islam

Department of Civil Engineering

BANGLADESH UNIVERSITY OF ENGINEERING AND TECHNOLOGY,

DHAKA, BANGLADESH

September, 2020

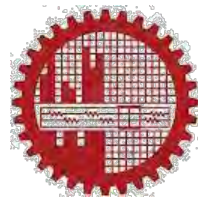**Seismic Assessment of RC Frame Building Designed Using Gross and Cracked Sections**

Md. Zahidul Islam

(Student ID: 1015042344P)

Submitted to the Department of Civil Engineering, Bangladesh University of Engineering and Technology (BUET), Dhaka. in partial fulfillment of the requirements for the degree

Of

MASTER OF ENGINEERING IN CIVIL AND STRUCTURAL ENGINEERING

Department of Civil Engineering

BANGLADESH UNIVERSITY OF ENGINEERING AND TECHNOLOGY

DHAKA, BANGLADESH

September, 2020

The thesis titled "Seismic Assessment of RC Frame Building Designed Using Gross and Cracked Sections" submitted by Md. Zahidul Islam, Roll No: 1015042344, Session: October/2015; has been accepted as satisfactory in partial fulfillment of the requirement for the degree of Master of Engineering in Civil and Structural Engineering on 22nd September, 2020.

BOARD OF EXAMINERS

Dr. Mohammad Al Amin Siddique
Professor
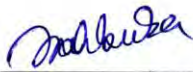Department of Civil Engineering
BUET, Dhaka-1000.

Chairman
(Supervisor)

Dr. Md. Shafiul Bari
Professor
Department of Civil Engineering
BUET, Dhaka-1000.

Member

Dr. Mahbuba Begum
Professor
Department of Civil Engineering
BUET, Dhaka-1000.

Member

Declaration

It is hereby declared that except for the contents where specific reference has been made to the work of others, the studies contained in this thesis is the result of investigation carried out by the author. No part of this thesis has been submitted to any other University or other educational establishment for a Degree, Diploma or other qualification (except for publication).

Signature of the Candidate

MD. ZAHIDUL ISLAM.

_____

(Md Zahidul Islam)

Dedication

This thesis is dedicated to my parents.

Acknowledgement

The author wishes to convey his profound gratitude to Almighty Allah for His graciousness, unlimited kindness and blessings, and for allowing him to complete the thesis.

The author wishes to express his sincere appreciation and gratitude to his supervisor, Dr. Mohammad Al Amin Siddique, Professor, Department of Civil Engineering, BUET, Dhaka, for his continuous guidance, invaluable suggestions and continued encouragement throughout the progress of the research work.

A very special debt of deep gratitude is offered to his mother and father for their continuous encouragement and cooperation during this study. Last but not the least; the author is deeply indebted to his beloved wife for supporting him all the time with love and inspiration.

ABSTRACT

Bangladesh is situated in a seismically active region with a moderate seismic risk. The country has been divided into four seismic zones following the concept of Maximum Considered Earthquake (MCE) with a return period of 2475 years. A number of infrastructures have already been built in order to fulfill the increasing demand of urban population. Bangladesh National Building Code (BNBC) has been updated to a draft BNBC 2017 to consider the realistic design guidelines. The code considers the cracked section properties for designing a structure at a factored load level. A comprehensive study is conducted in the current thesis to assess the seismic performance of buildings considering cracked section properties of the structural members. For comparative seismic assessment, a regular plan of 6-, 10-, and 15-storey RC frame buildings designed with gross section and cracked section (BNBC-2017 draft) properties of RC members using conventional force-based design approach. All the considered buildings are analyzed using nonlinear static pushover analysis. The obtained results show that the inter-storey drift at design load of RC frames designed using gross section property is well within the prescribed limit of maximum permissible inter-storey drift while that of cracked section properties is beyond the maximum permissible inter-storey drift limit. The higher column reinforcement demand is shown for buildings with cracked sections that those of gross sections and this value is higher for exterior and corner columns (27.4% increase for 6-storied) than those of the interior columns. Response reduction factors of the buildings with gross section properties result higher values than those of the cracked section buildings. R values always fall below the design R for the cracked section buildings and it is obtained 3.23 instead of R value of 5 for the considered 6-storied building.

TABLE OF CONTENTS

LIST OF FIGURES

LIST OF TABLES

LIST OF ABBREVIATIONS

ACI   American Concrete Institute

ASCE American Society of Civil Engineers

ATC   Applied Technology Council

BNBC Bangladesh National Building Code

BSSC Building Seismic Safety Council

ELF   Equivalent Lateral Force

FEMA Federal Emergency Management Association

NEHRP National Earthquake Hazard Reduction Program

SFRS Shear Force Resisting System

UBC   Uniform Building Code

IO   Immediate Occupancy

LS   Life Safety

CP   Collapse Prevention

Chapter 1

INTRODUCTION

1.1 General

Bangladesh is surrounded by a number of tectonic blocks responsible for many earthquakes in the past. Five major faults are significant for the occurrences of devastating earthquakes as global seismic hazard maps indicate that Bangladesh is located in a moderate to high seismic hazard zone. Over the last few decades, construction of reinforced concrete (RC) buildings has rapidly increased, replacing other construction materials, like adobe, wood and brick masonry, in Dhaka city as well as in other parts of the country. The seismic design as per Bangladesh National Building Code (BNBC) has been subjected to rapid developments to ensure ductile behavior and safe performance of the designed structures under possible future earthquakes. The seismic design standard/code of major countries across the world including BNBC 2006 to upcoming 2017(draft) use the force-based design (FBD) approach. The FBD approach of BNBC code defines the intended performance of no damage during minor earthquake and no collapse during major earthquake. In FBD approach, the ductility and good post-yield behavior with appropriate design and detailing are considered through the use of response reduction factor (R). The buildings are designed for the forces estimated using code procedure based on fundamental time period evaluated using the empirical equation and checked for the inter-storey drifts at the design loads. However, design forces and inter-storey drifts depend on modeling assumptions and vary significantly depending on how much effects of cracking on RC members are considered in analysis of structural model.

During analysis of RC structures under the combined effect of gravity and seismic loads, the designers take into account the appropriate, effective or gross moment of inertia to evaluate the flexural stiffness/rigidity of structural members such as slabs, beams, shear wall and columns. Due to the effects of gravity and seismic loads, few critical members of the structure will reach close to yielding and cracks are developed on bending tension side of RC members. Therefore, the flexural stiffness (EI) of RC members starts decreasing. Because of substantial decrease in flexural stiffness, the lateral deflection of RC members and structure is increased and it can be considerably larger as compared to that of the deflection evaluated based on gross flexural stiffness. Moreover, the

fundamental time period, deformation, internal forces and dynamic responses may be altered due to the reduction of flexural stiffness. Therefore, proper estimation of flexural rigidity of RC members is important for evaluating the accurate seismic responses of building and force and deformation demands imposed on the building. To take into account the cracking effects of RC frame member under forces, design code of major countries recommends the effective moment of inertia of frame elements as a certain fraction of gross moment of inertia. The upcoming BNBC- 2017(draft) recommends effective moment of inertia at factored load level of 70% of the gross inertia (I_{gross}) of columns and 35% of I_{gross} of beams for the structural analysis of RC structures. Current BNBC 2006 does not have any such provisions of effective moment of inertia for RC members explicitly. It seems that it is a common practice to analyze and design the structures using gross moment of inertia of slabs, beams, shear wall and columns as no information regarding the effective stiffness is mentioned. There might be a concern that the existing buildings, recently completed buildings as well as buildings under construction based on BNBC 2006, may get some safety issues from the serviceability and strength requirements evaluated based on effective flexural stiffnesses as per upcoming BNBC-2017(draft). This would result in concern in the minds of structural designers/civil engineers and the owners/people who would use it.

1.2 Background of the study

Seismic design codes are often subjected to improvements after each earthquake disaster and old constructions maybe left unprotected by new technology. The equivalent lateral force (ELF) design procedure is one of the most common seismic design methods adopted in different codes such as ASCE 7, Eurocode 8, BNBC-2006. ELF design is also called force-based design (FBD), which proposes minimum strength requirements as reduced by response reduction factor, R. In FBD, design forces and inter-storey drifts depend on modelling assumptions and vary significantly due to the effects of cracking of RC members. As per BNBC-2006, designers/engineers may consider gross moment of inertia to evaluate the flexural stiffness/rigidity of beams and columns of RC structures as no specific guidelines were stated. Therefore, forces and deformation demands imposed on the building will be varied depending on the appropriate flexural stiffness of RC members. Many researchers had evaluated the reduced factor for the stiffness of RC columns and beams to account for the cracking under seismic loadings. The upcoming draft BNBC-2017 recommends effective moment of inertia of 70% of gross inertia of

column and 35% of gross inertia of beam for the analysis of RC frame structures under factored load level.

Therefore, the present study will investigate the seismic responses of RC frame buildings analyzed and designed as per draft BNBC-2017 considering the gross/uncracked section and effective/cracked section property of the frame members. The seismic performance in terms of global pushover curve, maximum base shear, inter-storey drift of the RC frames will be evaluated using the nonlinear static or pushover analysis.

1.3. Objectives of the research

The objectives of the present study are as follows:

(i) To design RC frame buildings as per BNBC 2017(draft) considering gross/uncracked section and effective/cracked section to assess the level of seismic performance.

(ii) To evaluate the response reduction factor, R for such RC frame systems using nonlinear static (pushover) analysis.

(iii) To compare the maximum base shear, displacement at the base shear and inter-storey drift of the buildings based on gross and cracked section properties.

1.4. Outline of Methodology

In order to achieve the above selected objectives, the research work have been initiated by reviewing the seismic provisions of BNBC 2017(draft) and available literature. RC frame building with 6, 10 and 15-storied have been designed considering cracked and gross properties of RC members as per draft BNBC-2017. These structures have been then subjected to nonlinear static procedure (NSP). The analysis has included progressive damage of elements by inserting appropriate hinges as the structure has been laterally pushed through. The resulting capacity curve (Base shear vs. roof deflection) has represented structure's performance showing progressive yielding of members and ductility demand of a structure. Earthquake demand for the structure has been established as per site condition and draft BNBC-2017 specified seismic zone coefficient. NSP analysis has been carried out using the commercial finite-element software ETABS 18 in order to estimate the capacity curves using the nonlinear modeling parameters provided in ASCE/SEI 41-13. Belletti et al. (2013) shows that the more popular lumped plasticity model provides reasonably accurate results in predicting the force–deformation behavior of RC frame members. This modeling technique is widely used for seismic

performance evaluation. This approach has been used in the current study. The buildings have been considered to be supported by either rigid mat foundation or individual footing and assumed as fixed at the base. Seismic performance in terms of global pushover curves have been determined for each building. Finally, response reduction factor, R has been evaluated for such buildings.

1.5 Scope of the work

In this thesis, the comparative seismic assessment of 6, 10, 15-storied RC frame buildings designed with gross/uncracked section and effective/cracked section properties of the members using conventional force-based design approach. RC frames of different number of stories are designed considering seismic base shear coefficient based on empirically obtained period of the building as recommended in upcoming BNBC-2017(draft). All the considered frames are analyzed using nonlinear static or pushover analysis.

1.6 Organization of the thesis

The thesis paper is organized into total five chapters. Apart from chapter one, the following chapters are organized as follows:

Chapter 2: This chapter named "Literature Review" describes different RC framing systems, national and international code provisions like BNBC-2017 (upcoming BNBC), ASCE, Euro-code for seismic response, components of seismic response reduction factor, linear and nonlinear analysis procedures.

Chapter 3: This chapter named "Numerical Analysis" describes various RC building structures with different beam and column sizes, cracked section properties, loading and load combinations, hinge properties, hinge locations and seismic details. The chapter also includes "Model validation" section to validate the current analysis model compared with that of the model available in literature. In this chapter, previous research and modeling relevant to the similar type of structure is presented and compared the results in terms of nonlinear base shear coefficient versus top roof displacement curve (pushover curve).

Chapter 4: This chapter named "Results and Discussions" presents structural performance of all building models considered in the current study. Numerical results both from linear and nonlinear analyses are presented in this chapter. Response reduction factor, R for structural systems computed from different buildings have been compared.

The maximum base shear, displacement at the maximum base shear and inter-storey drift of the buildings based on gross and cracked section properties computed from different models have been provided.

Chapter 5: This chapter named "Conclusions and Recommendations" presents conclusions derived from the present study and recommendation for future research.

Chapter 2

LITERATURE REVIEW

2.1 Introduction

Seismic performance assessment is an important aspect of earthquake engineering. In seismic design both seismic demand and capacity are not only inter-dependent but also uncertain. To conduct seismic performance assessment considering gross and crack sections in case of reinforced concrete (RC) buildings, modeling of the structure with provision of material and geometric nonlinearity is essential. In nonlinear range, structural components go through the progressive cracking until failure. Building codes suggest reduced stiffness, i.e. moment of inertia, of structural elements to simulate this cracking phenomenon of the members under factored load levels. Therefore, modeling of building structures with cracked sections gives an insight of realistic behavior.

The damages and the economic losses during the major earthquakes required modification in seismic analysis. Design codes have been updated continuously considering previous damages of the structures. The upcoming BNBC-2017 (draft) recommends effective moment of inertia for structural members while BNBC-2006 does not have such provisions explicitly.

The design of building structures under earthquake loading has typically been based on results from conventional linear analysis techniques. The engineer normally faces a challenge for the design of reinforced concrete buildings because the material is composite and displays nonlinear behavior due to the complex interaction between its components – reinforcing bar and the concrete matrix. To effectively design reinforced concrete structures, modeling of the structural components is vital considering a linear-elastic analysis approach.

2.2 Seismic Performance of Buildings considering RC Cracked and Gross Section

If the applied moment on a concrete section is more than the cracking moment, then the section is said to be a cracked section. When the external load is applied in positive curvature then the compressive stress will develop above the neutral axis of a section and tensile stress will generate below the neutral axis. Concrete is very weak in tension and its tensile strength is considered to be one-tenth of its compressive strength. Since concrete is weak in tension and a time will arise when the tensile stress developed in

concrete is more than the tensile strength, the section will get cracked and whole tensile stresses is, therefore, now be borne up by reinforcing steel in a RC section. The concrete area is found to be ineffective as it already got cracked and is unable to withstand tensile stresses. Generally, the first tensile crack occurs at a stress value of 0.7 $\sqrt{f'c}$ MPa and this is called modulus of rupture or flexural tensile strength of concrete under bending. If the applied bending moment is less than the cracking moment, then the section is said to be an uncracked section. In such case, moment of inertia of a RC section can be taken as gross moment of inertia for the whole section. Concrete can easily take up such tensile stress and the whole concrete area is also found to be effective; referred to as uncracked section.

In RC buildings structures, the flexural stiffness reduction of structural elements such as beams, columns, shear walls and slabs due to concrete cracking plays an important role in the nonlinear load-deformation response. The concrete cracking may amplify the deflection of the building. The excessive lateral deflection may also result in large second-order P-delta effects. A review of the different cracking models proposed for finite element analysis of structural elements is given in the ASCE report (1982). Smith and Coull (1991) studied the cracked concrete stiffness in tall buildings. The main parameters affecting the stiffness of the cracked concrete elements are modulus of elasticity and so-called effective moment of inertia. The recommendations for main parameters vary significantly mainly due to different interpretations of test data and different behavior models.

Seismic analysis and design of reinforced concrete structures are based on linear response; however, it is universally accepted that under severe earthquakes inelastic response and cracking are accepted. Therefore, element properties should reflect this condition and inertias of beams, columns, shear walls and slabs should be reduced accordingly.

2.2.1 Effect of concrete cracking on the lateral response of RC buildings

Paulay (2001) investigated on seismic design and the ductile behavior of horizontal force-resisting structural elements and concluded that the entire building structure can be simulated adequately by simple bilinear force-displacement relationships. This helped displacement relationships between the system and its lateral force-resisting elements at a particular limit state. A redefinition of yield displacements and consequently stiffness

which allowed much more realistic predictions of the most important feature of seismic response were stated by the author. Paulay (2002) studied the estimations of displacement capacities of ductile system and provided redefinitions of some properties of reinforced concrete structure. He showed that for a RC coupled walls, flexural rigidities, $E_c I_e$, of prismatic components, whereas the modulus of elasticity of the concrete and I_e is the second moment of effective area of the cracked reinforced concrete section can be used. This rigidities is usually expressed in terms of a fraction of the second moment of the gross concrete sectional area, I_g. He mentioned that values of I_e/I_g, recommended in some codes or design practice, vary in a wide range of 0.2 to 1.0.

Chan and Wang (2006) studied different RC building plans which fulfill usefulness of stiffness measures as far as maximum lateral displacement and inter-storey drift. They found that the deflection profiles for the linear analysis and nonlinear cracking analysis of the linear-elastically structure are different. They also reported that there was a sizeable difference in the lateral deflection between the elastic analysis and the nonlinear cracking analysis of the structure and therefore resulted in an inadequate design when the concrete cracking effects considered.

An experimental program was conducted by Elwood and Eberhard (2006) to investigate existing and proposed models of the effective stiffness of reinforced concrete columns subjected to lateral loads. A total of 329 concrete columns was considered in the experimental study. They showed that existing models appropriate for design applications tend to overestimate the measured effective stiffness and are considered inaccurate. They showed that three-component model that explicitly accounts for deformations due to flexure, shear, and anchorage-slip provided a more accurate estimate of the measured effective stiffness for the database columns.

Ahmed et al. (2008) studied the effect of concrete cracking on the lateral response of building structure. They surveyed the different expressions of the modulus of elasticity, modulus of rupture, moment of inertia in cracked state proposed by different researchers and codes. They studied four and eleven storied buildings with different aspect ratios with an aim to figure out the effect of concrete cracking. They reported that top storey deflection and storey drift were increased to a sizable amount after incorporating the cracking of the concrete members. For high-rise structural system, the storey drifts after

incorporation of cracking effect had enhanced appreciably. The increase in storey drift was as high as 55%.

Pique and Burgos (2008) investigated on seismic analysis and design of reinforced concrete structures which were based on linear response. They considered different reduced inertias of beams and columns due to cracking under severe earthquakes. In their study, they reported that most world seismic standards do not establish effective stiffness for seismic analysis, although all of them accept inelastic incursions. They concluded that cracking must be considered in seismic analysis of building structures and thus to get realistic building's lateral displacement.

Luo et al. (2009) investigated the method of stiffness reduction adopted to consider inelastic characteristics of reinforced concrete in a concrete structure. They reported that bridge code of China still uses amplified coefficient of eccentricity to consider nonlinear characteristics of reinforced concrete. In their research, they adopted the numerical integral method to computerize simulation and analyzed the regulation of the stiffness change for rectangular section reinforced concrete bridge pier under different axial compression ratio and different forces of horizontal earthquake action. They suggested that the stiffness reduction factor of rectangular section reinforced concrete bridge pier can be taken as 0.3, which was an average value for the considered analyses.

Bonet et al. (2011) mentioned that structure codes (ACI-318) and (EuroCode–2) proposed the moment magnifier technique to consider the second-order effect to design slender reinforced concrete columns. However, the accuracy of this method depends on the effective stiffness EI of slender columns. They developed a new EI equation which can be effectively used for designing the slender reinforced concrete columns with sufficient accuracy.

Vidovic et.al. (2012) studied the most recent outline in the seismic design of structures as per Eurocode 8 considering the impact of cracking while at the same time assessing the stiffness of concrete element – the stiffness consequences for the size of the seismic forces and lateral displacements. They considered a residential building with a basement and six floors having different flexural stiffnesses as per different codes under seismic loadings. They concluded that horizontal displacements varied lesser than that of internal forces due to the variation of cracked stiffness of the structural elements of the building.

Liu et al. (2012) investigated the flexural stiffness reduction factor of reinforced concrete columns with equal L-shaped considering characteristics of material and geometrical nonlinearities. They concluded that the axial load level does have an influence on the stiffness reduction factor. In addition, they suggested that stiffness reduction factor of reinforced concrete columns with equal L-shaped sections and an axial load level below 0.35 has an average value of 0.4.

Causevic et.al. (2012) presented results obtained from analysis of two typical structures of six and eleven storied with a basement and ground floor. Both structures were analyzed in accordance with the Non Collapse Requirement (NCR) and the ductility class medium (DCM) was adopted as per Eurocode. From their analyses, it was observed that stiffness reduction resulted in an increase of section forces in slabs, and in a decrease of such forces in columns and beams. They also concluded that section forces in slabs, beams and columns were increased with the reduction of the RC wall stiffness.

Tang and Su (2014) reviewed the available simplified shear and flexural models suitable for structural walls. A database comprised of walls subjected to reverse-cyclic loads was formed to evaluate the performance of each model. They reported that for shear deformation dominated walls, use of intact shear stiffness following ACI318-11 or a 0.5 stiffness reduction factor following EC8 could result in underestimating the period at yield by 55% or 37%, respectively.

Das and Choudhury (2019) studied the performance of RC frame buildings considering three categories of member stiffness, namely, gross section stiffness, effective stiffness given in FEMA-356 and computed effective stiffness based on strength. They assessed the performance of the buildings with these three categories of stiffness and with different heights and plans. They concluded from the results of nonlinear analyses that the use of gross stiffness underestimated the response parameters of the building under seismic conditions. In addition, the inter-storey drifts of buildings analyzed with gross stiffness were much lower than those of buildings with effective stiffness based on strength. Therefore, to know the actual performance of the buildings under seismic action, actual effective stiffness based on strength need to be used.

2.3 Seismic design standards/codes of major countries across the world

Most of the standards/codes of major countries across the world including Bangladesh use the force-based design (FBD) approach. Analysis of RC structures using the FBD

under the gravity and seismic loads, the designers normally take into account the appropriate, effective or gross moment of inertia to evaluate the flexural stiffness/rigidity of beams, columns, walls and slabs to account the cracking effects of RC frame members. This section aids structural engineers by providing a summary of the range of stiffness modifiers recommended by different building codes. A literature review of codes, standards, and research articles is also provided in following sub-sections.

2.3.1 American Standard (ACI 318)

ACI 318-11 is referenced by the 2012 International Building Code (IBC). Sections 8.8.1 through 8.8.3 provide guidelines for effective stiffness values to be used to determine deflections under lateral loading. In general, 50% of the stiffness based on gross section properties can be utilized for any element, or stiffness can be calculated in accordance with Section 10.10.4.1. ACI 318-14 contains the similar recommendations for stiffness modifiers reformatted in Section 6.6.3.

2.3.2 New Zealand Standard (NZ 3101)

NZS 3101: Part 2 (2006 Edition) states that effective stiffness in concrete members is influenced by the amount and distribution of reinforcement, the extent of cracking, tensile strength of the concrete, and initial conditions in the member before loads are applied. This standard recommended effective stiffnesses for different members to simplify the complex analysis that would be required to address these factors. However, the level of loading used in NZS 3101 seems different from that of U.S. codes.

2.3.3 Canadian Standards (CSA A23.4-14)

CSA A23.4-14 provides recommended stiffness modification factors in Section 10.14.1.2. These factors are provided to determine the first-order lateral storey deflections based on an elastic analysis. The Canadian Standards are based on an earthquake with a 2% probability of exceedance in 50 years.

2.3.4 European Code (EN1994–2003)

According to Eurocode 8 (EN1994–2003), the elastic stiffness of the bilinear force-deformation relation in reinforced concrete elements should correspond to that of cracked sections and the initiation of yielding of the reinforcement. Unless a more accurate analysis of the cracked elements is performed, this standard recommends that the elastic

flexural and shear stiffness properties of concrete elements are taken as 50% of the corresponding stiffness of the uncracked element.

Part 3 of Eurocode 8 provides an equation based on moment-to-shear ratio and yield rotation, which can be used for determination of a more accurate effective stiffness. Both ultimate level and serviceability level loads are addressed in Eurocode 8 for linear and nonlinear analysis.

2.3.5 Turkish Standard (TEC 2007)

Turkish TS 500-2000 refers to the Turkish Earthquake Code (2007) which states that uncracked properties shall be used for components when performing certain types of analyses. However, stiffness modifiers for cracked section properties may be utilized for beams framing into walls in their own plane and for coupling beams of coupled structural walls when performing these types of analyses. Cracked section properties must be used for the analysis of existing structures. Cracked section properties may also be used when performing advanced analyses.

2.3.6 Indian Standard (IS 1893-2016)

The stresses in concrete and steel shall be calculated by the theory of cracked section in which the tensile resistance of concrete is ignored. If the calculated stresses are within the permissible stress specified section may be assumed to be safe. The maximum stress in concrete and steel may be found based on the cracked section theory. As per section 6.4.3.1 - moment of inertia has to take in RC frame and masonry structure as 70% of moment of inertia of column and 35% moment of inertia on beam. Reduced second area of moments need to be applied for slabs and walls as well, along with the beam and columns.

2.3.7 Bangladesh National Building Code (BNBC-2017 Draft)

Section 6.3.10.4.1 of draft BNBC-2017 shows that it shall be permitted to use the following properties for the members in the structure:

For Column: I= 0.7Ig, Beam: I= 0.35Ig, Wall (Cracked): I= 0.35Ig, Wall (Gross): I = 0.7Ig, Plates and Flat Slab: I = 0.25Ig.

Alternatively, the moments of inertia of compression and flexural members shall be permitted to be computed as follows:

Compression members:

$$I = (0.80 + 25\ A_{st}/A_g)\ (1 - M_u/(P_u\ h) - 0.5\ P_u/P_0)\ I_g \leq 0.875I_g$$

Where, P_u and M_u shall be determined from the particular load combination under consideration, or the combination of P_u and M_u determined in the smallest value of I. The value of I need not be taken less than $0.35I_g$.

Flexural members:

$$I = (0.10 + 25\rho)\ (1.2 - 0.2\ b_w/d)\ I_g \leq 0.5I_g$$

For continuous flexural members, I shall be permitted to be taken as the average of values obtained from Eq.6.6.16 for the critical positive and negative moment sections. The value of I need not be taken less than $0.25I_g$. The cross-sectional dimensions and reinforcement ratio used in the above formulas shall be within 10 percent of the dimensions and reinforcement ratio shown on the design drawings or the stiffness evaluation shall be repeated.

The effective moment of inertia of RC frame members suggested by the seismic code of major counties is shown in Table 2.1

Table 2.1: Effective moment of inertia of beam and column as per different codes

Different Codes	Beams	Columns	Wall un-cracked	Wall cracked
BNBC- 2017 (draft)	$0.35I_g$	$0.70I_g$	$0.70I_g$	$0.35I_g$
IS 1893-2016	$0.35I_g$	$0.70I_g$	$0.70I_g$	$0.70I_g$
ACI 318-14 (2000)	$0.35I_g$	$0.70I_g$	$0.70I_g$	$0.50I_g$
Eurocode-8 (1994–2003)	$0.50I_g$	$0.50I_g$	$0.50I_g$	$0.50I_g$
NZS 3101(1995)	$0.35I_g$	$0.40I_g$–$0.70I_g$	$0.50I_g$	$0.25I_g$–$0.40I_g$
CSA A23.4-14	$0.35I_g$	$0.70I_g$	$0.70I_g$	$0.35I_g$
TEC 2007	$0.4I_g$	$0.80I_g$	N/A	$0.40I_g$–$0.80I_g$

2.4 Structural performance levels and ranges

The performance of a building under any particular event is dependent on a wide range of parameters. These parameters are defined in ATC-40 (1996) and FEMA 356 (2000) qualitatively in terms of the safety afforded by the building to the occupants during and after the event; the cost and feasibility of restoring the building to pre-earthquake condition; and economic, architectural, or historic impacts on the larger community. These performance characteristics are directly related to the extent of damage that would be sustained by the building. Following sub-sections describe the different performance levels briefly:

2.4.1 ATC-40

A performance level describes a limiting damage condition: which may be considered satisfactory for a given building and a given ground motion. The limiting condition is described by the physical damage within the building, the threat to life safety of the building's occupants created by the damage, and the post-earthquake serviceability of the building. Target performance levels for structural and nonstructural systems are specified independently. Table 2.2 shows the performance levels of buildings as per ATC-40.

Table 2.2: Performance Level of Buildings (ATC-40)

Level of Performance	Description
Operational	Very little damage, temporary drift, structure retains original strength and stiffness, all systems are normal.
Immediate occupancy	Little damage, temporary drift, structure retains original strength and stiffness, elevator can be restarted, fire protection still works.
Life Safety	Fair damage, some permanent drift, some residual strength and stiffness left, damage to partition, building may be beyond economical repair.
Collapse Prevention	Severe damage, large displacement, little residual stiffness and strength but loading bearing column and wall function, being is closed to collapse.

2.4.2 FEMA 356

Building performance is a combination of the performance of both the structural and nonstructural components. Table A1(Appendix A) describes the approximate limiting levels of structural and nonstructural damage that may be expected of buildings rehabilitated to the levels defined in the standard. On average, the expected damage would be less.

Building performance in this standard is expressed in terms of target Building Performance Levels. These target Building Performance Levels are discrete damage states selected from among the infinite spectrum of possible damage states that buildings could experience during an earthquake. The particular damage states identified as target Building Performance Levels in this standard have been selected because they have readily identifiable consequences associated with the post-earthquake disposition of the building that are meaningful to the building community. These include the ability to resume normal functions within the building, the advisability of post-earthquake occupancy, and the risk to life safety. Due to inherent uncertainties in prediction of ground motion and analytical prediction of building performance, some variation in actual performance should be expected. Compliance with this standard should not be considered a guarantee of performance. Information on the reliability of achieving various Performance Levels can be found of (FEMA 274).

A wide range of structural performance requirements could be desired by individual building owners. The four Structural Performance Levels defined in this standard have been selected to correlate with the most commonly specified structural performance requirements. Table A2 (Appendix A) relates these Structural Performance Levels to the limiting damage states for common vertical elements of lateral-force-resisting systems. Table A3 (Appendix A) relates these Structural Performance Levels to the limiting damage states for common horizontal elements of building lateral force-resisting systems.

The federal emergency management agency in its report (FEMA-356, 2000) defines the structural performance level of a building to be selected from four discrete structural performance levels and two intermediate structural performance ranges. The discrete Structural Performance Levels are Immediate Occupancy (S-1), Life Safety (S-3), Collapse Prevention (S-5), and Not Considered (S-6). The intermediate Structural

Performance Ranges are the Damage Control Range (S-2) and the Limited Safety Range (S-4). The performance levels and ranges, as per FEMA are described in followings:

Immediate occupancy structural performance level (S-1)

Structural performance level S-1, immediate occupancy, may be defined as the post-earthquake damage state of a structure that remains safe to occupy, essentially retains the pre-earthquake design strength and stiffness of the structure, and is in compliance with the acceptance criteria specified in this standard for this structural performance levels defined in the appendix A.

Structural performance level S-1, immediate occupancy, means the post-earthquake damage state in which only very limited structural damage has occurred. The basic vertical and lateral-force-resisting systems of the building retain nearly all of their pre-earthquake strength and stiffness. The risk of life-threatening injury as a result of structural damage is very low, and although some minor structural repairs may be appropriate, these would generally not be required prior to re-occupancy.

Damage control structural performance range (S-2)

Structural performance range S-2, damage control, may be defined as the continuous range of damage states between the life safety structural performance level (S-3) and the immediate occupancy structural performance level (S-1).

Design for the damage control structural performance range may be desirable to minimize repair time and operation interruption, as a partial means of protecting valuable equipment and contents, or to preserve important historic features when the cost of design for immediate occupancy is excessive.

Life safety structural performance level (S-3)

Structural performance level S-3, life safety, may be defined as the post-earthquake damage state that includes damage to structural components but retains a margin against onset of partial or total collapse in compliance with the acceptance criteria specified in FEMA-356. Some structural elements and components are severely damaged, but this has not resulted in large falling debris hazards, either within or outside the building. Injuries may occur during the earthquake; however, the overall risk of life-threatening injury as a result of structural damage is expected to be low. It should be possible to

repair the structure; however, for economic reasons this may not be practical. While the damaged structure is not an imminent collapse risk, it would be prudent to implement structural repairs or install temporary bracing prior to re-occupancy.

Limited safety structural performance range (S-4)

Structural performance range S-4, limited safety, may be defined as the continuous range of damage states between the life safety structural performance level (S-3) and the collapse prevention structural performance level (S-5) defined in Table in the appendix A.

Collapse prevention structural performance level (S-5)

Structural performance level S-5, collapse prevention, may be defined as the post-earthquake damage state that includes damage to structural components such that the structure continues to support gravity loads but retains no margin against collapse in compliance with the acceptance criteria specified FEMA for this structural performance level.

Structural performance level S-5, collapse prevention, means the post-earthquake damage state in which the building is on the verge of partial or total collapse. Substantial damage to the structure has occurred, potentially including significant degradation in the stiffness and strength of the lateral-force resisting system, large permanent lateral deformation of the structure, and to more limited extent degradation in vertical load carrying capacity. However, all significant components of the gravity load resisting system must continue to carry their gravity load demands. Significant risk of injury due to falling hazards from structural debris may exist. The structure may not be technically practical to repair and is not safe for re-occupancy, as aftershock activity could induce collapse.

2.5 Nonlinear static analysis (Pushover analysis)

During seismic action, the building is expected to deform in-elastically and therefore seismic performance evaluation is required considering post-elastic behavior of the structure. Nonlinear static analysis or pushover analysis is generally carried out as an effective tool for performance evaluation of the structures under seismic loads. In nonlinear static analysis or pushover analysis, a building under constant gravity loads and monotonically increasing lateral forces during a seismic event is analyzed until a

target displacement is reached. Pushover analysis provides better understanding of seismic performance of buildings and also traces the progression of damage and failure of building's structural elements. By pushover analysis, one may get an insight about the behavior of building in non-linear zone.

2.5.1 Research studies on Pushover analysis

Structural engineering has started using the nonlinear static procedure (NSP) or pushover analysis professionally due to its simplicity in nature and easy in calculation. A review of literature is presented in brief summarizing the research works on pushover analysis for building structures provided below:

The pushover analysis method was firstly introduced by Freeman et al. (1975) as the Capacity Spectrum Method. The main purpose of this empirical approach was to use a simplified and quick method to assess the seismic performance of a series of 80 buildings located in a shipyard in USA. The study combined the use of analytical methods with site-response spectra to estimate values of peak structural response, peak ductility demands, equivalent period of vibration, equivalent percentages of critical damping, and residual capacities. It was concluded that it could perform, in most of the cases, a worthwhile evaluation of existing structures in a reasonable time-scale and cost.

Freeman (1978) presented the Capacity Spectrum method in a clearer manner together with its application to two instrumented 7-storey reinforced concrete structures. The data obtained from the recorded motions were compared with the analysis results showing reasonable agreement. He cautioned engineers that the elastic modelling assumptions, e.g. the choice between cracked or uncracked sections, the inelastic stiffness degradation, e.g. appropriate reduction of structural elements' stiffnesses in the post-elastic region, and the percentage of critical damping used to construct the demand spectra, and determination of the inelastic capacity needed careful judgment and some experience to be adequately defined and assessed. It was suggested that two levels of equivalent viscous damping should be assumed relating to the initial undamaged state and to the ultimate limit state in order to account for the effect of period lengthening that is usual when the structure enters the nonlinear region. Furthermore, it was concluded that more structures needed to be assessed to validate the method.

Saidi and Sozen (1981) produced a 'low-cost' analytical model which was named the Q-Model for calculating displacement histories of multi-storey reinforced concrete

structures subjected to ground motions. The Q-model, which was based on the idea of Gulkan and Sozen (1974), involved two simplifications, the reduction of a multi degrees of freedom (MDOF) model of a structure to a single degree of freedom (SDOF) oscillator and the approximation of the variation of the stiffness properties of the entire structure by a single spring to take account of the nonlinear force-displacement relationships that characterize its properties. Earthquake-simulation experiments of eight small-scale structures were performed and the displacement histories were compared with the results from nonlinear static analyses based on the Q-model. It was shown that the performance of the Q- Model in the simulation of high- and low- amplitude responses was satisfactory for most of the test structures. It was stated that the model would need to be further validated by more experimental and theoretical analyses.

Fajfar and Fischinger (1988) presented a variation of pushover analysis, the N2 method, and assessed it on a seven-storey RC frame-wall building structure that had been experimentally tested in Tsukuba, Japan as part of the joint U.S. – Japan research project. The authors used the uniform and inverted triangular load distributions to perform nonlinear static analyses of the structure. The pushover curves were compared to the dynamic experimental and analytical results showing considerable differences in their shapes. It was noted that the inverted triangular distribution was unconservative in estimating base shear demands due to the effect of higher modes. It was observed that the uniform distribution seemed more rational when shear strength demand was to be assessed. It was also observed that the nonlinear dynamic analysis of the equivalent SDOF system yielded in general non-conservative shear forces compared with the experimental and theoretical results. However, the target displacement at the ultimate limit state and the rotations of the floors were approximated satisfactorily compared with the experimental and theoretical results.

Gaspersic et al. (1992) extended the N2 method by attempting to include cumulative damage; a characteristic resulting from numerous inelastic excursions. The test structure was the seven-storey reinforced concrete building tested in the U.S. – Japan research project. The seismic demands for each element were computed in terms of the dissipated hysteretic energy using the Park-Ang model (Park et al. 1985). The conclusions drawn were that the dissipated hysteretic energy increased with increasing duration of ground motion, and it was significantly affected by the reduction of strength of the structural elements. They also concluded that when the fundamental period of the structure was

much larger than the dominant period of the ground motion, the higher mode effects became an important issue. In this case the input energy and dissipated hysteretic energy of a MDOF system were generally larger than the corresponding quantities in the equivalent SDOF system. The authors suggested that the N2 method was likely to underestimate quantities which governed damage in the upper part of a structure.

Mahaney et al. (1993) utilized the Capacity Spectrum Method in four case studies of structures to evaluate their seismic response after the Loma Prieta Earthquake. The analyzed structures included one-storey and two-storey wood-frame residences, an eleven-storey reinforced concrete shear wall building and several framed buildings with brick infilled walls. In that study the ADRS spectra format was firstly introduced. The results indicated that the damped elastic earthquake displacement demands did not necessary equal the actual inelastic displacement demands as had been assumed. This can be attributed to the short predominant period of some of the structures which were not in the permissible region of applicability of the equal displacement rule. However it was stated that the damage predicted by the Capacity Spectrum Method was in good agreement with the observed damage for the eleven-storey reinforced concrete shear wall building.

Fajfar and Gaspersic (1996) applied the N2 method to the standard seven-storey reinforced concrete building tested in Tsukuba, Japan in the joint U.S. – Japan collaboration, which had been tackled in previous studies. Three case studies were carried out. The first corresponded to the actual structure without any modeling modifications. Two additional variants of this model were considered. The first variant considered only the frame structure without the structural wall, and was denoted as Model 1. The second variant, Model 2, considered a weak first storey. These modifications however did not change the initial natural period of the structures. The conclusions drawn from the study were that for structures which vibrated primarily in the fundamental mode, the method could provide reliable estimates of global seismic demand. In most cases, the demands at the local level in terms of deformation, dissipated energy and damage indices could be adequate enough to be used in practice. The method could detect weaknesses such as storey mechanisms or excessive demands. However, it was also concluded that if higher mode effects became important, some demand quantities determined by the N2 method would be underestimated. Therefore, an appropriate magnification of selected quantities could be advantageous. No such

recommendations were provided. Additionally, the authors claimed that the N2 method appeared to be not very sensitive to changes in the assumed displacement shape and the corresponding vertical distribution of the loads, as well as the bilinear force-displacement idealization, which was not in agreement with other studies. The largest uncertainty on the interpretation and comparison of results was thought to have been introduced by the characteristics of each ground motion. Finally, it was acknowledged that bidirectional input and the influence of the coupling of the fundamental translational and torsional modes needed to be incorporated before the N2 method could be extended to the analysis of three-dimensional models of buildings.

Faella (1996) carried out both nonlinear static and nonlinear dynamic analyses using artificial and natural earthquake records on 3-, 6-, and 9-storey symmetrical reinforced concrete structures, designed to EC8, which were characterized as high ductility structures standing on stiff soil. Results showed that pushover analysis could identify collapse mechanisms, critical regions that would need particular detailing, and also inter-storey drifts and structural damage. It was suggested that for design purposes, inter-storey drifts and structural damage had to be computed for a top displacement larger than the target displacement calculated from the analyses. This could be achieved by the use of a coefficient which numerically increased as the number of storeys increased. However, he suggested that when carrying out pushover analyses it is necessary to compute the pushover curve at a target displacement higher than the one obtained from a nonlinear dynamic analysis. This would mean that a nonlinear dynamic analysis would be needed before conducting a pushover analysis. In this way though pushover analysis would not be needed therefore this approach is questionable. Finally, it was suggested that further analyses needed to be carried out to verify if this method could be an efficient tool for a range of input ground motion characteristics and for soft soil conditions.

Kunnath et al. (1996) performed a seismic evaluation of a 4-storey reinforced concrete building subjected to five strong ground motions. The prediction of displacements from pushover analyses and nonlinear time-history analyses showed fairly good agreement – with a tendency for pushover analyses to be on the unconservative side. The authors recognized the considerable differences in the time and computational effort required, for the types of analyses. In terms of time management pushover analysis appeared to be superior.

Fajfar et al. (1997) utilised the N2 method to analyze the seismic response of light masonry-infilled frame structures. A series of physical pseudo-dynamic tests were carried out on a full scale four-storey reinforced concrete structure. Pseudo- dynamic seismic tests were conducted first on the bare structure. Then some of the bare frames were infilled and the new structure was subjected to subsequent pseudo-dynamic tests using one artificial ground motion. The results showed that the presence of infilled frames changed the response of the structure significantly. The authors concluded that the N2 method was able to predict adequately the seismic demand and seismic damages since the predicted results were similar to the results obtained by nonlinear dynamic analyses for different accelerograms for all the test structures. The displacement and storey drift demands, and the hysteretic energy dissipation were generally overestimated by the N2 method. This was attributed to the slippage of the reinforcing bars during the dynamic tests which caused relatively slow energy dissipation. It is unclear though if this slippage had been accounted for in the pushover analyses conducted.

Tso and Moghadam (1997) proposed an extension of pushover analysis that included torsional effects, to compute the seismic response of two 7-storey reinforced concrete structures; one being symmetrical and the other asymmetrical. The method included the use of 3D elastic dynamic analyses of the models in order to provide the maximum target displacements for the lateral-load resisting elements. The force distributions across the structures derived from the dynamic analyses were used as static force distributions to carry-out a series of 2D pushover analyses. The results showed good estimates of floor displacements, inter-storey drifts and ductility demands for both types of structures.

Kilar and Fajfar (1997) tested the effectiveness of their proposed method on an asymmetric 21-storey reinforced concrete structural wall building. The results shown that a larger ductility is required in an asymmetrical structure in order to develop the same strength as a symmetrical structure. It was concluded that the procedure was an effective tool to estimate the ultimate strength and global plastic mechanism, and provided information on the sequence of plastic yield formation across the structure.

Bracci et al. (1997) introduced an adaptive pushover analysis and tested its effectiveness on a three-storey reinforced concrete frame building by comparing the analytical results with experimental values. The target displacement was found to be in agreement with the experimental displacement. The study focused mainly on identification of the failure

modes of the structure by inspecting the force-deformation relationships obtained from both experimental and analytical approaches.

Satyarno et al. (1998), attempted to refine pushover analysis by introducing a compound spring element in the computer program RUAUMOKO capable of modelling plastic hinge regions that could take into account the flexural and shear properties of typical beam-column joints of existing reinforced concrete frame structures. The idea behind this element was that shear and/or flexural failure modes can occur after certain critical regions of the structure sustain significant inelastic flexural rotations. The authors argued that there can be a shift in the structures' response from a flexural failure mode to a shear failure mode and this feature needs to be properly accounted for in pushover analyses. Additionally, the authors suggested an adaptive pushover method that utilized Rayleigh's equation for calculating the period of vibration of the structure at every force increment.

Aschheim et al. (1998) performed a comparison of the Capacity Spectrum Method and the Displacement Coefficient Method with results from nonlinear dynamic analyses for a large number of SDOF systems with various periods, strengths, and hysteretic models and on a three-storey reinforced concrete building. For the SDOF systems, the authors concluded that the displacement estimates from the pushover methods could be either conservative or unconservative, and showed great variability. None of these methods was reported to show any superiority on the accuracy of these estimates. Additionally, for the three-storey structure, the authors concluded that the pushover methods could both underestimate and overestimate significantly the displacement demands caused by various ground motions. In the case of short period structures, the displacement estimates were most probably overestimated. The main factor causing these differences was the variability of the individual ground motions used.

Gupta and Kunnath (1999) performed an evaluation of pushover analysis on four isolated reinforced concrete walls with 8, 12, 16 and 20-storeys. The authors utilized two conventional load patterns (FEMA and uniform), and a load pattern that changed continuously depending on the instantaneous dynamic properties of the system. The results were compared with the results of the nonlinear dynamic analyses. Two critical issues concerning these types of structures were identified: amplification of base shear demands due to higher mode effects and progressive yielding. It was shown that the adaptive load pattern was able to capture accurately the base shear amplification and

progressive yielding while the other two patterns calculated base amplification demands of less than 50% of the 'exact'.

Iwan (1999) investigated the applicability of the Capacity Spectrum Method for the analysis of structures subjected to near-fault ground motions. The method was applied to SDOF and MDOF bilinear hysteretic systems. The conclusions regarding SDOF systems were that the CSM method did not give satisfactory results except for a very limited short-period range being near the dominant pulse period of the ground motion. Additionally, the performance points obtained using the equivalent viscous damping resulted in underestimation of the true inelastic response of SDOF systems with periods shorter than the predominant period of the earthquake pulse. The author stated that studies of MDOF systems showed that elastic SDOF analyses and elastic MDOF analyses correlated well only for structural periods shorter than the ground pulse duration. It was concluded that the Capacity Spectrum Method provided a reasonable estimation of the maximum roof displacement. However, for taller buildings it proved to be insufficient to predict the demands in the upper storeys.

Matsumori et al. (1999) investigated the accuracy of pushover analysis in the estimation of ductilities across the floor levels on two 12-storey and three 18-storey reinforced concrete structures. The authors utilized two new lateral load patterns which were the sum and the difference of the storey shear distributions for the first two modes of vibration. Results showed that the ductility demands obtained were an upper bound when compared to nonlinear dynamic analysis results.

Chopra and Goel (2000) suggested an improved capacity-demand-diagram method that used constant ductility design spectra for estimating the deformation of inelastic SDOF systems. The method suggested that the target displacement would be given by the intersection point where the ductility factor calculated from the capacity diagram matched the value associated with the intersecting demand curve. The authors pointed out that the original ATC-40 procedure underestimated significantly the deformation of inelastic systems for a wide range of natural periods, T_n and ductilities, μ compared to the deformation demands determined from the inelastic design spectrum. Several deficiencies in the ATC-40 procedure A were found since it did not converge for some of the systems analyzed. Also in the cases in which it did converge it yielded deformation estimates and ductility factors that were significantly different to those obtained from a

nonlinear time- history analysis. Some of the analyses showed that the above parameters were underestimated with up to a 50% error. Furthermore, the authors concluded that the ATC- 40 procedures were deficient relative even to the elastic design spectrum in estimating the peak deformation of an inelastic system with period Tn in the velocity-sensitive or displacement-sensitive regions of the spectrum.

Yang and Wang (2000) applied the pushover method to three frame structures of 8, 12, and 15 storeys and compared the results with nonlinear time-history analyses. The results provided were estimates of roof displacement and floor rotations. In one case a difference of up to 30% could be observed but generally results could be deemed satisfactory. The differences in the results were mainly attributed by the authors to the frequency contents of the ground motions used. Also it was noted that the bilinear representation of the pushover curves introduced errors in the estimation of the base shear and the yield displacement. These in turn resulted in differences in the calculated responses between analyses.

Albanesi et al. (2000) proposed the use of variable-damping response spectra in the pushover method proposed in ATC-40 document to evaluate seismic response of nonlinear structures in terms of the maximum displacement and acceleration, given the structural initial elastic period, the yielding acceleration and the hardening ratio in the plastic range. The somewhat improved procedure was used to study elasto-plastic and Takeda degrading hysteretic SDOF systems and also a two-storey and a seven-storey existing reinforced structures. The results showed much variation in responses between hysteretic models and not any clear improvement on the effectiveness of the method. The degrading Takeda model was found to be more appropriate for modeling concrete behaviour than the elasto-plastic model even though the applicability of the latter was thought to be satisfactory.

Peter and Badoux (2000) applied the capacity spectrum method to a 9-storey reinforced concrete building with reinforced concrete and masonry structural walls. The structure was subjected to two strong ground motions. Three types of lateral load patterns were used to simulate seismic behaviour in a static manner. These were the uniform distribution, the modal distribution and the modal adaptive force distribution. The conclusion the authors drew from their study were that the CSM method was adequate to estimate seismic demands such as inter-storey drifts. Furthermore, the uniform load

pattern proved to be quite effective. A need for more reliable structural models was acknowledged.

Gupta and Kunnath (2000) investigated the effectiveness of the adaptive-spectra pushover procedure with respect to the other conventional pushover methods and the nonlinear time- history analyses on five reinforced concrete structures of 4, 8, 12, 16, and 20 storeys. The results indicated increasing deviations in inter-storey drift responses for increasing height of buildings, between the conventional pushover methods and the nonlinear time-history analyses. It was also noted that great care should be taken when interpreting results from pushover analyses because they could obscure real deficiencies in a structural system and lead the engineer to recommend retrofitting of the structure when it is not needed while failing to address the real deficiencies.

Fajfar (2000) applied the N2 method to a four-storey reinforced concrete frame structure subjected to three ground motions. The results were said to have been compared with experimental data provided from pseudo-dynamic tests of the model. The method was deemed acceptable for estimating seismic demands in planar structures. It was noted though that the type of spectra used were not adequate for estimating seismic response from near-fault ground motions, for soft soils, for hysteretic loops with significant stiffness or strength deterioration and for systems with low strength.

Requena and Ayala (2000) discussed two variations of adaptive pushover analysis mainly concerned with the estimation of the contribution of the higher modes of vibration in the seismic response of building structures. These variations have been discussed in section 2.4.5, named as approach 2-A, and approach 2-B. The approaches together with the fundamental mode distribution were tested on a 17-storey reinforced concrete frame and results of maximum displacement, inter-storey drifts and plastic hinge locations were compared with results from nonlinear dynamic analyses. Good agreement was achieved by both proposed methods with approach 2-B being slightly more efficient than 2-A. Furthermore, the authors investigated the changes in the first three modes of vibration of the structure when it behaved nonlinearly through a nonlinear static analysis. The authors concluded that stiffness degradation of the structure influenced more the fundamental mode shape than mode shapes corresponding to higher modes. Furthermore, it was suggested that the changes in the modes of vibration need to be considered in this type of analysis

Memari et al. (2001) performed a comparative evaluation of current seismic assessment methodologies on a 32-storey reinforced concrete building. The authors suggested that pushover analysis is a good tool for approximating seismic demands in the lower storeys of tall structures. The predictions have a better agreement with the nonlinear time-history analyses for larger peak ground acceleration values. The mode of failure though for the structure could not be safely predicted by pushover analysis, something that is worrying since the identification of the failure mode of a structure by pushover analysis has been considered as one of the virtues of the method.

Mwafy and Elnashai (2001) studied the seismic response of twelve reinforced concrete buildings using nonlinear static and nonlinear dynamic analyses. The buildings were divided into three general groups: four 8-storey irregular frames, four 12-storey regular frames and four 8-storey dual frame-wall structures. It was found out that in all cases the responses of the buildings were sensitive to the shape of the lateral load pattern. Also the multi-mode pattern did not appear to provide enhanced results with respect to the other conventional load patterns.

Lew and Kunnath (2001) examined the effectiveness of nonlinear static procedures to capture the seismic response of two steel – 6-storey and 13-storey - and two reinforced concrete buildings – 7-storey and 20-storey. The conclusions that were drawn from this study were that nonlinear static procedures were not effective in capturing inter-storey drifts and locations of plastic hinges for any type of the tested structures especially at higher-storeys. The peak displacement profiles calculated from all procedures were in agreement though.

Albanesi et al. (2002) suggested an energy-based approach for pushover analysis and studied its efficiency on two reinforced concrete frame structures – a three-storey three-bay frame and a seven-storey two-bay frame. The results were compared with nonlinear dynamic analyses results and with the conventional Capacity Spectrum Method results using both force- and displacement- control incremental analyses. The capacity curves derived using all methods were very similar for the three- storey structure but quite different for the seven-storey structure, showing that deviations in the response can occur due to using either force-controlled or displacement-controlled nonlinear static analyses. The use of force-controlled or displacement-controlled nonlinear static analyses in the Capacity Spectrum method can cause significant differences in the estimation of the

seismic demands. Furthermore, the results showed in general underestimation of maximum displacement and base shear from both the conventional and the proposed method with respect to the dynamic analyses results.

Jingjiang et al. (2003) proposed a two-phase load pattern: an inverted triangular load pattern until the base shear reached some fraction β of its maximum value followed by an exponential form pattern defined as (x/H) a where x is the distance from the ground to the floor, (H) is height of the building and a is a characteristic parameter for different types of buildings. The authors performed pushover analyses with two more load patterns –uniform and triangular- for three groups of reinforced concrete buildings. These groups were three frame buildings of 4-, 6- and 8-storeys, two frame-wall buildings of 9- and 20-storeys and three shear walls of 6-, 10- and 16-storeys. It was concluded that the inverted triangular and the proposed load patterns were the most effective in estimating the target displacements for the frame buildings. Regarding the second group the uniform and the proposed load patterns were satisfactory for the 9-storey but unsatisfactory for the 20-storey building. The conclusions drawn for the last group were that the uniform and the proposed load patterns produced good results for low-rise shear walls but poor for mid- and high-rise walls. However, vague explanation was provided of the criteria needed to determine at which magnitude of base shear the conventional load pattern should change to the proposed one. For the frame structures the authors changed the load pattern at a half the value of maximum base shear while for the remaining buildings the load pattern was altered at 70-80% of the maximum base shear.

Antoniou and Pinho (2004) presented a displacement-based adaptive pushover procedure. The method used monotonic lateral incremental displacements instead of monotonic lateral incremental forces to obtain the capacity curves. The authors applied it to twelve reinforced concrete buildings and compared the results with the force-based method and with nonlinear time-history analysis. It was concluded that the method was able to provide improved predictions of demands with respect to the conventional method but could not reproduce results from the nonlinear time-history analysis. This was appointed to the static nature of the method that was used to the possible incorrect updating of the displacement vector.

Kunnath (2004) applied a number of load distributions based on the modal combination rule, to an eight-storey and a sixteen-storey reinforced concrete building. The pushover

analyses results provided from the DCM method, were compared with those from nonlinear time-history analyses of a typical ground motion. These indicated quite good agreement in the estimation of the inter-storey drifts in the eight-storey building but inappropriate for the upper levels in the case of the sixteen-storey building.

Makarios (2004) attempted to optimize mathematically the definition of an equivalent single-degree-of-freedom system needed in pushover analysis. This was done by optimizing the capacity curve when it is transformed to a bilinear form. The proposal was evaluated on a nine-storey reinforced concrete regular-frame building. The method could provide with two iterations a reasonable accuracy of the target displacement with an error of 1 to 8%

Papanikolaou and Elnashai (2005) evaluated the conventional and adaptive pushover analyses on eight structural building models. These comprised two twelve-storey regular reinforced concrete structures of high and low ductility class, two eight-storey shear wall type structures of high and low ductility class, two eight-storey irregular structures of high and low ductility class, a four-storey reinforced concrete frame structure with irregularity in plan. The obtained results were compared with nonlinear dynamic analyses. It was shown that pushover analysis can approximate displacement demands for structures that are free of irregularities in plan and elevation. The adaptive pushover procedure did not improve the results much in any of the cases thus not showing any clear advantages over the conventional pushover procedure.

Dolsek and Fajfar (2005) extended the N2 method to approximate the seismic response of two 4-storey infilled reinforced concrete frame structures. The basic differences from the standard N2 method were the multi-linear instead of bilinear idealization of the pushover curve thus taking into consideration the strength degradation of the infill and the new proposed R-μ-T relationships. The results obtained showed an overestimation of storey drifts in the first storey and underestimation in the rest of the storeys with respect to the nonlinear dynamic analysis results.

Kalkan and Kunnath (2007) investigated the accuracy of pushover procedures for the seismic evaluation of buildings. These were the conventional pushover analysis using the mode shape load distribution and the Uniform load distribution, the Modified Modal Pushover Analysis, MMPA, the Upper-bound Pushover Analysis, and the Adaptive Modal Combination Procedure, AMC. These were applied to a 6- and 13-storey steel

building, and to a 7- and a 20-storey RC moment frame building. The results from these analyses were compared to the results from nonlinear dynamic analyses based on the behaviour of these buildings to far-field and near-fault ground motions. The quantities of interest in this study were the displacement demands, inter-storey drifts and rotation demands. The study found that the conventional pushover analysis overestimated the displacement demands in the low and intermediate storeys for all buildings and ground motions. The upper-bound pushover analysis on the other hand underestimated the displacement demands. The MMPA and the AMC procedures overestimated the displacement demands but with the smallest error. These last two procedures predicted very similar results. Regarding the inter-storey drift demands the conventional pushover procedures significantly underestimated the drifts in the upper storeys and overestimated them in the lower storeys for most of the buildings. The upper-bound pushover analysis on the other hand, overestimated the drifts in the upper storeys and underestimated them in the lower storeys. The MMPA and the AMC methods performed slightly better with reasonable accuracy in the lower storeys but with overestimation in the upper storeys for most of the buildings. Finally the plastic rotation demands were compared between the MMPA, AMC and nonlinear dynamic analyses only. It was found that that the MMPA was able to capture the rotation demands mostly in the lower storeys. The AMC procedure was the most effective for estimating this quantity across the buildings' floors.

Cimellaro et al. (2014) proposed bidirectional pushover analysis on models with irregular in shape. The extended N2 method and Proposed Bidirectional pushover analysis were analyzed to the irregular models and the results were compared with nonlinear response history analysis (NRHA) in terms of inter-storey drift and floor rotations, proves acceptable. In the first case of analysis classical N2 method was performed and in the second case N2 method is applied in X and Y directions separately with load factors 1 and 0.6 and results are combined in SRSS combination. The same methodology is applied as bidirectional pushover analysis by applying bidirectional seismograms in both directions simultaneously. Seismograms are taken from ITACA website with peak ground acceleration 0.15g. From the results proved that factor 1 and 0.3 indicated in European seismic code for nonlinear static analysis is not sufficient when bi-directional ground motions are applied.

Ahmed and Raza (2014) carried out study on seismic vulnerability of RC buildings by considering plan irregularities using pushover analysis. Various models were considered

in order to identify the performance of the structures to withstand against disaster for building structures. They have conducted study on "G+9" storey building situated in zone V having plan irregularities like, rectangular, diaphragm discontinuity, and Y-shaped building. Pushover analysis has been performed using FEM based analytical software ETABS 9.7.4 version. They have presented their results in terms of pushover demand, capacity spectrum and plastic hinges. They have concluded that base shear for rectangular model is greater than diaphragm discontinuity and Y-shaped models. Point displacements are greater for diaphragm discontinuity model as there is an opening in the centre for that model. Finally, they concluded that among the three models considered for study purposes, rectangular model is most vulnerable to seismic effect.

Cavdar et al. (2018) have conducted pushover analysis and nonlinear dynamic analysis for a building which was collapsed in Turkey earthquake in 2003. Their objective was to perform the pushover analysis and NDA for different earthquakes to test the reliability and usability of performance levels. The mode superposition method considering the Wilson-ɵ algorithm was used for solving the dynamic equilibrium equations. A performance evaluation was performed using the current Turkish Earthquake Code, TEC (2007). It is concluded that pushover can provide a reasonably accurate estimation of performance level when a reinforced-concrete shear-wall building is not severely damaged. If the building is seriously collapsed, pushover analysis underestimates the building performance, regardless of the lateral load distributions.

2.5.2 Capacity

The overall capacity of a structure depends on the strength and deformation capacities of the individual components of the structure. In order to determine capacities beyond the elastic limits, some form of nonlinear analysis, such as the pushover procedure, is required. This procedure uses a series of sequential elastic limits, some form of nonlinear analysis, superimposed to approximate a force displacement capacity diagram of the overall structure. The mathematical model of the structure is modified to account for reduced resistance of yielding components. A lateral force distribution is again applied until additional components yield. This process is continued until the structure becomes unstable or until a predetermined limit is reached. The capacity curve approximates how structures behave after exceeding their elastic limit.

2.5.3 Demand (displacement)

Ground motions during an earthquake produce complex horizontal displacement pattern in structures that may vary with time. Tracking this motion at every time-step to determine structural design requirements is judged impractical. Traditional linear analysis methods use lateral forces to represent a design condition. For nonlinear methods it is easier and more direct to use a set of lateral displacements as a design condition. For a given structure and ground motion, the displacement demand is the estimate of the maximum expected response of the building during the ground motion.

2.5.4 Performance

Once a capacity curve and demand displacement is defined, a performance check can be done. A performance check verifies that structural and nonstructural components are not damaged beyond the acceptable limits of the performance objective for the forces and displacement imposed by the displacement demand. Fig. 2.1 shows a typical capacity curve of a structure. Severity of earthquakes as classified in ATC-40, 1996 is defined below.

A. The serviceability earthquake (SE)

The serviceability earthquake (SE) is defined probabilistically as the level of ground shaking that has a 50 percent chance of being exceeded in 50-year period. This level of earthquake ground shaking is typically about half of the level of ground shaking of the design earthquake. The SE has a mean return period of approximately 75 years. Damage in the nonstructural elements is expected during serviceability earthquake.

B. The design earthquake (DE)

The design earthquake (DE) is defined probabilistically as the level ground shaking that has a 10 percent chance of being exceeded in a 50-year period. The DE represents an infrequent level of ground shaking that can occur during the life of the building. The DE has a mean return period of approximately 475 years. Minor repairable damage in the primary lateral load carrying system is expected during design earthquake. For secondary elements, the damage may be such that they require replacement.

C. The maximum earthquake (ME)

The maximum earthquake (ME) is defined deterministically as the maximum level of earthquake ground shaking which may ever be accepted at the building site within the

known geologic frame work. The maximum earthquake (ME); 5% chance of being exceeded in 50 years.

As per draft BNBC-2017, maximum considered earthquake (MCE) motion may be considered to correspond to having a 2% probability of exceedance within a period of 50 years. The country has been divided into four seismic zones with different levels of ground motion with peak ground acceleration (PGA) on very stiff soil/ rock (site class SA) in units of g (acceleration due to gravity). The zone coefficients (Z) of the four zones are: Z=0.12 (Zone 1), Z=0.20 (Zone 2), Z=0.28 (Zone 3) and Z=0.36 (Zone 4).
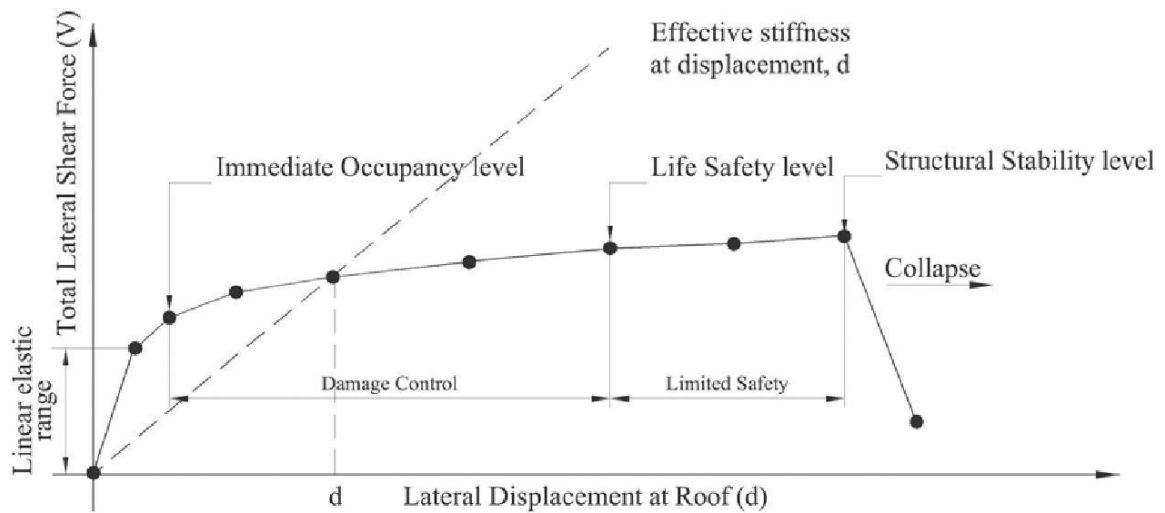
Figure 2.1: Typical capacity curve considering the performance level (ATC-40)

In Fig. 2.1, the discrete points indicated by the symbol '•'represent the occurrence of important events in the lateral response history of the structure. Such an event may be the initiation of yield in a particulars structural element or a particular type of damage. Each point is determined by a different analysis sequence. Then, by evaluating the cumulative effects of damage sustained at each of the individual events, and the overall behavior of the structure's increasing lateral displacements, it is possible to determine and indicate on the capacity curve those total structural lateral displacements that represent limits on the various structural performance levels, as has been done in Fig. 2.1.

2.6 ADRS curve

The capacity spectrum method, a nonlinear static procedure, provides a graphical representation of the global force-displacement capacity curve of the structure (i.e. pushover curve) and compares it to the response spectra representations of the earthquake

demands. This method is a very useful tool in the evaluation and retrofit design of concrete structures. The graphical representation provides a clear picture of how a structure responds to earthquake ground motion, and, as illustrated below, it provides an immediate and clear picture of how various retrofit strategies, such as adding stiffness or strength, will affect the structure response to earthquake demands The capacity spectrum curve for the structure is obtained by transforming the capacity curve from lateral force (V) vs. lateral displacement (d) coordinates to spectral acceleration (Sa) vs. spectral displacement (Sd) coordinates using the modal shape vectors, participation factors and modal masses obtained from a modal analysis of the structure. In order to compare the structure's capacity to the earthquake demand, it is required to plot the response spectrum and the capacity spectrum on the same plot. The conventional response spectrum plotted in spectral acceleration vs. period coordinate has to be changed in to spectral acceleration vs. spectral displacement coordinate. This form of response spectrum is known as acceleration displacement response spectrum (ADRS). Capacity spectrum method requires plotting the capacity curve in spectral acceleration and spectral displacement domain. This representation of spectral quantities is knows as Acceleration displacement response spectra in brief ADRS, which was introduced by Mahaney et al. (1993). Spectral quantities like spectral acceleration, spectral displacement and spectral velocity is related to each other to a specific structural period T. Building code usually provide response spectrum in spectral acceleration vs. period format which is the conventional format. Each point on the curve defined in Fig. 2.2 is related to spectral displacement by mathematical relation, $S_d = (1/4\pi^2)$ Sa*T^2 Converting with this relation response spectrum in ADRS format may be obtained.
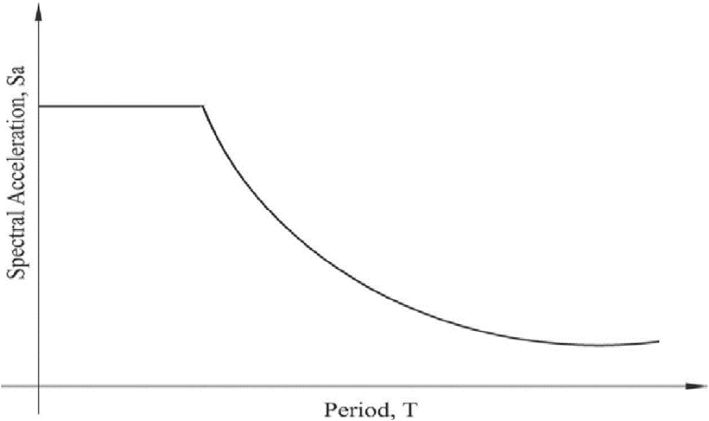
Figure 2.2: Code specified response spectrum in Spectral acceleration vs. Period. (ATC-40)
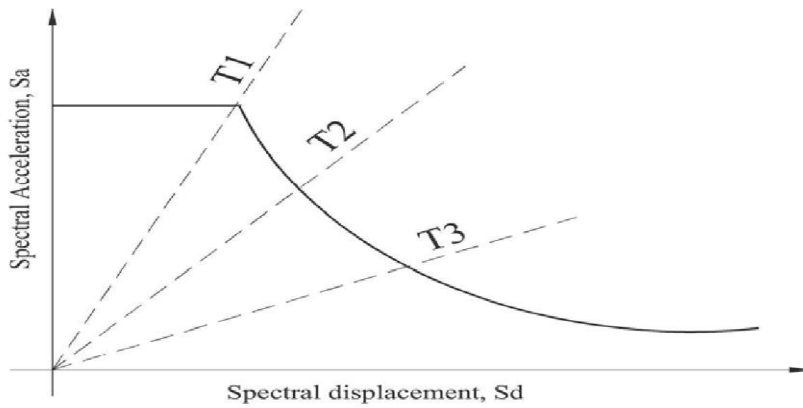
Figure 2.3: Response spectrum in ADRS format (ATC-40)

T1= Time Period at ½ Second

T2= Time Period at 1 Second

T3= Time Period at 2 Second

Any line from the origin of the ADRS format represent a constant period Ti which is related to spectral acceleration and spectral displacement by the mathematical relation,

$T=2\pi\sqrt{(Sd/Sa)}$

Capacity Spectrum Capacity spectrum is a simple representation of capacity curve in ADRS domain. A capacity curve shown in Fig. 2.3 is the representation of base shear (V) to roof displacement (d). In order to develop the capacity spectrum from a capacity curve it is necessary to do a point by point conversion to first mode spectral coordinates.
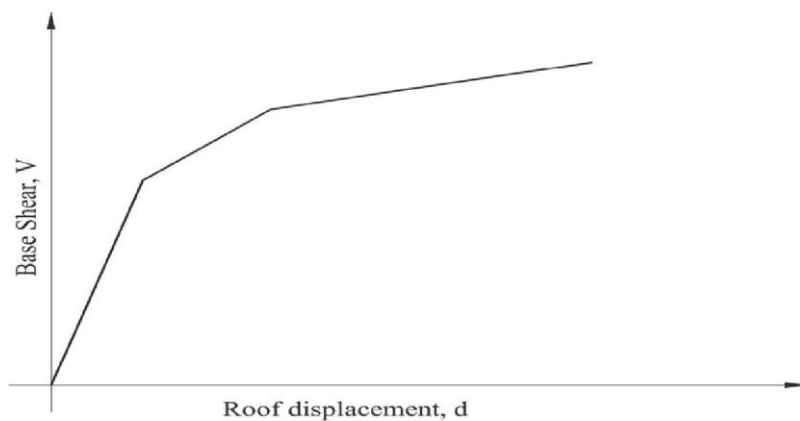
Figure 2.4: A typical capacity curve (ATC-40)

Any point corresponding values of base shear, Vi and roof deflection, Δi may be converted to the corresponding point of spectral acceleration, Sai and spectral displacement, Sdi on the capacity spectrum using relation,

$S_{ai} = (V_i/W)/\alpha_1$

$S_{di} = \Delta_{Roof}/(PF_1 \times \phi_{1,Roof})$

$$PF_1 = \left[\frac{\sum\limits_{1}^{N}(w_i\phi_{i,1})/g}{\sum\limits_{1}^{N}(w_i\phi^2_{i,1})/g} \right]$$

Modal mass coefficient for the   first mode, α_1 is calculated using equation,

$$\alpha_1 = \frac{\left[\sum\limits_{1}^{N}(w_i\phi_{i,1})/g\right]^2}{\left[\sum\limits_{1}^{N}w_i/g\right]\left[\sum\limits_{1}^{N}(w_i\phi^2_{i,1})/g\right]}$$

Where

PF1   =   modal participation factor for the first natural mode.

α1   =   modal mass coefficient for the first natural mode

Φ1,
roof   =   roof level amplitude of the first mode.

wi/g   =   mass assigned to level i

Φi1   =   amplitude of mode 1 at level i

 N= level N, the level which is the uppermost in the main portion of the structure

V= base shear

W= building dead weight plus likely live loads
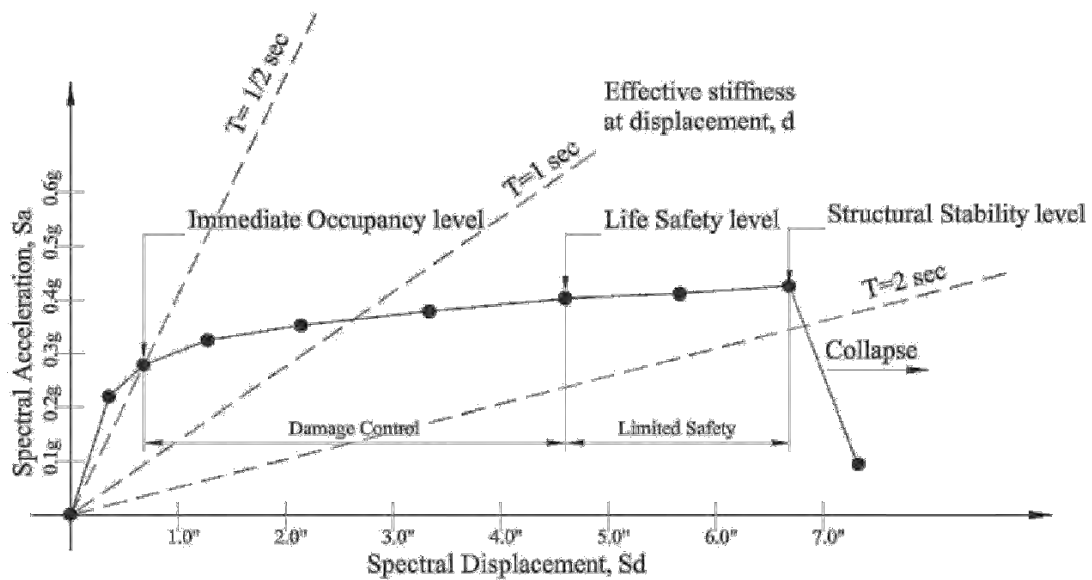
Figure 2.5: Capacity spectrum (ATC-40)

Δroof=   roof displacement

Sa   =   spectral acceleration

Sd   =   spectral displacement

where, ω is the radial frequency of the effective (or secant) first-mode response of the structure if pushed by an earthquake to that spectral displacement.

Using the relationship $T=2\pi/\omega$, it is possible to calculate, for each of these radial lines, the effective period of the structure if it is pushed to a given spectral displacement

Fig. 2.4 shows a typical capacity spectrum converted from capacity curve of Fig. 2.3 of a typical structure. It is seen in the capacity spectrum that up to some displacement corresponding to point A, the period is constant T_1. That is the structure is behaving elastically. As the structure deflects more to point B, it goes to inelastic deformation and its period lengthens to T_2.

When the capacity curve is plotted in Sa vs. Sd coordinates, radial lines drawn from the origin of the plot through the curve at various spectral displacements have a slope (ω),

The capacity spectrum method initially characterizes seismic demand using an elastic response spectrum. This spectrum is plotted in spectral ordinates (ADRS) format showing the spectral acceleration as a function of spectral displacement.

2.7 Nonlinear analysis and demand capacity curve

Inelastic behavior is intended in most structures subjected to infrequent earthquake loading, the use of nonlinear analyses is essential to capture behavior of structures under seismic effect. Nonlinear static procedures (NSP) for the seismic assessment of existing structures (or design verification of new ones) has gained considerable popularity in recent years, backed by a large number of extensive verification studies that have demonstrated its relatively good accuracy in estimating the seismic response of buildings. Due to its simplicity, the structural engineers has been using the nonlinear static procedure or pushover analysis. Static pushover approach is based on applying the lateral–load distribution pattern prescribed by the seismic code. The pushover analysis is performed by using a step-by-step displacement-controlled technique until the structure reached a predetermined level of maximum lateral deformation. Modeling for such analysis requires the determination of the nonlinear properties of each component in the structure, quantified by strength and deformation capacities, which depend on the modeling assumptions. Pushover analysis is carried out for either user-defined nonlinear hinge properties or default hinge properties, available in some programs based on the ASCE 41-13, FEMA-356 and ATC-40 guidelines.

The NSPs may be divided into following two main categories:

The first category of NSPs consists on Capacity Spectrum Method (CSM), suggested by Freeman and coworkers (1975 and 1998) and implemented in ATC-40 guidelines (1996). Since inelastic behavior is intended in most structures subjected to infrequent earthquake loading, the use of nonlinear analyses is essential to capture behavior of structures under seismic effects. The employment of Nonlinear Static Procedures (NSP) in the seismic assessment of existing structures (or design verification of new ones) has gained considerable popularity in the recent years, backed by a large number of extensive verification studies that have demonstrated its relatively good accuracy in estimating the seismic response of buildings.

Due to its simplicity, the structural engineering profession has been using the nonlinear static procedure (NSP) or pushover analysis. Modeling for such analysis requires the determination of the nonlinear properties of each component in the structure, quantified by strength and deformation capacities, which depend on the modeling assumptions. Pushover analysis is carried out for either user-defined nonlinear hinge properties or

default-hinge properties, available in some programs based on the FEMA-356 and ATC-40 guidelines introducing the Adaptive Capacity Spectrum Method (ACSM). In (ACSM) method basically consists of having a structural model with nonlinear material properties displaced to a target displacement under monotonically increasing lateral loading. The output of such an analysis is the demand in different structural elements, which is compared with their related capacities. Thus, it represents a relatively simple alternative to estimate the nonlinear behavior of structures. All of them present improvements with respect to their predecessors, such as the inclusion of higher modes contribution and the consideration of progressive damage. In this study capacity spectrum method (CSM) is used because it gives a visual representation of capacity-demand equation, suggests possible remedial action if the equation is not satisfied and easily incorporates several limit states, expressed as station on the load displacement curve of the structure. Another procedure for calculating demand displacement is 'Displacement Coefficient Method' which provides a direct numerical process for calculating the displacement demand. Displacement Coefficient Method has not been explored. Performance analysis of the structures under this thesis was made using Capacity Spectrum Method.

2.8 Seismic performance evaluation

The essence of virtually all seismic evaluation procedures is a comparison between some measures of the "demand" that earthquake place on structure to a measure of the "capacity" of the building to resist the induced effects. Traditional design procedures characterize demand and capacity as forces. Base shear (total horizontal force at the lowest level of the building) is the normal parameter that is used for this purpose. The base shear demand that would be generated by a given earthquake, or intensity of ground motion is calculated, and compares this to the base shear capacity of the building. If the building were subjected to a force equal to its base shear capacity some deformation and yielding might occur in some structural elements, but the building would not collapse or reach an otherwise undesirable overall level of damage. If the demand generated by the earthquake is less than the capacity, then the design is deemed acceptable.

2.9 Nonlinear static procedure for capacity evaluation of structures

Instead of comparing forces, nonlinear static procedures use displacements to compare seismic demand to the capacity of a structure. This approach included consideration of

the ductility of the structure on an element by element basis. The inelastic capacity of a building is then a measure of its ability to dissipate earthquake energy. The current trend in seismic analysis is toward these simplified inelastic procedures.

The recommended central methodology is on the formulation of inelastic capacity curve for the structure. This curve is a plot of the horizontal movement of a structure as it is pushed to one side. Initially the plot is a straight line as the structure moves linearly. As the parts of the structure yield, the plot begins to curve as the structure softens. This curve is generated by building a model of the entire structure from nonlinear representations of all of its elements and components. Most often this is accomplished with a computer and structural analysis software.

All structural actions may be classified as either deformation controlled or force-controlled using the component force versus deformation curves shown in Fig. 2.6 The Type 1 curve depicted in Fig. 2.5 is representative of ductile behavior where there is an elastic range (point 0 to point 1 on the curve) followed by a plastic range (points 1 to 3) with non-negligible residual strength and ability to support gravity loads at point 3. The plastic range includes a strain hardening or softening range (points 1 to 2) and a strength-degraded range (points 2 to 3).
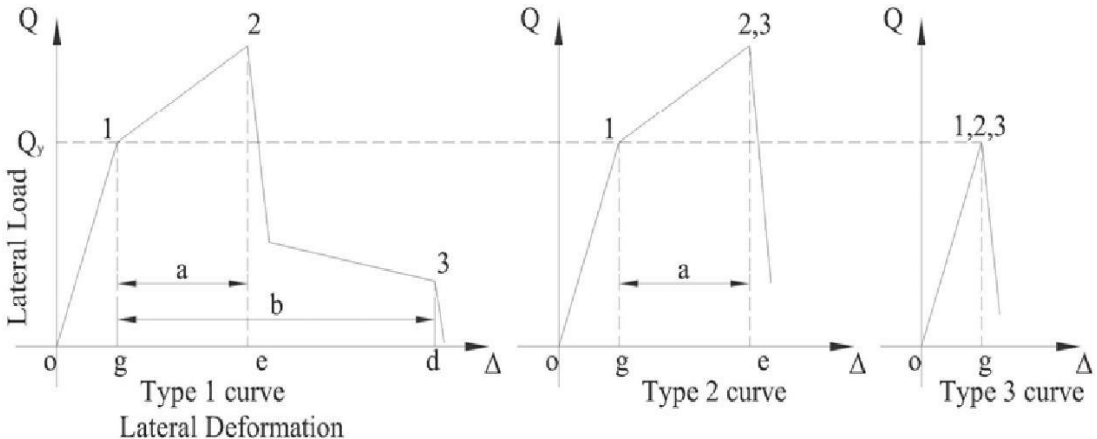
Figure 2.6: Component force versus deformation curves (FEMA-356)

Primary component actions exhibiting this behavior shall be classified as deformation-controlled if the strain-hardening or strain-softening range is such that e > 2g; otherwise,

they shall be classified as force controlled. Secondary component actions exhibiting Type 1 behavior shall be classified as deformation-controlled for any e/g ratio. The Type 2 curve depicted in Fig. 2.5 is representative of ductile behavior where there is an elastic range (point 0 to point 1 on the curve) and a plastic range (points 1 to 2) followed by loss of strength and loss of ability to support gravity loads beyond point 2. Primary and secondary component actions exhibiting this type of behavior shall be classified as deformation-controlled if the plastic range is such that e >2g; otherwise, they shall be classified as force controlled. Type 3 curve depicted in Fig. 2.5 is representative of a brittle or non-ductile behavior where there is an elastic range (point 0 to point 1 on the curve) followed by loss of strength and loss of ability to support gravity loads beyond point1. Primary and secondary component actions displaying Type 3 behavior shall be classified as force-controlled (FEMA-356).

Acceptance criteria for primary components that exhibit Type 1 behavior are typically within the elastic or plastic ranges between points 0 and 2, depending on the performance level. Acceptance criteria for secondary elements that exhibit Type 1 behavior can be within any of the performance ranges. Acceptance criteria for primary and secondary components exhibiting Type 2 behavior will be within the elastic or plastic ranges, depending on the performance level. Acceptance criteria for primary and secondary components exhibiting Type 3 behavior will always be within the elastic range. Figure 2.5 provides some examples of possible deformation- and force-controlled actions in common framing systems.

2.10 Acceptability limit

A given component may have a combination of both force and deformation controlled actions. Each element must be checked to determine whether its individual components satisfy acceptability requirements under performance point forces and deformations. Together with the global requirements, acceptability limits for individual components are the main criteria for assessing the calculated building response.
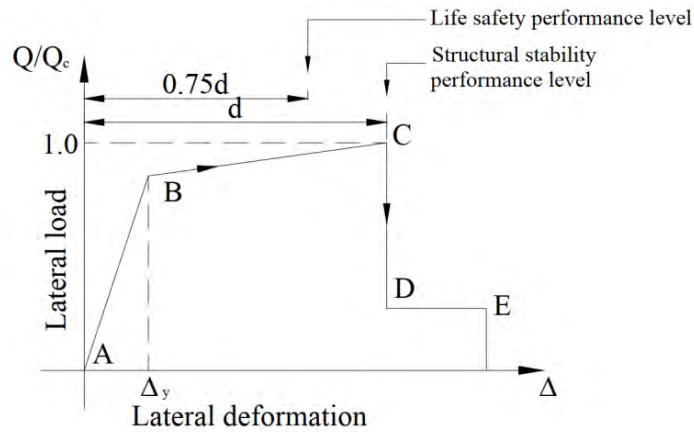
Figure 2.7: Force deformation action and acceptance criteria (ATC-40)

Fig. 2.6 shows a generalized load deformation relation appropriate for most concrete components. The relation is described by linear response from A (unloaded component) to an effective yield point B, linear response at reduced stiffness from B to C, sudden reduction in lateral load resistance to D, response at reduced resistance to E, and final loss of resistance thereafter. The following main points relate to the depicted load-deformation relation:

Point A corresponds to the unloaded condition. The analysis must recognize that gravity loads may induce initial forces and deformations that should be accounted for in the model. Therefore, lateral loading may commence at a point other than the origin of the load-deformation relation.

Point B has resistance equal to the nominal yield strength. The slope from B to C, ignoring the effects of gravity loads acting through lateral displacements, is usually taken as between 5% and 10% of the initial slope. This strain hardening, which is observed for most reinforced concrete component, may have an important effect on the redistribution of internal forces among adjacent components. The abscissa at C corresponding to the deformation at which significant strength degradation begins.

The drop in resistance from C to D represents initial failure of the component. The residual resistance from D to E may be non-zero in some cases and may be effectively zero in others. Where specific information is not available, the residual resistance usually may be assumed to be equal to 20% of the nominal strength. Point E is a point defining the maximum deformation capacity. Deformation beyond that limit is not permitted because gravity load can no longer be sustained.

2.11 Structural response reduction factor, R

Response reduction factors were first proposed by the Applied Technology Council (ATC) in the ATC 3-06 report published in 1978. The National Earthquake Hazard Reduction Program (NEHRP) provisions, first published in 1985, are based on the seismic design provisions set forth in ATC 3-06. Similar factors, modified to reflect the allowable stress design approach, were adopted in the Uniform Building Code (UBC) a decade late in 1988. The concept of response reduction factor, R was proposed based on the premise that well-detailed seismic framing systems could sustain large inelastic deformations without collapse (ductile behavior) and develop lateral strength in excess of their design strength (often termed as reserve strength). The R factor was assumed to represent the ratio of the forces that would develop under the specified ground motion if the framing system were to behave entirely elastically (termed hereafter as elastic design) to the prescribed design forces at the strength level (assumed equal to the significant yield level).

The commentary to the 1988 NEHRP provisions (BSSC, 1988) defines the R factor as an empirical response modification (reduction) factor intended to account for both damping and ductility inherent in a structural system at displacements great enough to approach the maximum displacement of the system. The components of R can be defined in several ways; each depends on the performance level under consideration. In this report only the life-safety performance level was considered explicitly.

A typical force-displacement relationship for a building frame is shown in Figure 2.7, which is used to estimate yield forces and yield displacement relationship.
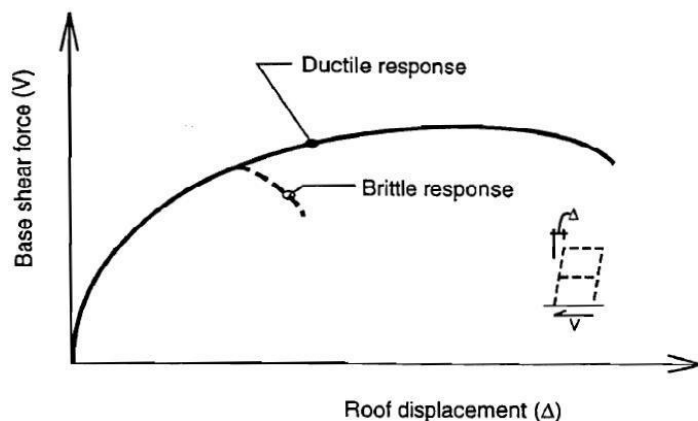
Figure 2.8: Sample base shear force versus roof displacement relationship (ATC 19)

Paulay and Priestley (1992) assumes a priori knowledge of the yielding strength, Vy of the frame. The elastic stiffness of the frame calculated from the force-displacement curve at the force corresponding to 0.75Vy. Elastic stiffness, K is defined as the slope of the idealized bilinear curve as shown in Figure 2.8(a).
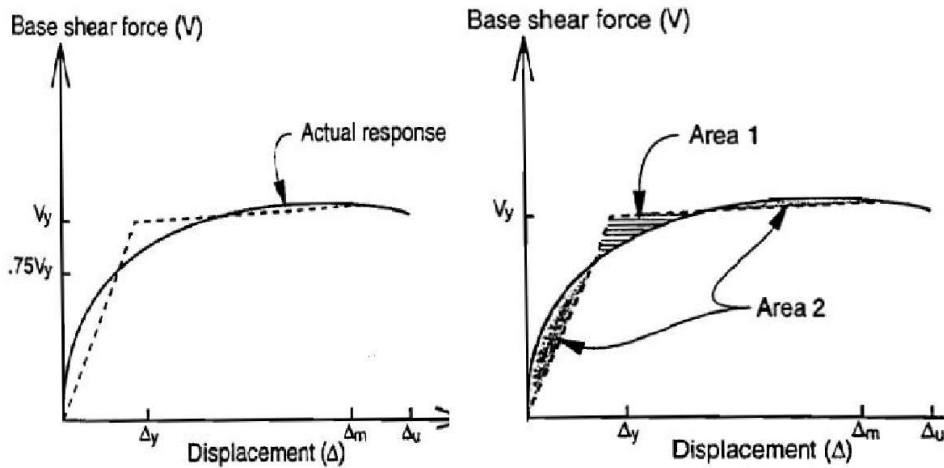
Figure 2.9: Bilinear approximations to a force-displacement relationship (ATC 19)

The second method, equal energy method, assumes that area enclosed by the curve above the bilinear approximation is equal to the area enclosed by the curve below the bilinear approximation illustrated in Fig 2.8 (b). Here, V_y = Yield force, Δ_y = yield displacement, V_0 = maximum force, Δ_m = displacement corrosponding to a limit state, Δ_u = displacement immediately prior to failure.

The ability of a building frame to be displaced beyond the elastic limit is termed as ductility. From Figure 2.8, displacement ductility is defined as the difference between Δ_m to Δ_y. Maximum displacement ductility is defined as the difference between Δ_u to Δ_y. displacement ductility ratio is defined as ratio of Δ_m to Δ_y namely $\mu_\Delta = \frac{\Delta m}{\Delta y}$.

In the mid-1980s, University of California at Berkeley researchers proposed splitting reduction factor R into three factors that account for contributions from reserve strength, ductility and viscous damping, as

$R = R_s \times R_\mu \times R_\zeta$

where, R_s = strength factor, R_μ = ductility factor and R_ζ = damping factor.

Figure 2.9 shows base shear vs. top displacement relationship curve to calculate response reduction factor R.

Researches (ATC 10; Freeman, 1990; ATC 19) have been conducted since the first formulation for R. A new formulation for R has been introduced in which R is expressed as the product of three factors:

$R = R_s R_\mu R_\zeta$

where, R_s = period dependent strength factor, R_μ = period dependent ductility factor and R_ζ = Damping factor, for 5% damping considered $R_\zeta = 1$,

Ductility factor, $R_\mu = \dfrac{Ve}{Vy}$

R_μ can also be estimated approximately from the structural ductility ratio (μ), the foundamental period of vibration (T) and the characteristics of earthquake. Here relationship proposed by Newmark and Hall (1982) to estimate R_μ, is used to in the present study.

R_μ = 1 for T < 0.2 s

$R_\mu = \sqrt{(2\mu- 1)}$ for 0.2 s < T < 0.5 s

$R_\mu = \mu$ for T > 0.5 s
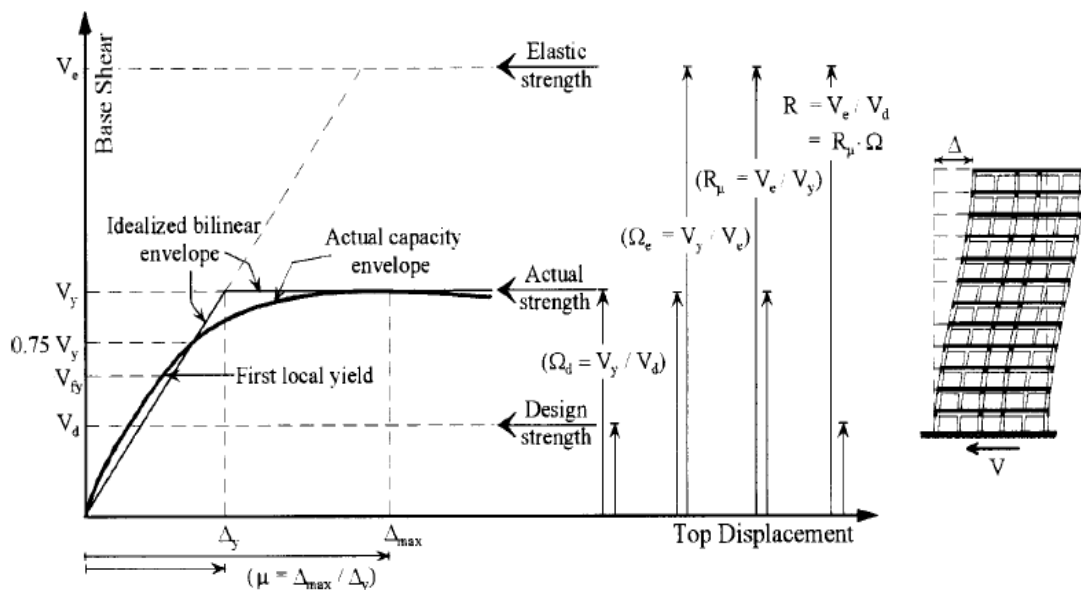
Figure 2.10: Base shear vs. top displacement relationship (Mwafy and Elnashai ,2002)

The structural ductility (μ) can be defined as:

$$\mu = \frac{\Delta max}{\Delta y}$$

The over strength factor (R_s) is defined as the ratio of the yield base shear (V_y) to the design base shear (V_d) as follows:

$$R_s = \frac{Vy}{Vd}$$

Finally, response reduction factor, $R = R_s \times R_\mu \times R_\zeta$

Table 2.3 shows damping factor for different percentage of damping as per UBC 1994 and Wu and Hanson method (1989).

Table 2.3: Damping factor as a function of viscous damping (ATC 19)

Viscous damping (% of critical)	1994 UBC ($R\zeta$)	Wu and Hanson, ($R\zeta$) 1989
2	0.80	-
5	1.00	1.00
7	-	-
10	1.20	1.19
12	-	-
15	-	1.39
20	1.50	1.56

2.12 Determination of target displacement (BNBC-2.5.12.3)

The displacement coefficient method provides a direct numerical process for calculating the displacement demand. The following step-by-step process is excerpted from FEMA 273 Guidelines and ATC 40. This excerpt refers to the target displacement which is the same as the performance point.

Target displacement, $\delta t = C_0 C_1 C_2 C_3 S_a \left(\frac{Te}{2\Pi}\right)^2 g$ and $Te = Ti\sqrt{\left(\frac{Ki}{Ke}\right)}$

T_e = effective fundamental period of the building in the direction under consideration,

T_i = elastic fundamental period (in seconds) in the direction under consideration calculated by elastic dynamic analysis

K_i = elastic lateral stiffness of the building in the direction under consideration

K_e = effective lateral stiffness of the building in the direction under consideration

C_0 = modification factor to relate spectral displacement and likely building roof displacement

Estimates of C_0 can be calculated using one of the following:

- The first modal participation factor at the level of the control node
- The modal participation factor at the of the control node calculated using a shape vector corresponding to the deflected shape of the building at the target displacement

Table 2.4 shows value of C_0 which is dependent on number of storey.

Table 2.4: Values for modification factor C_0 (ATC 40)

No of Stories	Modification Factor, C_0
1	1.0
2	1.2
3	1.3
5	1.4
10+	1.5

Figure 2.11 shows a typical base shear versus roof displacement graph to calculate target displacement.
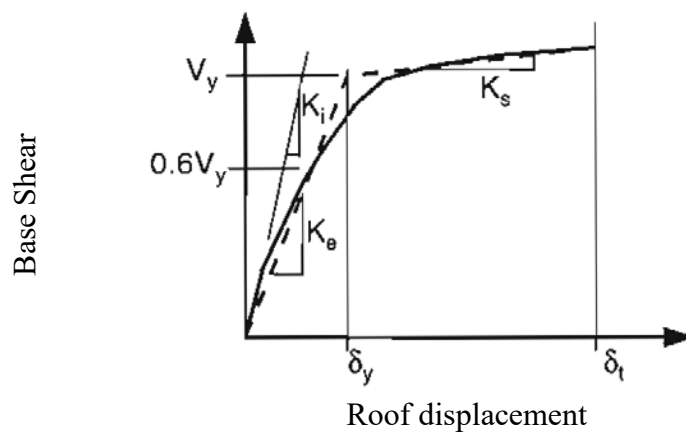
Figure 2.11: Bilinear representation of capacity curve for displacement co-efficient method (ATC 40)

C_1 = modification factor to relate expected maximum inelastic displacements to displacements calculated for linear elastic response = 1.0 for $T_e \geq T_0$

$= [1.0+(R-1) \; T_0/ \; T_e]/R$ for $T_e < T_0$

C_1 need not exceed 2.0 for Te <0.1 sec

T_0 = a characteristic period of the response spectrum, defined as the period associated with the transition from the constant segment of the spectrum to constant velocity segment of the spectrum.

Figure 2.12 shows spectral acceleration variation which is dependent on time.
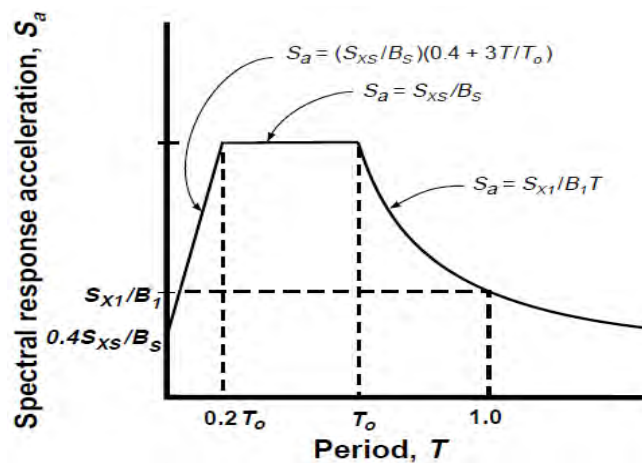
Figure 2.12: General response spectrum (FEMA 273)

where $T_0 = (S_{X1} \times B_S) / (S_{XS} \times B_1)$

Here, S_{XS} = Spectral response acceleration at short periods for any hazard level and any damping, g and S_{X1} = Spectral response acceleration at a one-second period for any hazard level and any damping, g

B_S = Coefficient used to adjust short period spectral response for the effect of viscous damping and B_1 = Coefficient used to adjust one-second period spectral response for the effect of viscous damping

B_S and B_1 are considered from Table 2.5

The damping coefficient should be based on linear interpolation for effective damping values other than those given.

For 5% damping Bs and B1 = 1.0

So $T_0 = (SX_1 / SX_S)$

$SX_1 = Fv \times S_1$ and $SX_S = Fa \times Ss$

Table 2.5: Damping coefficients Bs and B1 as a function of effective damping, β

Effective damping, β (percentage of critical)	*Bs*	*B1*
< 2	0.8	0.8
5	1.0	1.0
10	1.3	1.2
20	1.8	1.5
30	2.3	1.7
40	2.7	1.9
> 50	3.0	2.0

Spectral response acceleration parameter Ss and S1 for different seismic zone are mentioned at Table 2.6.

Table 2.6: Spectral response acceleration parameter Ss and S_1 for different Seismic Zone: (BNBC-2017)

Parameters	Zone - 1	Zone – 2	Zone - 3	Zone - 4
S_s	0.3	0.5	0.7	0.9
S_1	0.12	0.2	0.28	0.36

Site co-efficient Fa for different seismic zone and soil are mentioned at Table 2.7.

Table 2.7: Site co-efficient Fa for different seismic zone and soil (BNBC 2017)

Parameters	Zone - 1	Zone - 2	Zone – 3	Zone - 4
SA	1.0	1.0	1.0	1.0
SB	1.2	1.2	1.2	1.2
SC	1.15	1.15	1.15	1.15
SD	1.35	1.35	1.35	1.35
SE	1.4	1.4	1.4	1.4

Site co-efficient Fv for different seismic zone and soil are mentioned at Table 2.8.

Table 2.8: Site co-efficient Fv for different seismic zone and soil (BNBC 2017)

Parameters	Zone - 1	Zone - 2	Zone – 3	Zone - 4
SA	1.0	1.0	1.0	1.0
SB	1.5	1.5	1.5	1.5
SC	1.725	1.725	1.725	1.725
SD	2.7	2.7	2.7	2.7
SE	1.75	1.75	1.75	1.75

R = ratio of inelastic strength demand to calculated yield strength coefficient calculated as $R = \frac{Sa/g}{Vy/W} \times \frac{1}{Co}$

W= Seismic weight of the structure (dead load and participation of live load)

C_2 = modification factor to represent the effect of hysteresis shape on the maximum displacement response. Values of C_2 for different framing systems and performance levels are listed in Table 2.9

Table 2.9: Values for modification factor C_2 (ATC 40)

	T = 0.1 Second		$T \geq T_0$ Second	
Structural performance Level	Framing Type 1[1]	Framing Type 2[2]	Framing Type 1[1]	Framing Type 2[2]
Immediate Occupancy	1.0	1.0	1.0	1.0
Life safety	1.3	1.0	1.1	1.0
Collapse prevention	1.5	1.0	1.2	1.0

Note:

1: Structures in which more than 30 percent of the shear at any level is resisted by components or elements whose strength and stiffness may deteriorate during the design earth quake. Such elements include: ordinary moment resisting frames, concentrically-braced frames, frames with partially restrained connections, tension-only braced frames, unreinforced masonry walls, shear-critical walls and piers or any combination of the above

2. All frames not assigned to Framing Type 1.

C_3 = modification factor to represent increased displacements due to second order effects. For buildings with positive post-yield stiffness (Figure 2.13.a), C_3 shall be set equal to 1.0. for buildings with negative post-yield stiffness (Figure 2.13.b), C_3 shall be calculated as

$$C_3 = 1 + \frac{[\alpha](R-1)^{3/2}}{Te}$$

(a) Positive post yield slope (FEMA 356)
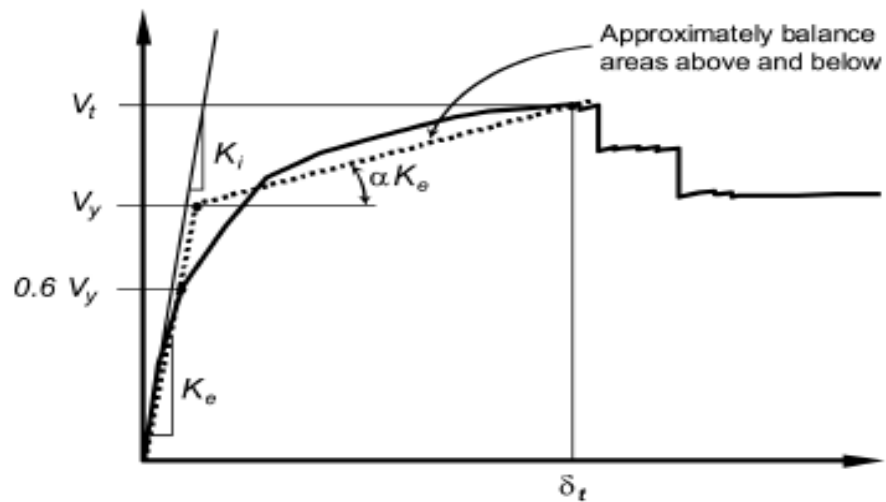
(b) Negative post yield slope
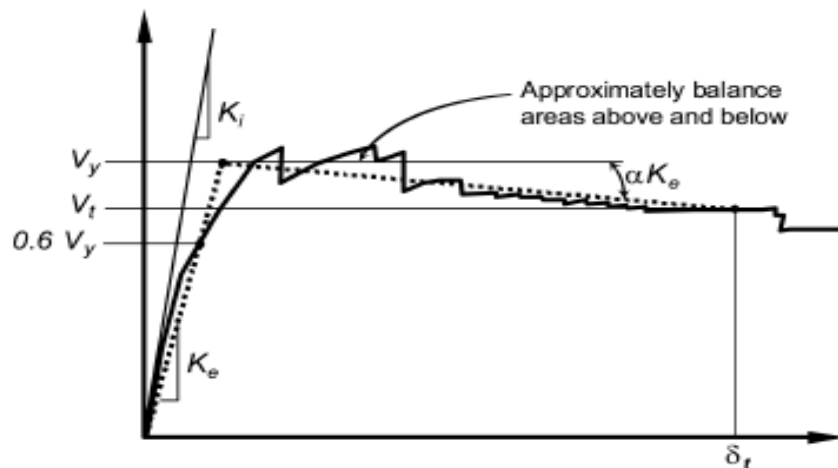
Figure 2.13 Idealized force-displacement curves (FEMA 356)

Where R and Te were defined above and α is the ratio of post-yield stiffness to elastic stiffness when the nonlinear force-displacement relation is characterized by a bilinear relation.

α = Ratio of post-yield stiffness to effective elastic stiffness, where the nonlinear force displacement relation is characterized by bilinear relation

S_a = Response spectrum acceleration, at the effective fundamental period, Te and damping ratio of the building in the direction under consideration, in g.

Vy = Yield strength calculated using the capacity curve.

2.13 Seismic Performance Level of RC Building

The seismic performance of structural systems under earthquake loading is no doubt an area requiring extensive research. In fact, many research bodies all over the world have been engaged in investigating the seismic response of various types of structural systems. In general, research on the seismic performance of structural systems can be classified into two groups: analytical research and experimental research. Because of innovation in the fields of electronics and the mechanics, the progress of those two groups of research has been remarkable.

For earthquake resistant design, evaluation of the seismic performance of buildings, it is essential to determine if an acceptable solution in terms of capacity and performance is achieved. The nonlinear static analysis (pushover analysis) is a promising tool for seismic performance evaluation of existing and new structures. Pushover analysis gives an estimate of seismic capacity of the structural system and its components based on its material characteristics and detailing of member dimensions. The method there by evaluates the seismic performance of the structure and quantifies its behaviour characteristics (strength, stiffness and deformation capacity) under design ground motion. This information can be used to check the specified performance criteria. Modelling the inelastic behaviour of the structural elements for different levels of performance is an important step towards performance evaluation of building. National Earthquake Hazards Reduction Program (NEHRP) guidelines for the seismic rehabilitation of buildings FEMA 273/356 require realistic values of the effective cracked stiffness of reinforced concrete (RC) members up to yielding for reliable estimation of the seismic force and deformation demands. Yielding consisting of two parts, namely; (i) linear elastic stiffness up to cracking and (ii) stiffness from cracking up to yielding, in the present study both of them are considered in the analysis. From different research, it

has been shown that linear elastic analysis with 5% damping can satisfactorily approximate inelastic seismic deformation demands.

Assessing the capacity of existing building as per the present codes of practice is an important task in seismic evaluation. In order to enhance the performance of existing buildings to the present level of ductile design prescribed by present codes and find the retrofit or design a rehabilitation system, there is an urgent need to assess accurately the actual lateral load resistance and the potential failure modes. Building performance of structural components in terms of target building performance levels are commonly studied with the nonlinear static analysis.

Pushover analysis is static nonlinear analysis carried out to develop capacity curve or pushover curve of the building (Fig. 2.14). It requires execution of nonlinear static analysis that allows monitoring progressive yielding of the structures. The building is subjected a lateral load. The load magnitude increase until the building reaches target displacement. This target displacement represents the top displacement when the building is subjected to design level ground excitation.
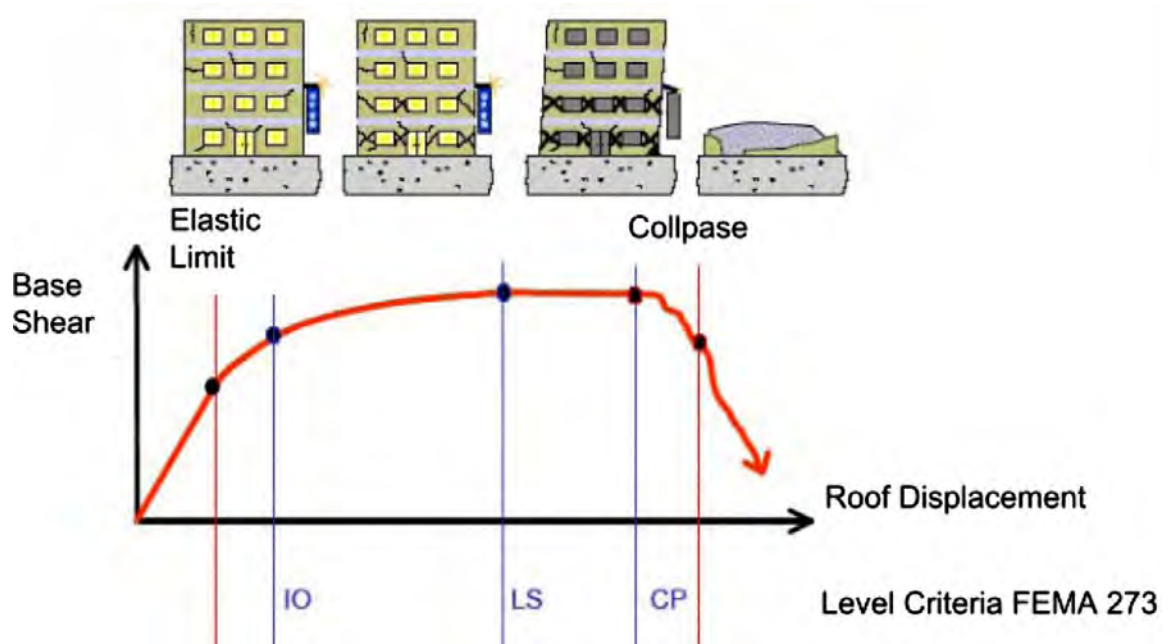
Figure 2.14 Seismic performance of RC building (Hakim et al. 2014)

2.14 Summary:

In this chapter, brief details of RC cracked and gross sections, code provisions, seismic performance assessment and nonlinear static analysis (pushover analysis) have been provided. The response reduction factor R is also discussed. It is observed that static nonlinear procedure can be effectively used to assess the seismic performance of RC buildings. The present research investigates the seismic responses of RC frame buildings analyzed and designed using the force-based design concept considering the gross/un-cracked section and effective/cracked section properties of RC members. The effective/cracked section property of the RC beams, slabs, and columns is considered as per the provisions of the upcoming BNBC-2017 (draft). The seismic performances of the RC frames designed using gross section and cracked section are evaluated using the nonlinear static (pushover) analysis. The seismic response reduction factor, R has been also evaluated considering RC cracked and gross section properties using nonlinear static or pushover analysis.

Chapter 3
NUMERICAL ANALYSIS

3.1 Introduction

An elastic analysis gives a good indication of the elastic response of structures, but it cannot predict failure mechanisms and account for redistribution of forces during an earthquake excitation. Inelastic analysis procedures help to demonstrate how buildings really response by identifying modes of failure. The use of inelastic procedures for design and evaluation is an approach that help engineers to understand better when the buildings will be subjected to major earthquakes. Application of this procedure resolves some of uncertainties associated with the code and elastic procedures. Details of structural modeling and all considerations of buildings for design and analysis have been described in this chapter. A comprehensive numerical analysis have been conducted for 6-, 10- and 15-storied buildings having the same plan configuration. Typical height of the floor is considered the same for all buildings and designated as M1 for 6-storied, M2 for 10-storied and M3 for 15-storied. Structural design of these buildings has been conducted first by using equivalent static analysis as per BNBC 2017 (draft) for seismic loads. Both the gross and cracked sections are considered for determining size and associated reinforcements for reinforced concrete structural elements. A nonlinear static or pushover analysis has been performed for all the buildings to assess the seismic performance.

3.2 Provisions for earthquake loads in BNBC

3.2.1 Design response spectrum

The earthquake ground motion for which the building has to be designed is represented by the design response spectrum. Both static and dynamic analysis methods are based on this response spectrum. This spectrum represents the spectral acceleration for which the building has to be designed as a function of the building period, taking into account the ground motion intensity. The spectrum is based on elastic analysis but in order to account for energy dissipation due to inelastic deformation and benefits of structural redundancy, the spectral accelerations are reduced by the response reduction factor R. For important structures, the spectral accelerations are increased by the importance factor I. The design basis earthquake (DBE) ground motion is selected at a ground shaking level that is 2/3 of the maximum considered earthquake (MCE) ground motion. The effect of local soil

conditions on the response spectrum is incorporated in the normalized acceleration response spectrum C_s. The spectral acceleration for the design earthquake is given by the following equation:

$$S_a = 2/3(ZI/R) \, C_s$$

Sa= Design spectral acceleration (in units of g which shall not be less than $0.67\beta ZIS$)

β = coefficient used to calculate lower bound for Sa. Recommend devalue for β is 0.11

Z=   Seismic zone coefficient

I=   Structure importance factor

R=   Response reduction factor

C_s = Normalized acceleration response spectrum, which is a function of structure (building) period and soil type (site class).

$$Cs = S[1 + T/T_B(2.5\eta - 1)] \quad \text{for } 0 \le T \le T_B$$

$$Cs = 2.5 S\eta \quad \text{for } T_B \le T \le T_C$$

$$Cs = 2.5 S\eta[T_C/T] \quad \text{for } T_C \le T \le T_D$$

$$Cs = 2.5 S\eta[T_C T_D /T^2] \quad \text{for } T_D \le T \le 4\text{sec}$$

C_s depends on S and values of T_B, T_C and T_D, (Figure 6.2.25, draft BNBC 2017) which are all functions of the site class.

S=   Soil factor which depends on site class and is given in Table 6.2.16

T=   Structure (building) period as defined in Sec2.5.7.2

T_B=   Lower limit of the period of the constant spectral acceleration branch given in Table 6.2.16 as a function of site class.

T_C=   Upper limit of the period of the constant spectral acceleration branch given in Table 6.2.16 as a function of site class

T_D=   Lower limit of the period of the constant spectral displacement branch given in Table 6.2.16 as a function of site class

η =   Damping correction factor as a function of damping with a reference value $\eta=1$ for 5% viscous damping.

3.2.2 Equivalent static force method

In this method, the dynamic earthquake effect is represented by an equivalent static load at different levels in proportion to mass at that level. Bangladesh is considered to be divided into four region of different possible earthquake ground response (0.12g, 0.20g, 0.28g and 0.36g) shown in Table 3.1 and Fig. 3.1.The seismic design base shear force, V in a given direction shall be determined from the following relation:

$$V = S_a W$$

Where,

S_a = Lateral seismic force coefficient calculated using Eq. 6.2.34 (Sec 2.5.4.3). It is the design spectral acceleration (in units of g) corresponding to the building period T (computed as per Sec 2.5.7.2).

W = Total seismic weight of the building defined in Sec 2.5.7.

Table 3.1: Seismic zone location and zone coefficient of BNBC-2017(draft)

Seismic Zone	Location	Seismic Intensity	Seismic Zone Coefficient, Z
1	Southwestern part including Barisal, Khulna, Jessore, Rajshahi	Low	0.12
2	Lower Central and Northwestern part including Noakhali, Dhaka, Pabna, Dinajpur, as well as Southwestern corner including Sunderbans	Moderate	0.20
3	Upper Central and Northwestern part including Brahmanbaria, Sirajgang, Rangpur	Severe	0.28
4	Northeastern part including Sylhet, Mymensingh, Kurigram	Very Severe	0.36

For different site classes SA to SE, the soil factor and different period limit of spectral acceleration mentioned at Table 3.2. Figure 3.2 shows typical shape of elastic response spectrum coefficient curve.
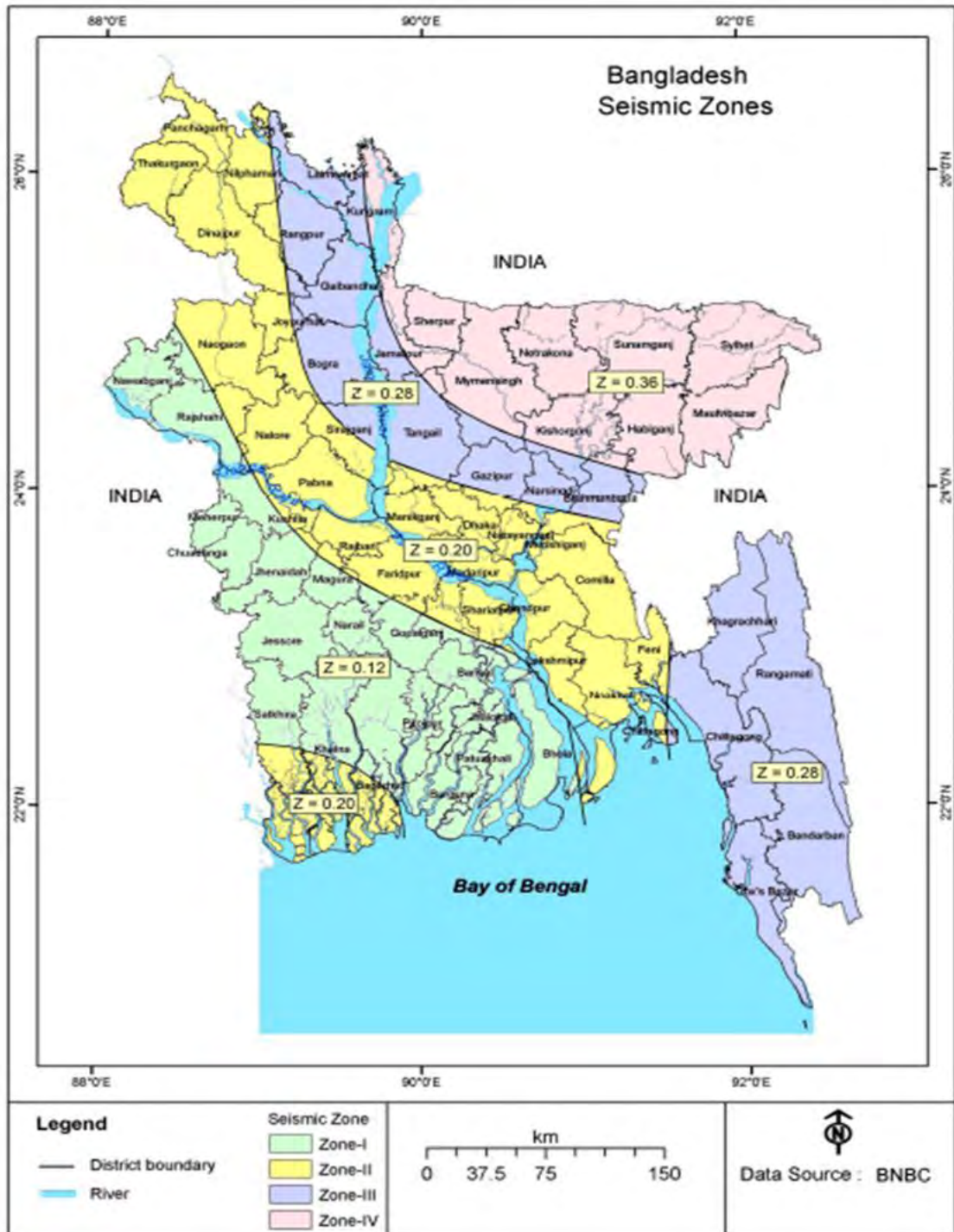
Figure 3.1: Seismic zoning map of Bangladesh

Table 3.2: Site dependent soil factor and other parameters defining elastic response spectrum

Soil type	S	T_B (S)	T_C (S)	T_D (S)
SA	1.0	0.15	0.4	2.0
SB	1.2	0.15	**0.5**	2.0
SC	1.15	0.20	0.6	2.0
SD	1.35	0.20	0.8	2.0
SE	1.4	0.15	0.50	2.0
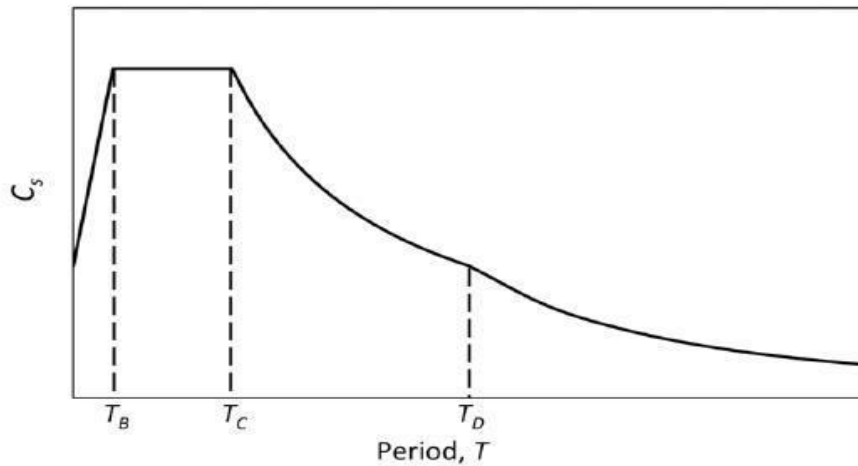
Figure 3.2: Typical shape of elastic response spectrum co-efficient, Cs (BNBC-2017 draft)

Figure 3.3 shows normalized design acceleration response spectrum for different site classes as per draft BNBC 2017. Response reduction factor, R which depends on the type of structural system is given in Table 6.2.19 of draft BNBC-2017.
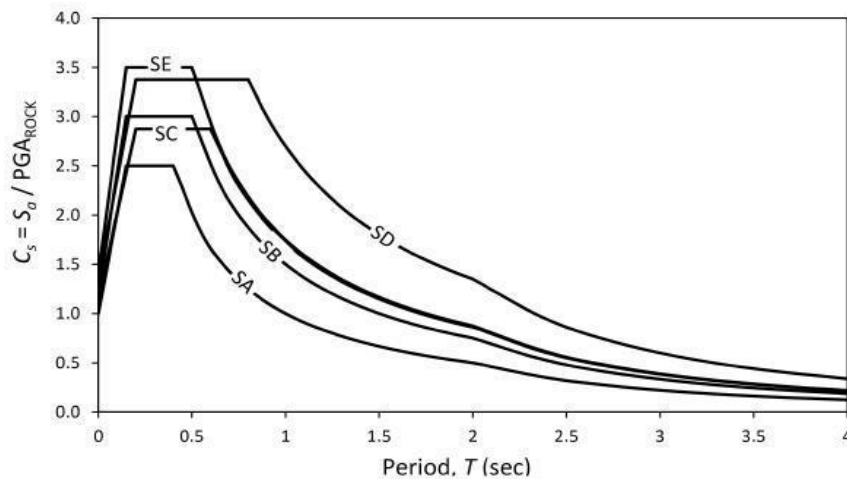
Figure 3.3: Normalized design acceleration response spectrum for different site class (BNBC-2017 draft)

3.2.3 Building period

The fundamental period, T of the building in the horizontal direction under consideration shall be determined using the following guidelines:

Structural dynamics procedures (such as Rayleigh method or modal eigenvalue analysis), using structural properties and deformation characteristics of resisting elements, may be used to determine the fundamental period T of the building in the direction under consideration. This period shall not exceed the approximate fundamental period determined by approximate period by more than 40 percent.

The building period T (in sec) may be approximated by the following formula:

$T = C_t (h_n)^m$

Where,

h_n = Height of building in metres from foundation or from top of rigid basement. This excludes the basement storeys, where basement walls are connected with the ground floor deck or fitted between the building columns. But it includes the basement storeys, when they are not so connected. C_t and m are obtained from Table 6.2.20, BNBC as shown in Table 3.3.

Table 3.3: Values for coefficients to estimate approximate period

Structure type	C_t	m	
Concrete moment-resisting frames	0.0466	0.9	Note: Consider moment resisting frames as frames which resist 100% of seismic force and are not enclosed or adjoined by components that are more rigid and will prevent the frames from deflecting under seismic forces.
Steel moment-resisting frames	0.0724	0.8	
Eccentrically braced steel frame	0.0731	0.75	
All other structural systems	0.0488	0.75	

3.2.4 Vertical distribution of lateral forces

In the absence of a more rigorous procedure, the total seismic lateral force at the base level, in other words the base shear V, shall be considered as the sum of lateral forces F_x induced at different floor levels, these forces may be calculated as:

$$F_x = V \times [Wx(hx)^k] / \sum_{i=1}^{n} W_i h_i^k$$

where,

F_x= part of base shear force included at level x

W_i and W_x = part of the total seismic weight of the structure (W) assigned to level i or x

h_i and h_x = the height from the base to level i or x

k =1 for structure period ≤ 0.5s

   =2 for structure period ≥ 2s

   = Linear interpolation between 1 and 2 for other periods

N= Number of stories

Storey shear and its horizontal distribution:

The design storey shear V_x, at any storey x is the sum of forces F_x in that storey and all the stories above it, given by the following equation,

$$Vx = \sum_{i=x}^{n} Fi$$

where, F_i = portion of base shear included at level i

3.3 Equivalent static analysis

Basic design considerations (materials properties, loading and load combinations etc.) and design outputs of linear static analysis have been discussed in the following sections.

3.3.1 Design considerations

Guidelines and considerations were followed from BNBC 2017 (draft) for structural analysis and design. Other necessary codes, standards, specifications like ACI 318-08, ASCE 7-10, ATC- 40 have been utilized as required in structural design and detailing.

3.3.2 Design data

Type of structure   : RC Moment Resisting Frame
Seismic zone   : II
Zone factor   : 0.2
Number of storey: M1 (G+5), M2(G+9), M3(G+14)
Typical floor height   : 3m
Ground floor height   : 3m

Periphery outside Infill wall   : 250 mm thick

Inside Wall: 125 mm thick

Live load   : 2.0 kN/m^2

Roof Live load: 1.0 kN/m^2

3.3.3 Description of building frame

No. of bays along X axis: 4

No. of bays along Y axis: 4

Spacing along X axis: 5m

Spacing along Y axis: 5m

No. of floors: M1 (G+5), M2 (G+9), M3 (G+14)

Table 3.4 shows various parameters to calculate seismic base shear force as per draft BNBC-2017.

Table 3.4: Seismic load consideration parameters (BNBC 2017)

`Seismic Zone (Z)	Table: 6.2.14, for Zone 2, Z = 0.20
Response reduction factor (R)	Table 6.2.19: for Building Frame Systems-moment Resisting Frame Systems (no shear wall), Intermediate Reinforced Concrete Moment Frames R=5
Structural importance factor (I)	Table 6.2.17: I = 1.0
Site co-efficient (S)	Table 6.2.16: for SC type soil, S = 1.15
Numerical co-efficient (C_t)	Table: 6.2.20, C_t = 0.0466 for h in meter, m = 0.9 for Concrete Moment Resisting Frame
Diaphragm eccentricity	0.05 times * width of the structure perpendicular to direction considered

To get structural behavior, column base supports have been considered as fixed supported for all the building models.

3.4 Load combinations from BNBC 2017: (Art 2.7.3.1)

Ultimate Strength Design (USD) method and loads and load combinations have been followed as per BNBC 2017 to check adequacy of all structural members. Following load combinations are considered for the design of all the building models. Since the seismic

response of these buildings are the prime focus, only the load combinations associated with gravity loads and seismic loads are considered.

1.2 DL + 1.6 LL

1.2 DL ±1.0 E+ 1.0 LL

0.9D ± 1.0E

where, DL = Dead load, LL=Live load,

E = total seismic load effect

From Art 2.5.13 of draft BNBC 2017: $E = E_h + E_v$

E_h = effect of horizontal seismic forces

E_v = effect of vertical seismic forces

$E_v = 0.50\ (a_h)\ D$

a_h = expected peak ground acceleration (in g) for design = (2/3) ZS for all the structures at Dhaka (zone-2), Z=0.2,

S=1.15 for Seismic Design Category C (SDC)

$E_v = 0.50 \times (2/3)\ ZS \times D = 0.5\ x\ (2/3) \times 0.2 \times 1.15\ D = 0.077\ D$

So, 1.2 D±1.0 E+ 1.0 L = 1.2 D ± 1.0 E_h+0.077 D+1.0 L = 1.277 D+1.0 L ± 1.0 E_h

From Art 2.5.13: $E = E_h - E_v$

0.9 D ± 1.0 E= 0.9 D ± 1.0 E_h - 0.077D = 0.823D± 1.0 E_h

Figure 3.4 shows the typical plan layout for 6-, 10- and 15-storied buildings. Column designation C1 is used for corner column, C2 for exterior and C3 for the interior columns of the building. Figures 3.5 to 3.7 show the elevation of 6-, 10- and 15-storied buildings, respectively. Figure 3.8 shows the typical beam layout for all the buildings.
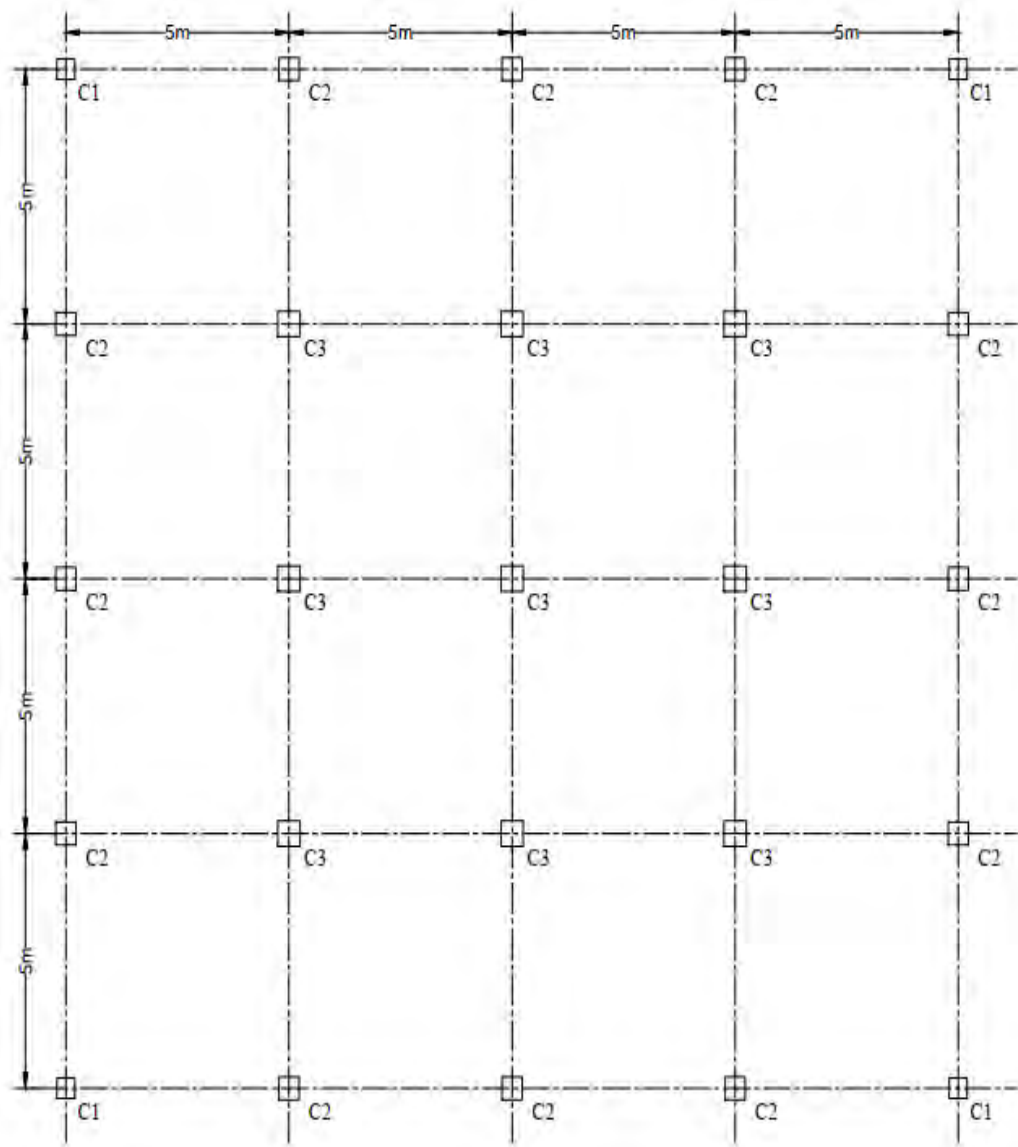
Figure 3.4: Typical plan for 6,10,15-storied RC buildings
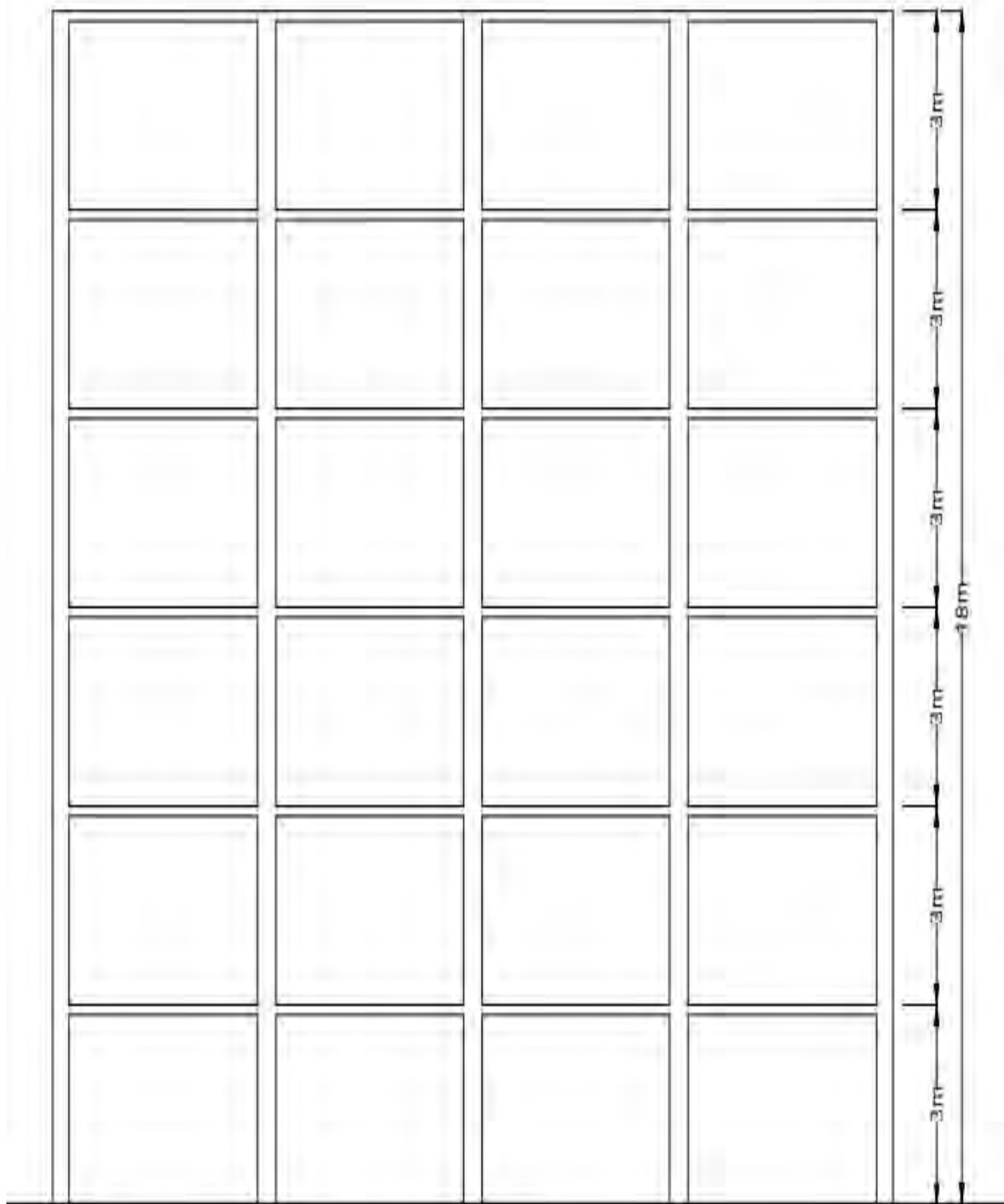
Figure 3.5: Elevation for 6-storied RC building
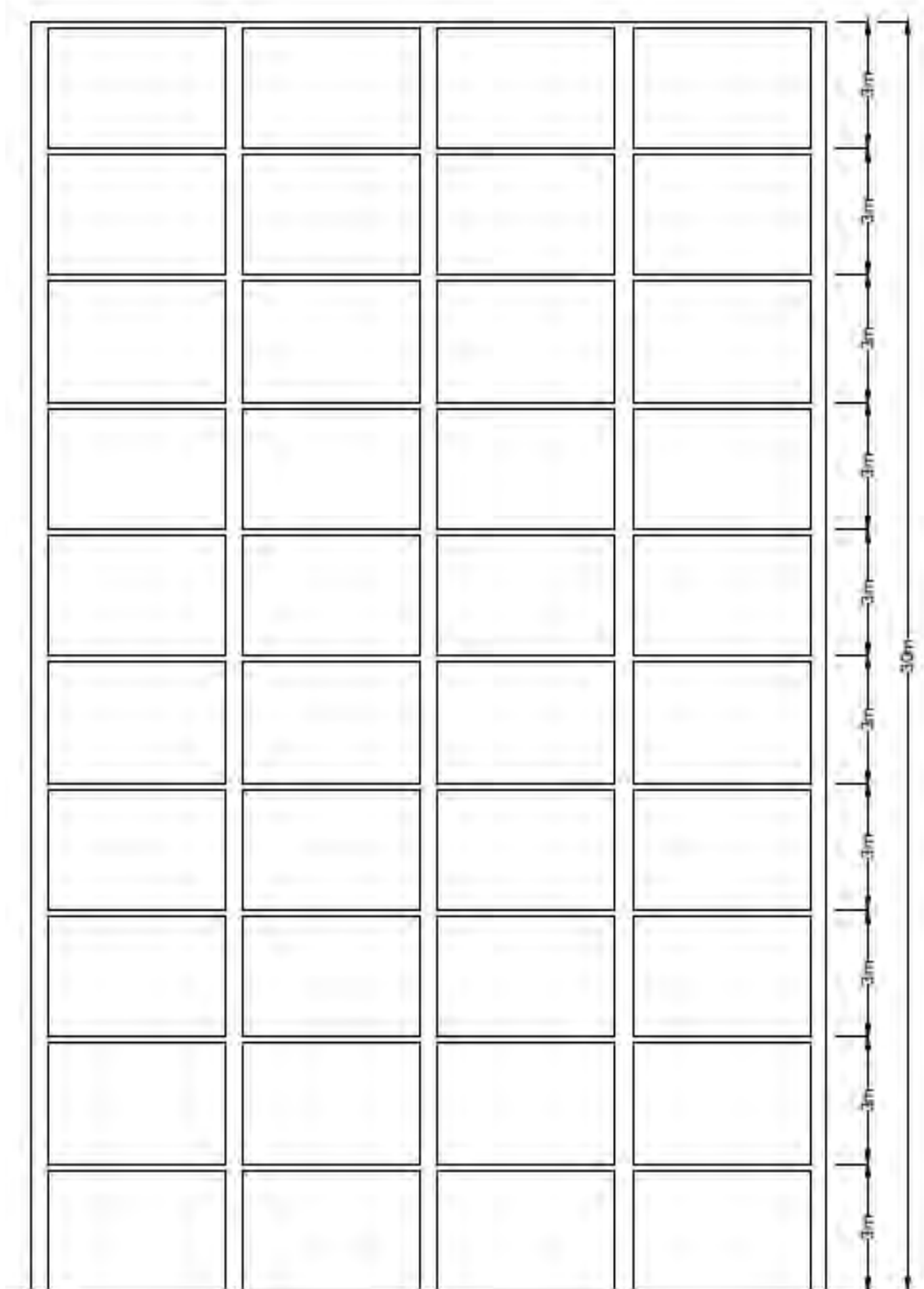
Figure 3.6: Elevation for 10-storied RC building
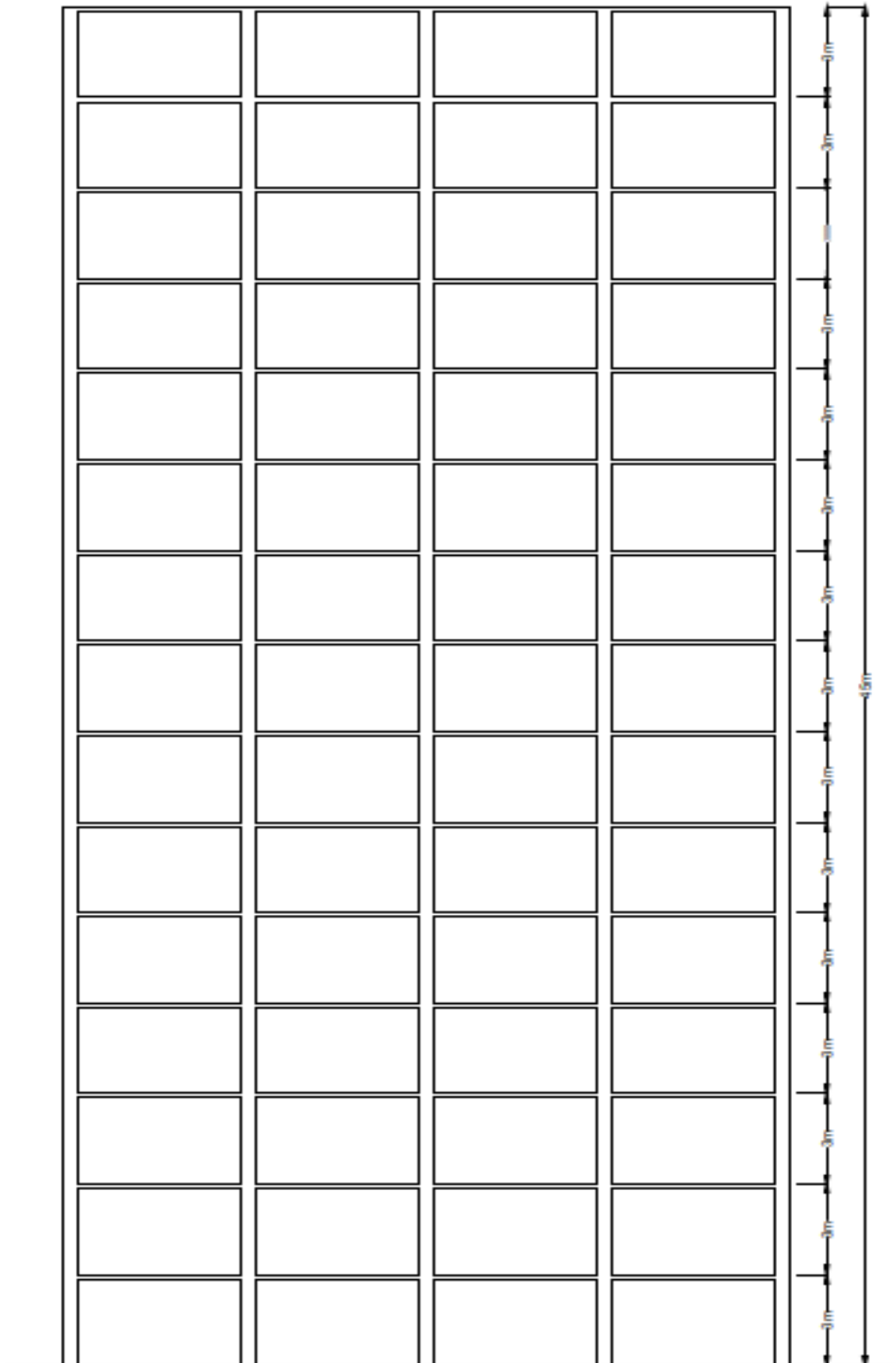
Figure 3.7: Elevation for 15-storied RC building
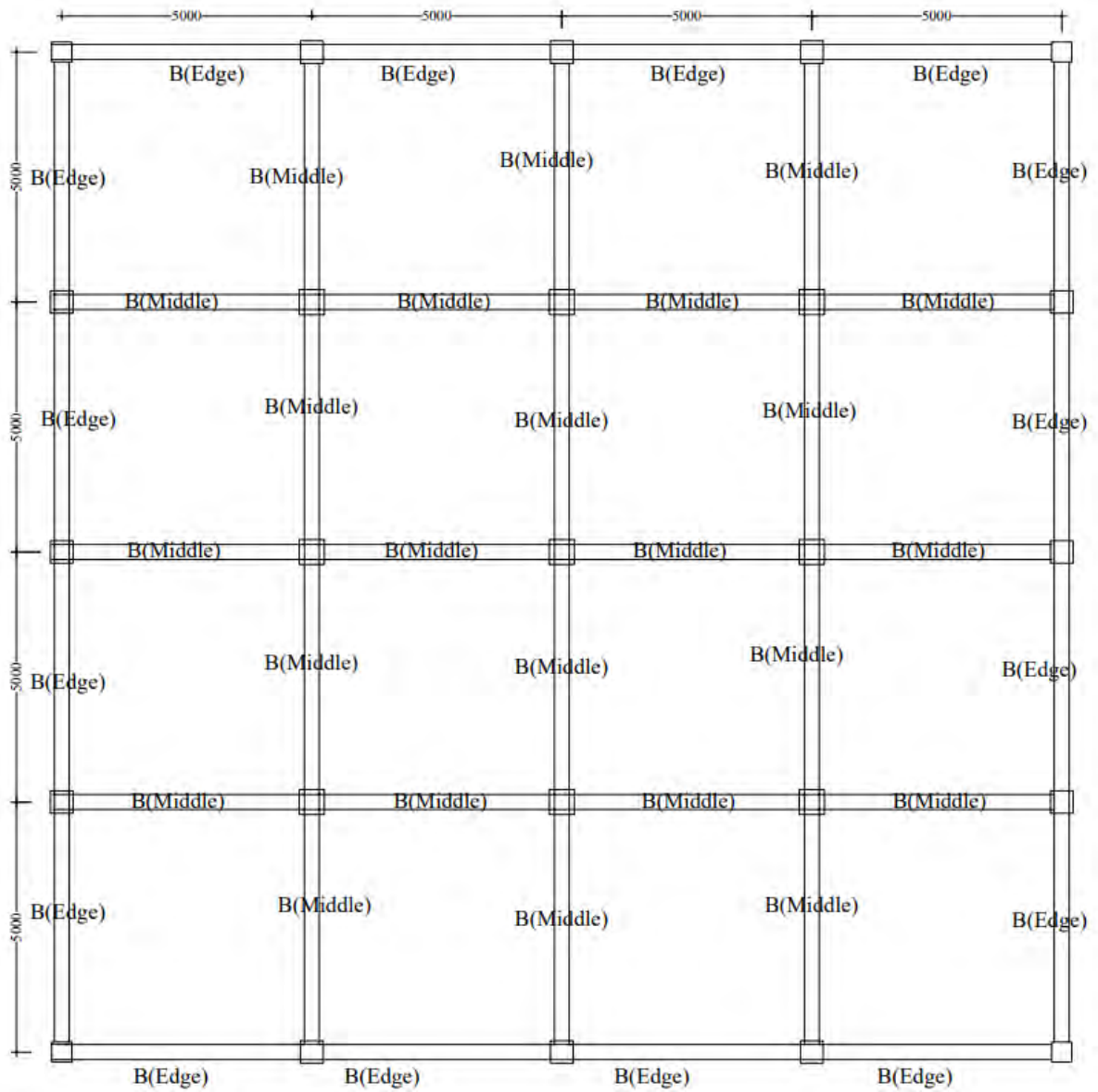
Figure 3.8: Typical beam layout for 6,10,15-storied RC buildings

Tables 3.5 to 3.7 present building details such as beam, column cross-sections and reinforcement details using gross and cracked sections.

Figures 3.9 to 3.11 show the three-dimensional (3D) view of the 6, 10, 15-storied RC buildings, respectively.

Table 3.5: Details of 6-storied RC building designed using gross and cracked sections

Members	Floor	Width (mm)	Depth (mm)	Reinforcement Gross section (mm^2)	Reinforcement Cracked section (mm^2)	% increase in reinf. for cracked section
Beam(Edge)	1-3	300	500	1075(top)	1104(top)	2.6%
				563(bot)	563(bot)	-
Beam(Edge)	4-6	300	500	777(top)	831(top)	6.5%
				443(bot)	443(bot)	-
Beam(Middle)	1-3	300	500	1255(top)	1255(top)	-
				611(bot)	611(bot)	-
Beam(Middle)	4-6	300	500	922(top)	922(top)	-
				443(bot)	443(bot)	-
Column (C1)	0-1	350	350	3165	4359	27.4%
Column (C1)	1-2	350	350	3218	4396	26.8%
Column (C1)	2-3	350	350	2116	2687	21.3%
Column (C1)	3-4	350	350	1323	1771	25.3%
Column (C1)	4-6	350	350	1225	1225	-
Column (C2)	0-1	400	400	4945	6347	22.1%
Column(C2)	1-2	400	400	3387	4466	24.2%
Column (C2)	2-3	400	400	2000	2382	16%
Column (C2)	3-6	400	400	1600	1600	-
Column(C3)	0-1	450	450	6535	7831	16.5%
Column(C3)	1-2	450	450	2854	2888	1.2%
Column(C3)	2-6	450	450	2025	2025	-

Table 3.6: Details of 10-storied RC building designed using gross and cracked sections

Members	Floor	Width (mm)	Depth (mm)	Reinforcement Gross section (mm^2)	Reinforcement Cracked section (mm^2)	% increase in reinf. for cracked section
Beam (Edge)	1–5	300	550	1114(top)	1125(top)	---
				669(bot)	669(bot)	---
Beam (Edge)	6–10	300	550	895(top)	915(top)	-
				493(bot)	493(bot)	-
Beam (Middle)	1–5	300	550	1100(top)	1100(top)	-
				775(bot)	775(bot)	-
Beam (Middle)	6–10	300	550	938(top)	938(top)	-
				582(bot)	582(bot)	-
Column (C2)	0-1	450	450	8469	9510	10.9%
Column (C2)	1-2	450	450	6295	6812	7.6%
Column (C2)	2-3	450	450	4071	4172	2.4%
Column(C2)	3-4	450	450	2566	2566	-
Column (C2)	4-10	450	450	2025	2025	-
Column (C3)	0-1	500	500	10279	11444	10.2%
Column(C3)	1-2	500	500	6838	7107	3.8%
Column(C3)	2-3	500	500	4506	4506	-
Column(C3)	3-4	500	500	2512	2512	-
Column (C1)	1-2	400	400	4231	4766	11.2%
Column (C1)	2-3	400	400	3049	3339	8.7%
Column (C1)	3-4	400	400	1936	2108	8.2%
Column(C1)	4-10	400	400	1652	1652	-

Table 3.7: Details of 15-storied RC building designed using gross and cracked sections

Members	Floor	Width (mm)	Depth (mm)	Reinforcement Gross section (mm^2)	Reinforcement Cracked section (mm^2)	% increase in reinf. for cracked section
Beam(Edge)	1-10	300	600	1155(top)	1186(top)	2.6%
				709(bot)	711(bot)	0.3%
Beam(Edge)	10-13	300	600	896(top)	896(top)	-
				5463bot)	543(bot)	-
Beam(Edge)	14-15	300	600	543(top)	543(top)	-
				207(bot)	207bot)	-
Beam(Middle)	1-10	300	600	1261(top)	1261(top)	-
				711(bot)	711(bot)	-
Beam(Middle)	11-13	300	600	985(top)	985(top)	-
				543(bot)	543(bot)	-
Beam(Middle)	14-15	300	600	549(top)	549(top)	-
				238(bot)	238(bot)	-
Column(C1)	0-1	500	500	7583	8442	10.2%
Column(C1)	1-2	450	450	6818	7516	9.3%
Column(C1)	2-3	450	450	5330	5711	6.7%
Column(C1)	3-4	450	450	4116	4502	8.2%
Column(C1)	4-5	450	450	2830	3146	8.6%
Column(C1)	5-15	450	450	2025	2025	-
Column(C2)	0-1	600	600	11885	12815	4.4%
Column(C2)	1-2	550	550	9047	9466	4.4%
Column(C2)	2-3	550	550	7187	7187	-
Column(C2)	3-4	550	550	5345	5345	-
Column(C2)	4-5	550	550	3593	3593	-
Column(C2)	5-15	550	550	3025	3025	-
Column(C3)	0-1	650	650	13319	14723	9.5%
Column(C3)	1-2	600	600	9977	10162	1.8%
Column(C3)	2-3	600	600	8005	8046	0.5%
Column(C3)	3-4	600	600	6035	6035	-
Column(C3)	4-5	600	600	4117	4117	-
Column(C3)	5-15	600	600	3600	3600	-

3.5 Design outputs

Structural analysis and design of buildings considering the same framing system but different no. of floors (height) have been performed using equivalent static analysis and ultimate strength design method as per BNBC 2017 guidelines. From Tables 3.5 to 3.7, it is shown that reinforcement demand for cracked section RC columns are usually higher than those with gross-section properties. For beams, this reinforcements' demand are comparable when gross and cracked sections are considered.
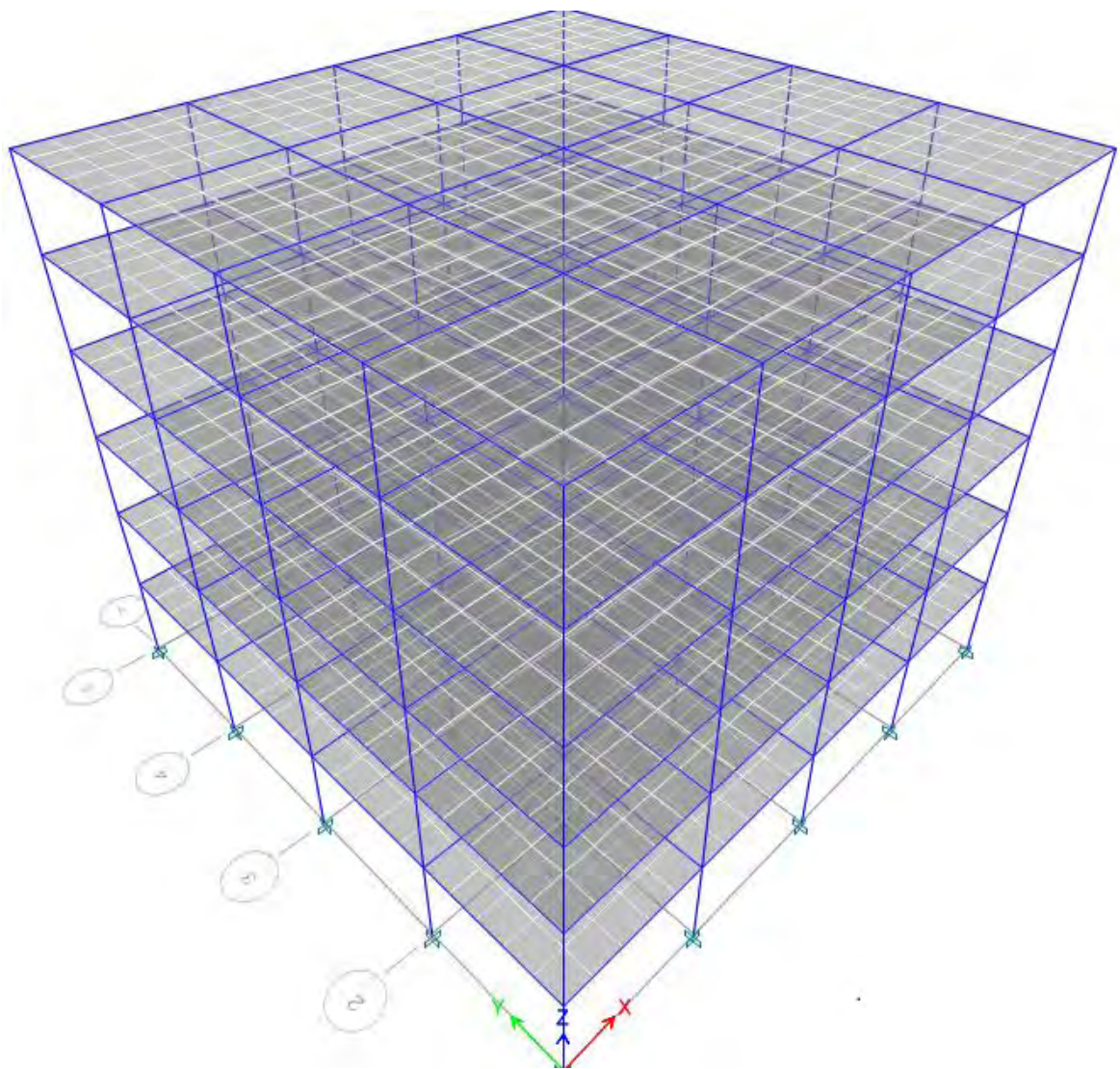
Figure 3.9: 3D view of 6-storied RC building
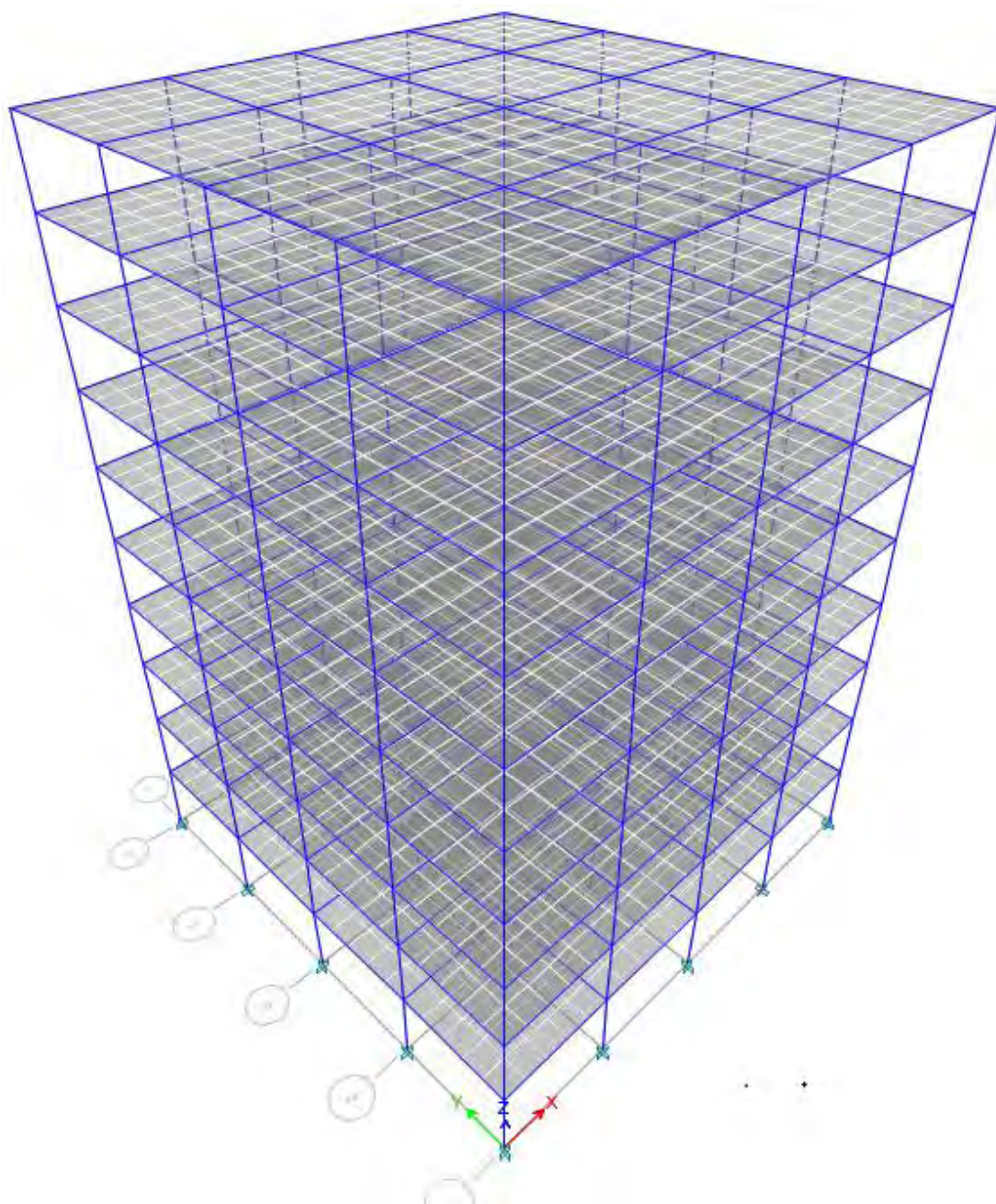
Figure 3.10: 3D view of 10-storied RC building
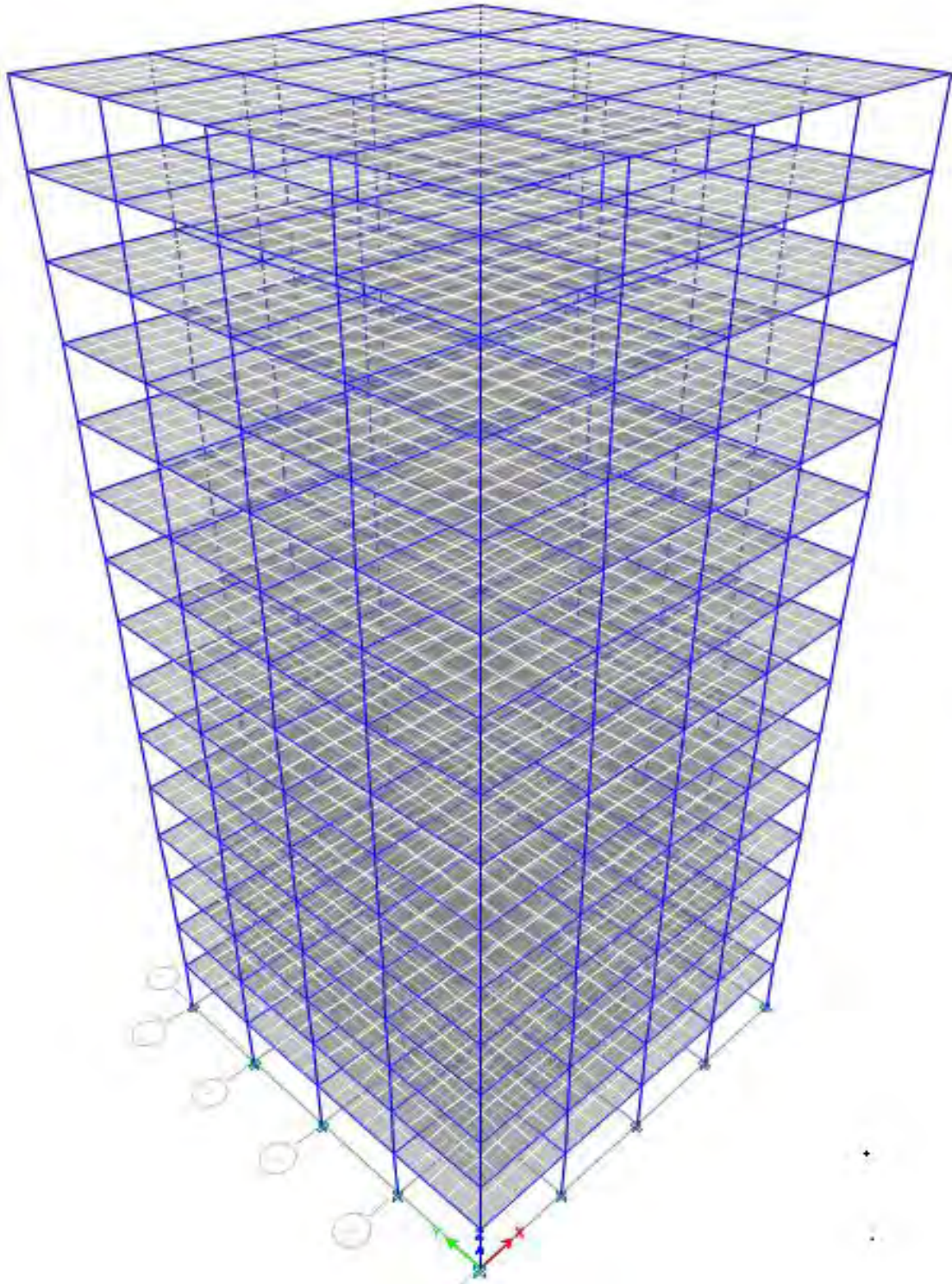
Figure 3.11: 3D view of 15-storied RC building

3.6 Nonlinear static or Pushover analysis (NSA)

Nonlinear static analysis (NSA) has been performed for the considered buildings with similar framing system having the same geometric plan but with different storey levels.

Diaphragm eccentricity has been considered 5% as per draft BNBC-2017. The finite element analysis of the studied structures has been carried out in commercially available finite element software ETABS 17. In this research work, reinforced concrete (RC) moment resisting frame has been considered for all the building models as per draft BNBC-2017. Plasticity was assumed to be lumped at probable hinge locations in RC members. Coupled axial force and biaxial bending moment hinge (P–M–M hinges) and uniaxial flexural hinges (M3 hinges) are assigned at the both ends of the columns and beams, respectively. The design compressive strength and strain at peak stress of concrete are taken as 25 N/mm^2 and 0.002, respectively. Modulus of elasticity for concrete is taken as $E_c = 2.35 \times 10^4$ N/mm^2. The idealized force–deformation curve shown in Figure 3.12 is assigned to each plastic hinge which are in-built in commercial software ETABS. The lateral seismic force distribution obtained using draft BNBC 2017 is used as loading pattern for the pushover analysis. The generalized load–deformation relation shown in Figure 3.12 represents linear response from A to an effective yield point B, further a linear response at decreased stiffness from B to C. Neglecting effects of vertical loads acting through lateral displacements, the slope from point B to C can be taken as 0–10% of the initial slope in absent of any specific experiment value. Ordinate of point C represents the maximum strength of the member and an abscissa represents the deflection at which notable strength reduction takes place. Line DE indicates the remaining strength of the structure. Modeling parameters and acceptance criteria for different performance levels in RC frame members are considered as per FEMA 356 (2000) guidelines as shown in Tables 3.8 and 3.9 for columns and beams, respectively.

(a) Deformation
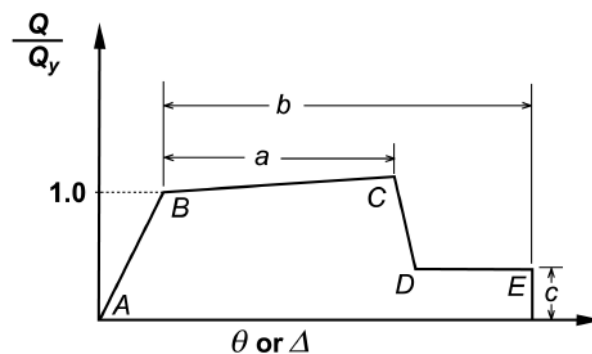
(b) Deformation ratio
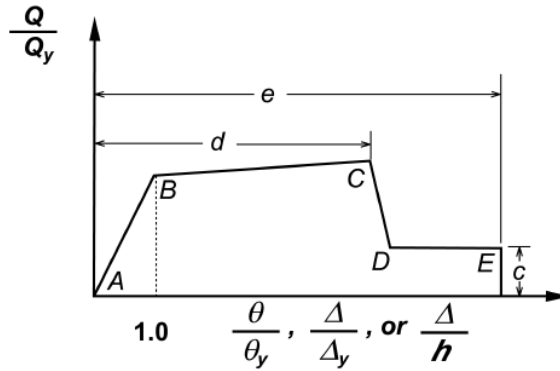
(c) Component or element deformation criteria
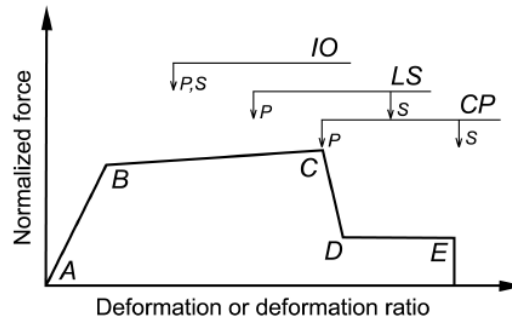
Figure 3.12: Generalized components force-deformation relationship for modeling and acceptance criteria (FEMA 356)

Table 3.8: Modeling parameters and numerical acceptance criteria for nonlinear procedure reinforced concrete column (ATC-40)

			Modeling Parameters[4]			Acceptance Criteria[4]				
						Plastic Rotation Angle, radians				
						Performance Level				
			Plastic Rotation Angle, radians		Residual Strength Ratio		Component Type			
							Primary		Secondary	
Conditions			a	b	c	IO	LS	CP	LS	CP
i. Columns controlled by flexure[1]										
$\dfrac{P}{A_g f'_c}$	Trans. Reinf.[2]	$\dfrac{V}{b_w d \sqrt{f'_c}}$								
≤ 0.1	C	≤ 3	0.02	0.03	0.2	0.005	0.015	0.02	0.02	0.03
≤ 0.1	C	≥ 6	0.016	0.024	0.2	0.005	0.012	0.016	0.016	0.024
≥ 0.4	C	≤ 3	0.015	0.025	0.2	0.003	0.012	0.015	0.018	0.025
≥ 0.4	C	≥ 6	0.012	0.02	0.2	0.003	0.01	0.012	0.013	0.02
≤ 0.1	NC	≤ 3	0.006	0.015	0.2	0.005	0.005	0.006	0.01	0.015
≤ 0.1	NC	≥ 6	0.005	0.012	0.2	0.005	0.004	0.005	0.008	0.012
≥ 0.4	NC	≤ 3	0.003	0.01	0.2	0.002	0.002	0.003	0.006	0.01
≥ 0.4	NC	≥ 6	0.002	0.008	0.2	0.002	0.002	0.002	0.005	0.008

Table 3.9: Modeling parameters and numerical acceptance criteria for nonlinear procedure reinforced concrete beam (ATC-40)

			Modeling Parameters[3]			Acceptance Criteria[3]				
							Plastic Rotation Angle, radians			
							Performance Level			
			Plastic Rotation Angle, radians		Residual Strength Ratio			Component Type		
								Primary		Secondary
Conditions			a	b	c	IO	LS	CP	LS	CP
i. Beams controlled by flexure[1]										
$\dfrac{\rho-\rho'}{\rho_{bal}}$	Trans. Reinf.[2]	$\dfrac{V}{b_w d \sqrt{f'_c}}$								
≤ 0.0	C	≤ 3	0.025	0.05	0.2	0.010	0.02	0.025	0.02	0.05
≤ 0.0	C	≥ 6	0.02	0.04	0.2	0.005	0.01	0.02	0.02	0.04
≥ 0.5	C	≤ 3	0.02	0.03	0.2	0.005	0.01	0.02	0.02	0.03
≥ 0.5	C	≥ 6	0.015	0.02	0.2	0.005	0.005	0.015	0.015	0.02
≤ 0.0	NC	≤ 3	0.02	0.03	0.2	0.005	0.01	0.02	0.02	0.03
≤ 0.0	NC	≥ 6	0.01	0.015	0.2	0.0015	0.005	0.01	0.01	0.015
≥ 0.5	NC	≤ 3	0.01	0.015	0.2	0.005	0.01	0.01	0.01	0.015
≥ 0.5	NC	≥ 6	0.005	0.01	0.2	0.0015	0.005	0.005	0.005	0.01

[1]

For informational purposes, limit states (IO, LS, CP) are specified and which are reported in analysis. These numerical limits are applicable for a member, whose failure is taken place by flexural demands, and assuming that shear/brittle failure do not occur earlier than these limits are achieved.

Beam-column framing elements have been considered as line elements with properties concentrated at component centerlines in a FEM model. Beam – column joints have been considered as monolithic rigid joint. Beams and columns have been modeled using concentrated plastic hinge models.

3.7 Model Validation

This section focusses on model preparation and comparison of results for a building available in literature. Validation of building models is an essential step towards having confidence in the results for the simulation performed on the structures. Maximum output parameters obtained from analysis have been compared for the considered building models.

3.7.1 Validation of RC frame structure

A finite element model has been developed considering provided information and obtained results were compared with those values available in literature. For this, a research work by Prajapati and Amin (2019) has been considered. They investigated the effect of stiffness properties of RC frame members on the response of building systems. The considered building was reinforced concrete with 8-storied and specifically those with the plan having fairly limited bays. A two dimensional (2-D) models have prepared in commercially available software ETABS and obtained results have been compared.

3.7.2   Details of example buildings

In this thesis, a regular symmetric RC frame building of 8-storey, which represent 'medium' period structures, is selected for model validation. The considered RC frame building has three bays of 5 m each in both horizontal directions as shown in Figure 3.13. Height of each storey is considered as 3.5m. Thickness of interior and exterior masonry wall is taken as 115 mm and 230 mm, respectively. The slab thickness is assumed as 150 mm. The live load of 3 kN/m^2 and floor finish of 1 kN/m^2 are assumed on the slabs. The study building was assumed rest on soft soil and to be located in zone-V of IS 1893, which is the most seismically intensive region of Indian seismic map. The RC frames were designed using M25 grade of concrete and Fe415 steel. The RC frame buildings with cracked section property were designed using SAP2000 software as per Indian design codes of IS: 456-2000, IS 1893-2016 and IS: 13920-1993. Additional details of the RC frame building such as total height, fundamental time period, seismic weight and design seismic base shear of RC frames evaluated using equivalent static analysis (seismic co-efficient method) are available in Prajapati and Amin (2019).

3.7.3 Description of the model validation

Summary of the considered building is provided below having elevation shown in Figure 3.14:

No. bays along X axis: 3

No. of bays along Y axis: 3,

Spacing along X axis: 5m,

Spacing along Y axis: 5m

Storey height: 3.5m

No. of floors: G + 7

Sizes of column: C1, C2, C3 = 600 x 600 mm for Level-1 to Level-4

Sizes of column: C1, C2, C3 = 500 x 500mm for Level-5 to Level-8

Sizes of beam: B1= 300 x 600 mm for Level-1 to Level-4

Sizes of beam: B1 = 275 x 550 mm for Level-5 to Level-8

Figure 3.13: Plan for model validation of 8-storied RC example building
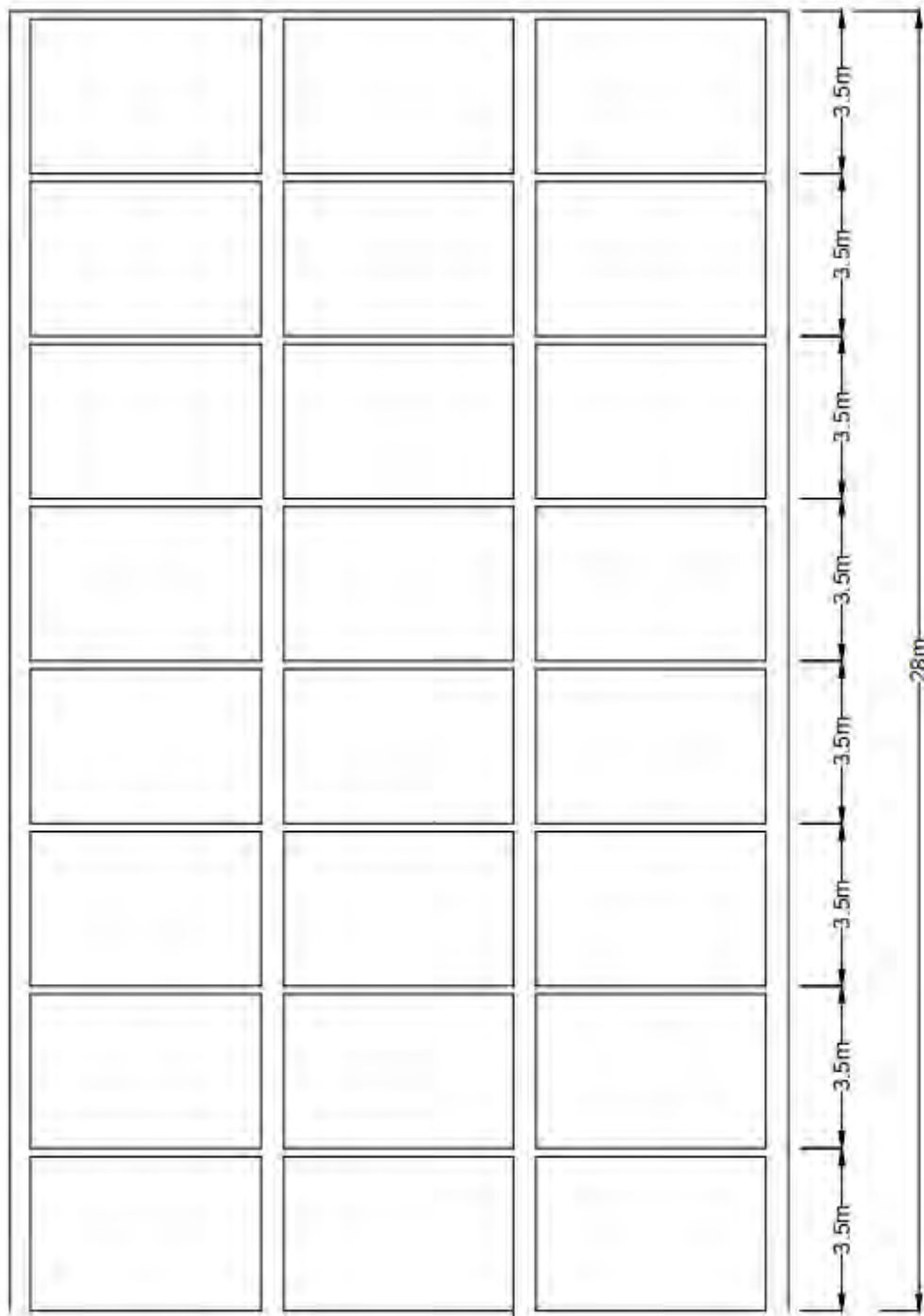
Figure 3.14: Elevation for model validation of 8-storied RC example building

Figure 3.15 shows the comparison of pushover curves obtained by Prajapati and Amin (2019) by using SAP 2000 software and the present study with ETABS software. From the figure, it is shown that the modeling assumptions and acceptance criteria are in good agreement. In addition, Table 3.10 presents the comparison of seismic weight and associated base shear for the considered building obtained from the analyses.
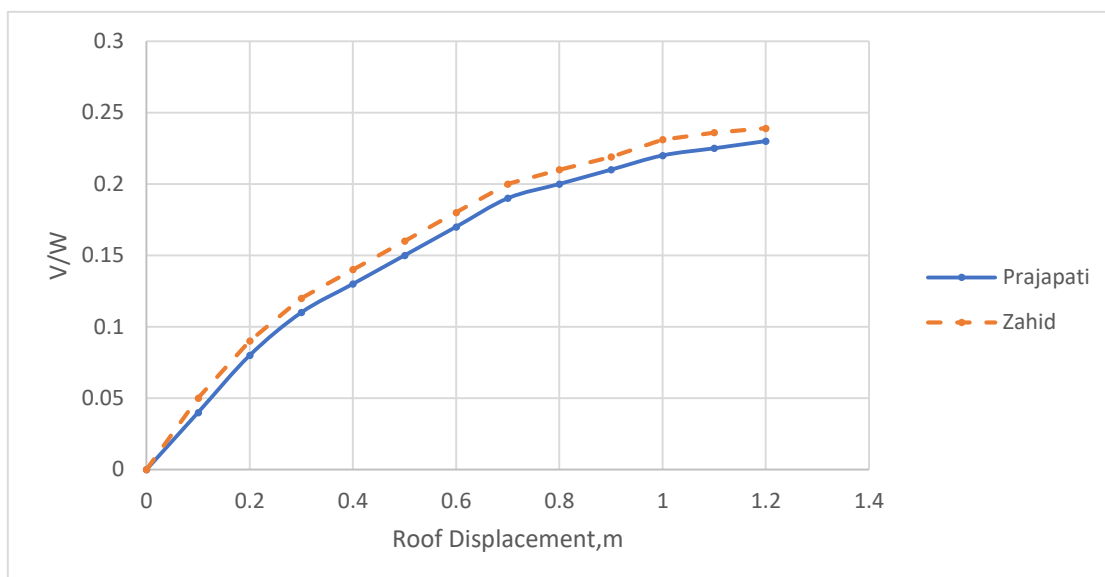
Figure 3.15: A comparison of pushover curves for 8-storied building using cracked section properties

Table 3.10: A comparison of seismic weight and base shear for 8-storied model building

Description	Prajapati and Amin (2019)	Present analysis	Present analysis/ Prajapati and Amin (2019)
Seismic Weight (W)	6213 kN	6222 kN	1.00
Base shear (V)	671 kN	667 kN	0.99

3.8 Pushover curves for the buildings considered in the thesis

After model validation using the commercial software ETABS, a number of analyses have been performed on the considered buildings ranged from 6- storied to 15 –storied with the identical plan configuration. Figures 3.16 to 3.18 present the comparison of pushover curves considering gross and cracked section properties of RC frame members for 6-, 1-0- and 15-storied buildings, respectively.
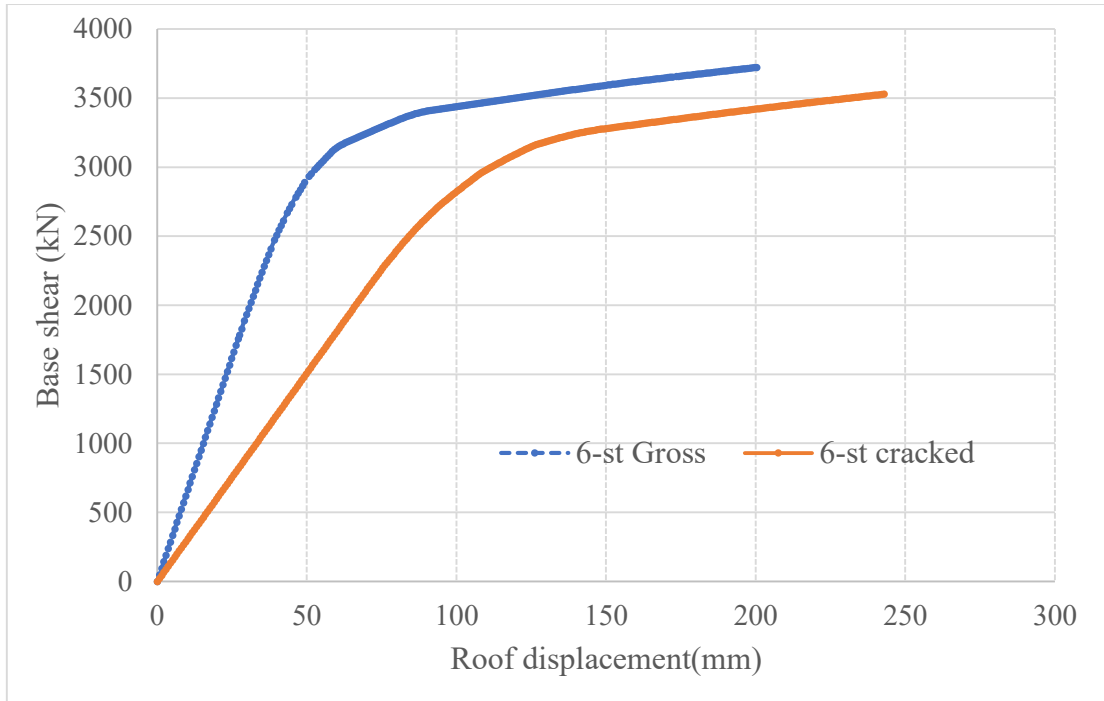
Figure 3.16: Comparison of pushover curves between 6-storied Cracked and Gross sections
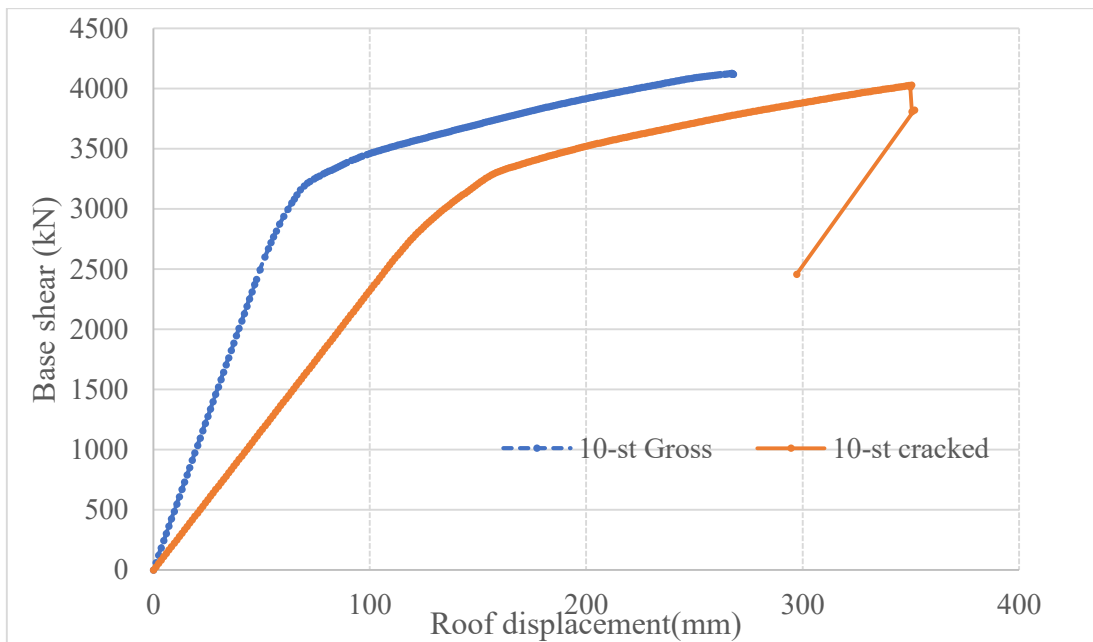
Figure 3.17: Comparison of pushover curves between 10-storied Cracked and Gross sections
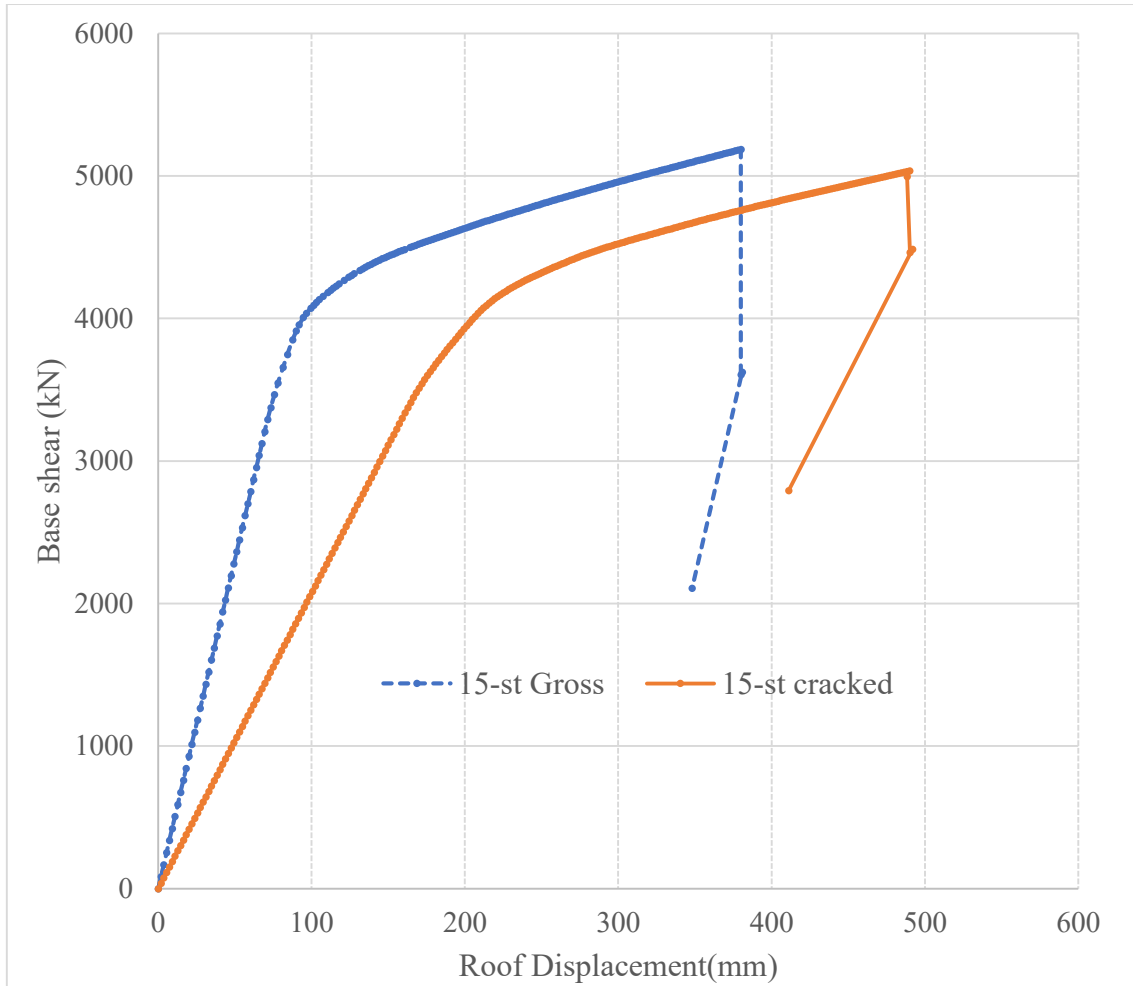
Figure 3.18: Comparison of pushover curves between 15-storied Cracked and Gross sections

Chapter 4
RESULTS AND DISCUSSIONS

4.1 Introduction

In this chapter, all results and outputs obtained from numerical analysis conducted considering gross and cracked section properties of the buildings in Chapter 3 are discussed. Results obtained from nonlinear static analyses (NSA) are compared for both the gross and cracked considerations of the structural members. Buildings with 6-, 10-, and 15-storied having the similar plan configurations and design criteria have been considered for discussions.

4.2 Seismic Performance of RC structures considering nonlinear static analysis

Nonlinear static analyses have been performed for the buildings designed as per upcoming BNBC 2017(draft). In the design phases, both the gross and cracked section properties of the structural members are considered. Analysis results of pushover curves are presented in Appendix –B. Some of obtained results are presented in this chapter. Table 4.1 shows the seismic performance level at Design Basis Earthquake (DBE) and Maximum Considered Earthquake (MCE) and also the performance point

Table 4.1: Seismic Performance of the considered RC frame buildings

Storey	Building Type	Performance (DBE)	Performance (MCE)	Performance Point	
				V/W	D(mm)
6-st	Gross Section	IO	IO	0.064	28
6-st	Cracked Section	IO	IO	0.084	76
10-st	Gross Section	IO	LS	0.050	50
10-st	Cracked Section	IO	LS	0.056	114
15-st	Gross Section	LS	LS	0.041	72
15-st	Cracked Section	LS	CP	0.042	150

Table 4.1 shows the seismic performance level of RC frame for hazard level corresponding to design basic earthquake (DBE) and maximum considered earthquake (MCE). The performance level of 6-st RC frame building with both the gross section and

cracked section are found "IO" for DBE and MCE. The performance level of 10-st RC frame building having the gross section and cracked section are obtained "IO" for DBE. However, the performance level of 10-st RC frame building with gross section and cracked section are found "LS" for MCE. The performance level of 15-st RC frame building with gross section and cracked section are found "LS" for DBE. The performance level of 15-st RC frame building with gross section is found "LS" for MCE while that of cracked section is found "CP" for MCE.

4.2.1 Hinge formations for the gross and cracked sections of the buildings

Figure 4.1 shows the plastic hinge formation for 6-storied cracked building at load level while Figure 4.2 shows the 3-D view of the hinge formation of the building. In a similar pattern, Figure 4.3 shows the hinge formation for the 6-storied gross/uncracked building while Figure 4.4 shows the 3-D view of the hinge formation for the same building.

Figures 4.5 to 4.12 present the hinge formations 10 and 15-storied buildings both considering Cracked and Gross section properties of the building.
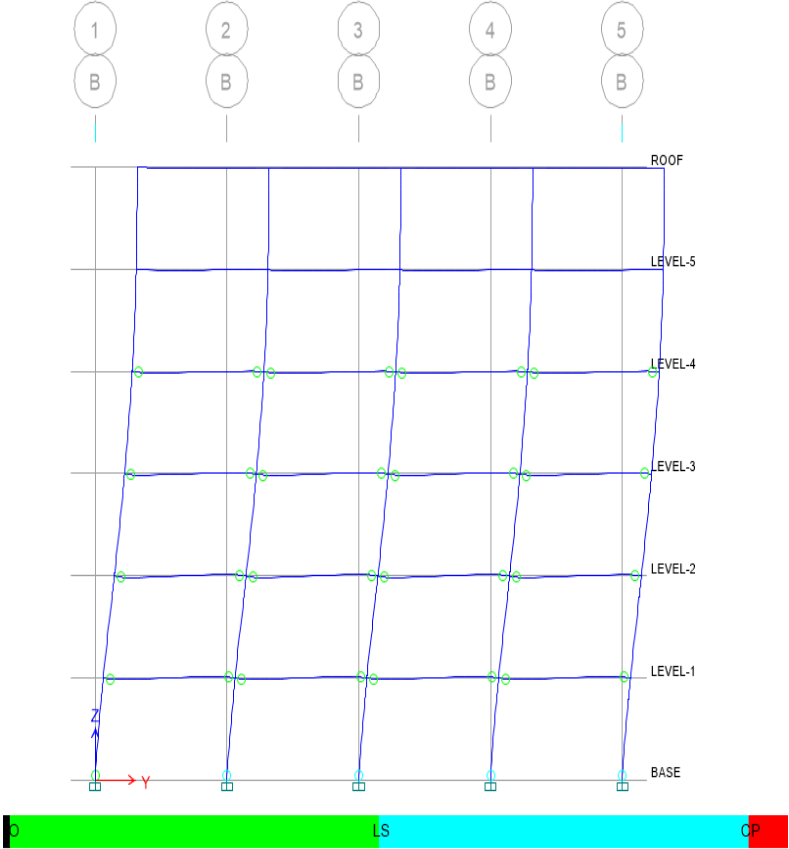
Figure 4.1: 2D view of Plastic hinge formation at performance point for 6-storied RC Gross section building
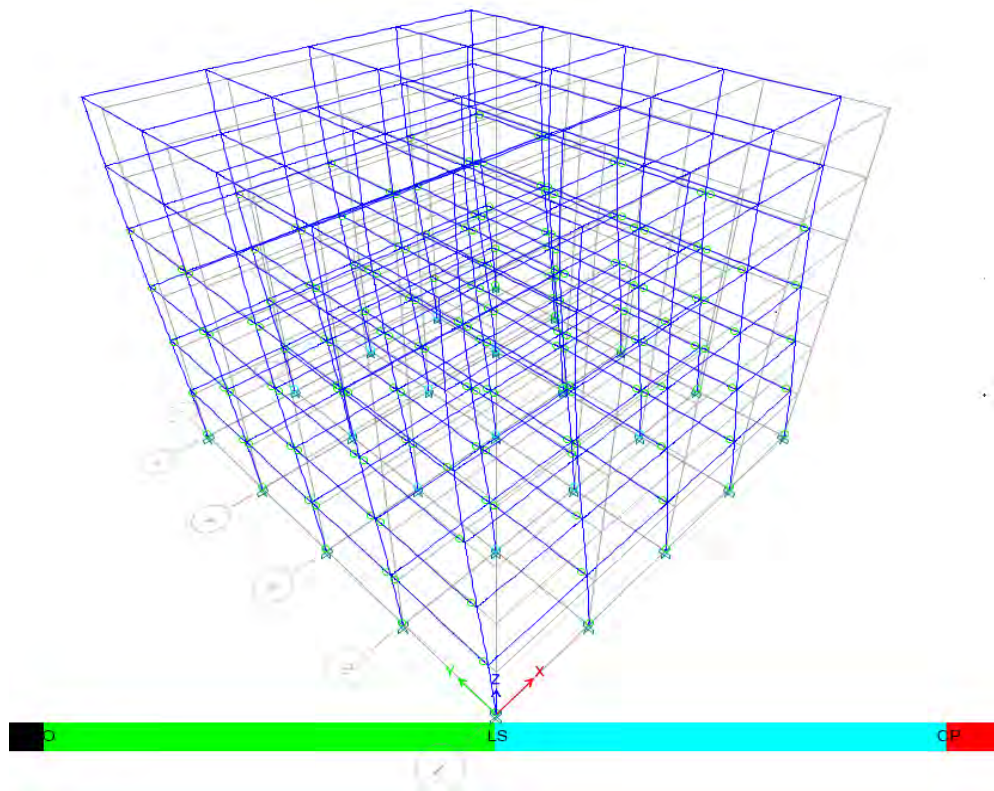
Figure 4.2: 3-D view of plastic hinge formation at performance point for 6-storied RC Gross section building
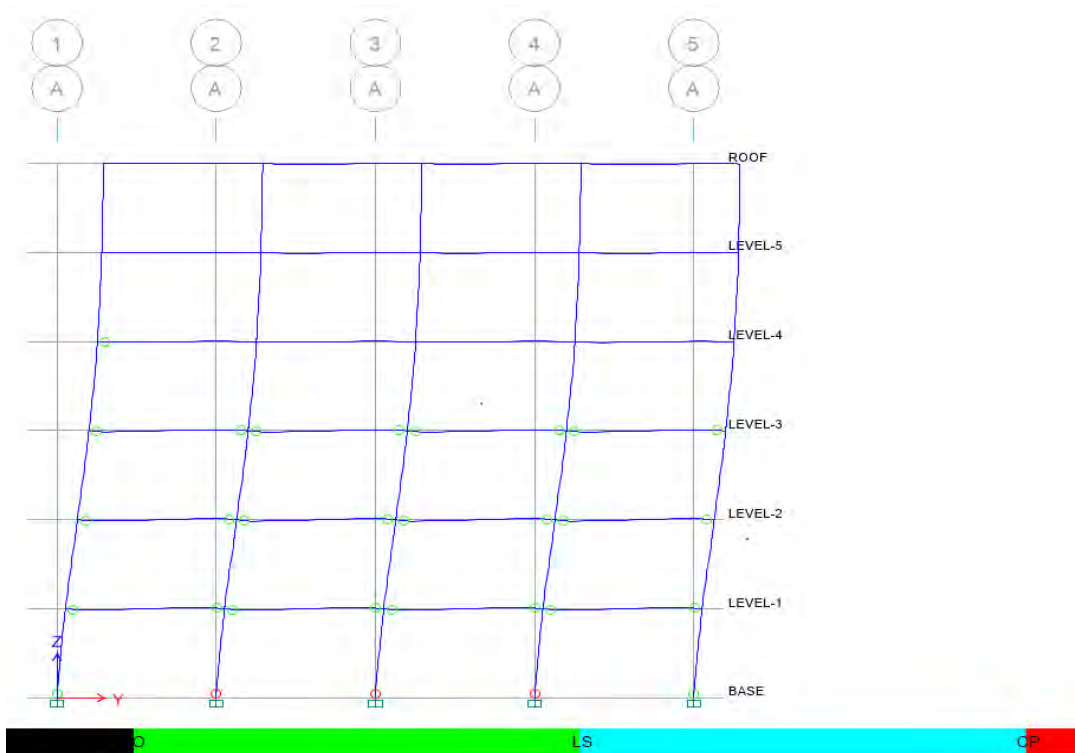
Figure 4.3:2D view of plastic hinge formation at performance point for 6-storied RC Cracked section building
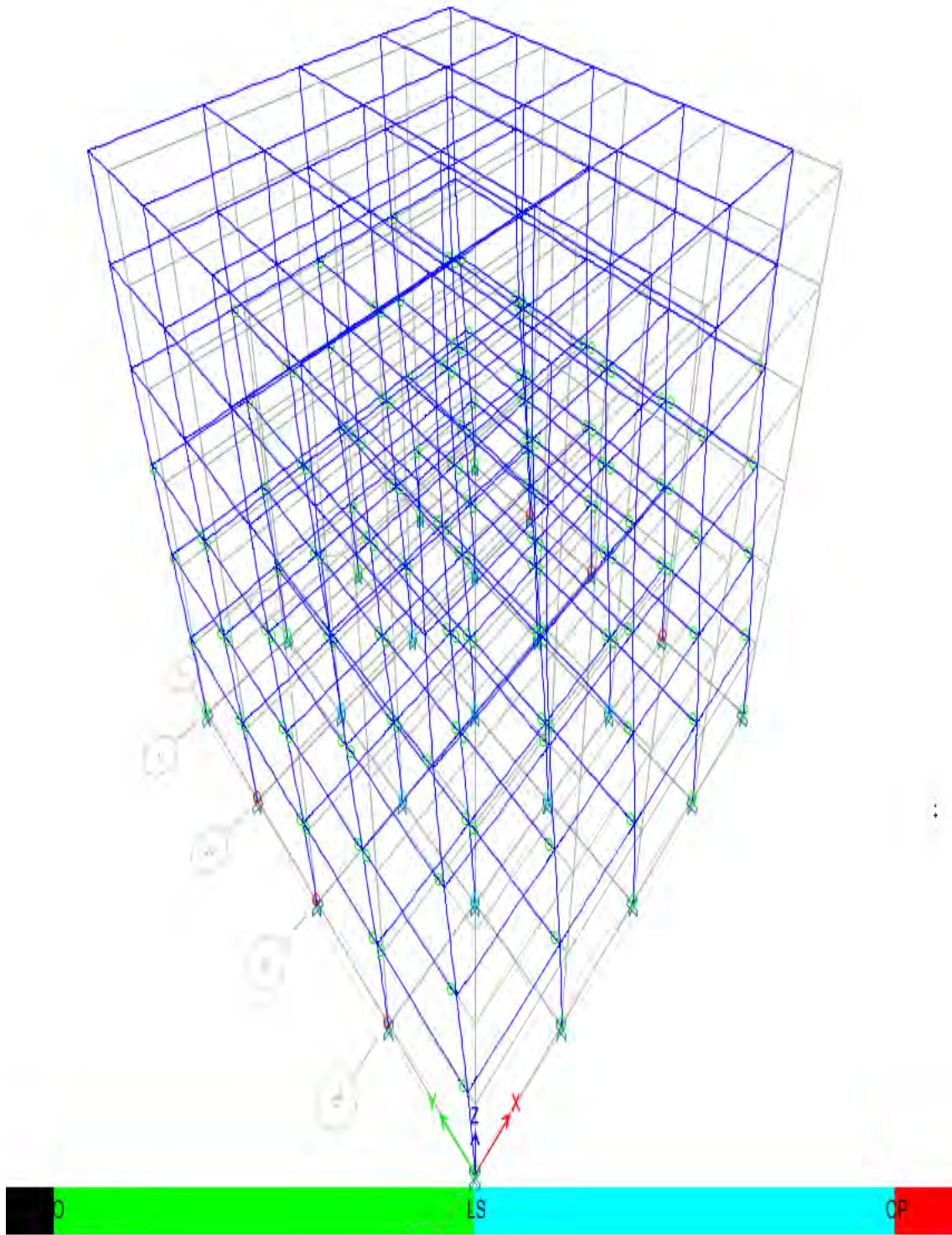
Figure 4.4: 3-D view of plastic hinge formation at performance point for 6-storied RC Cracked section building
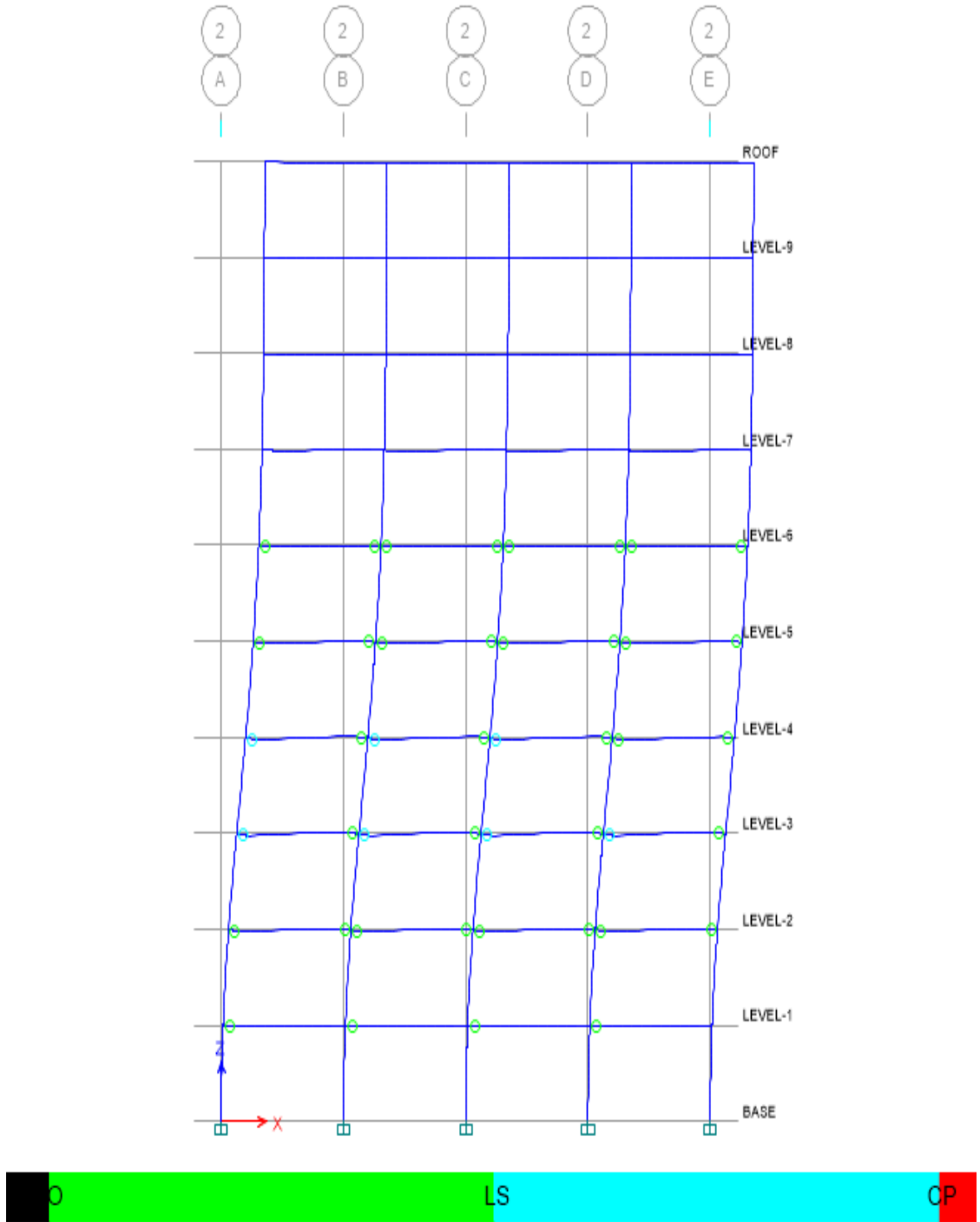
Figure 4.5: 2D View of plastic hinge formation at performance point for 10-storied RC Cracked section building
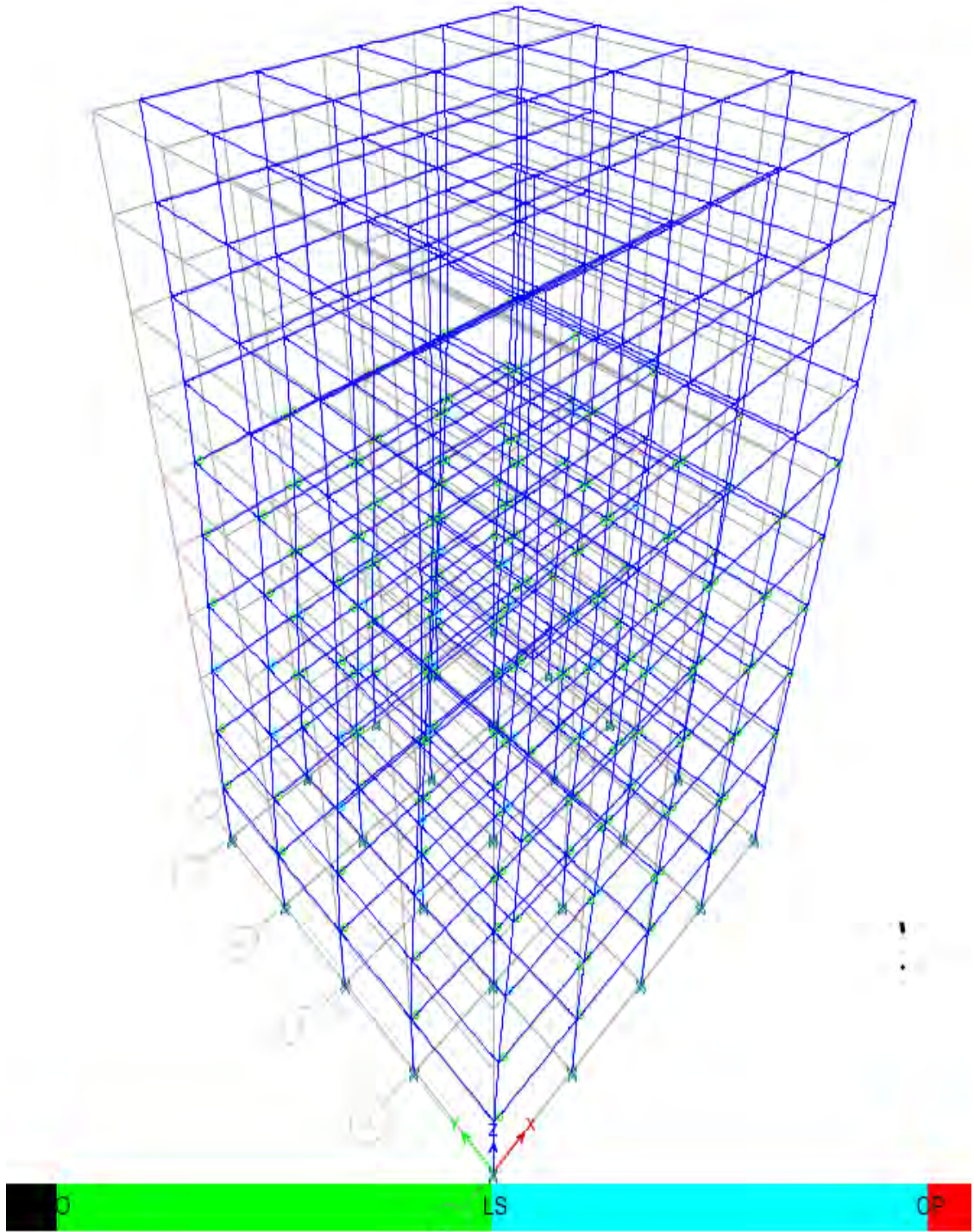
Figure 4.6: 3-D view of plastic hinge formation at performance point for 10-storied RC Cracked section building
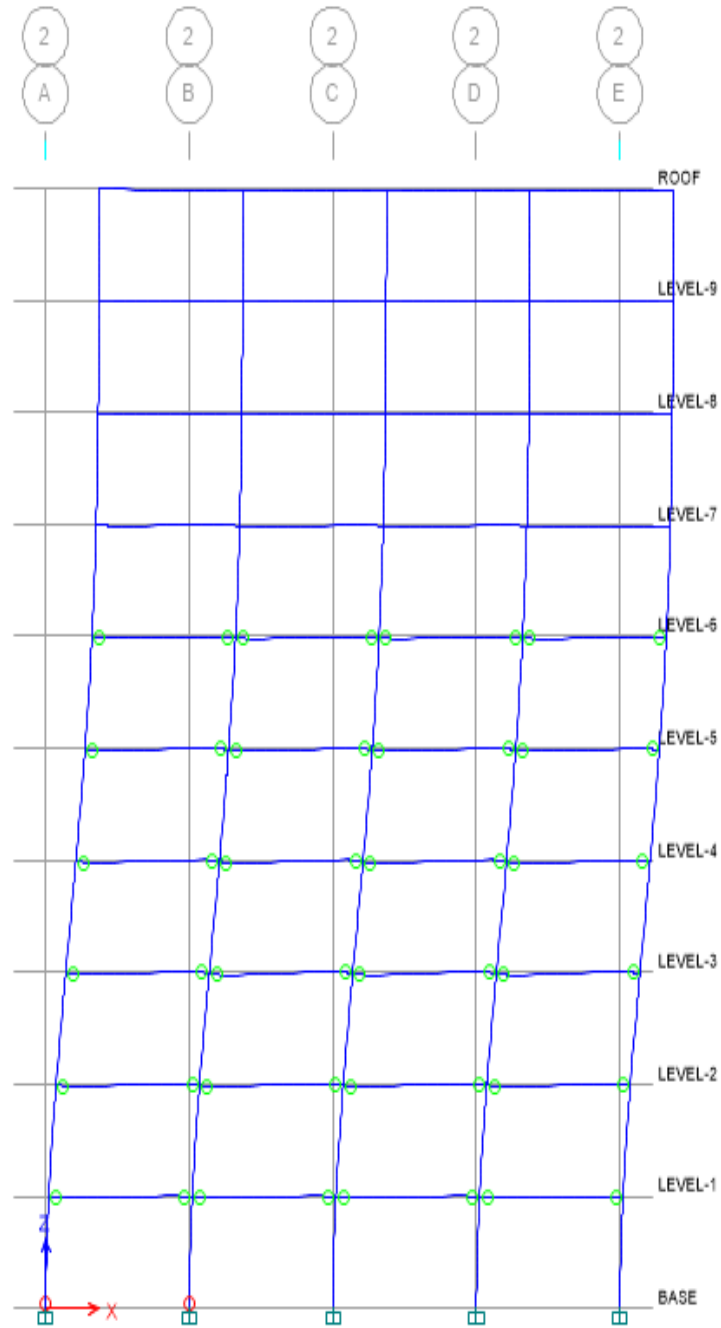
Figure 4.7: 2D View of plastic hinge formation at performance point for 10-storied RC Gross section building
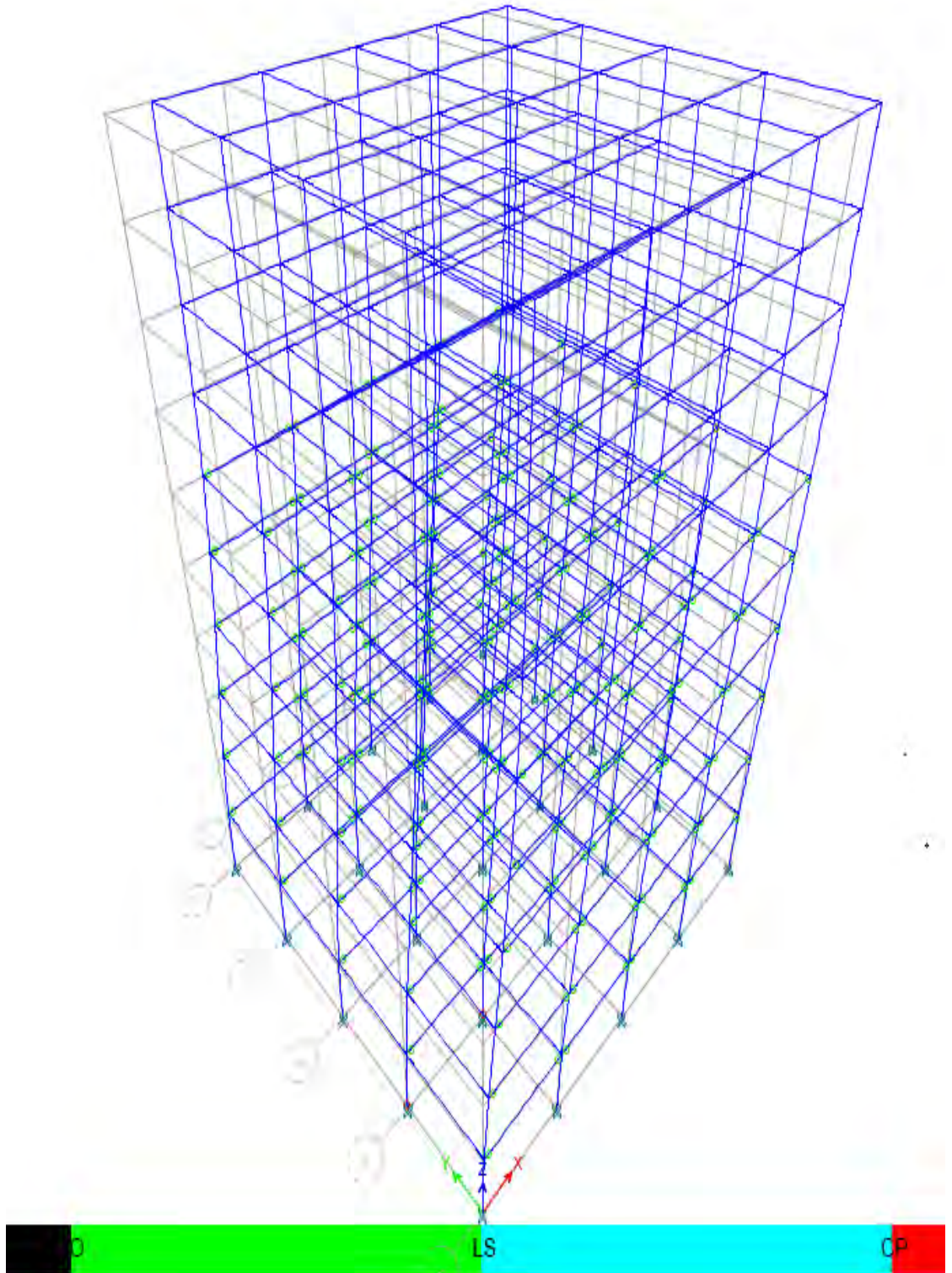
Figure 4.8: 3-D view of plastic hinge formation at performance point for 10-storied RC Gross section building
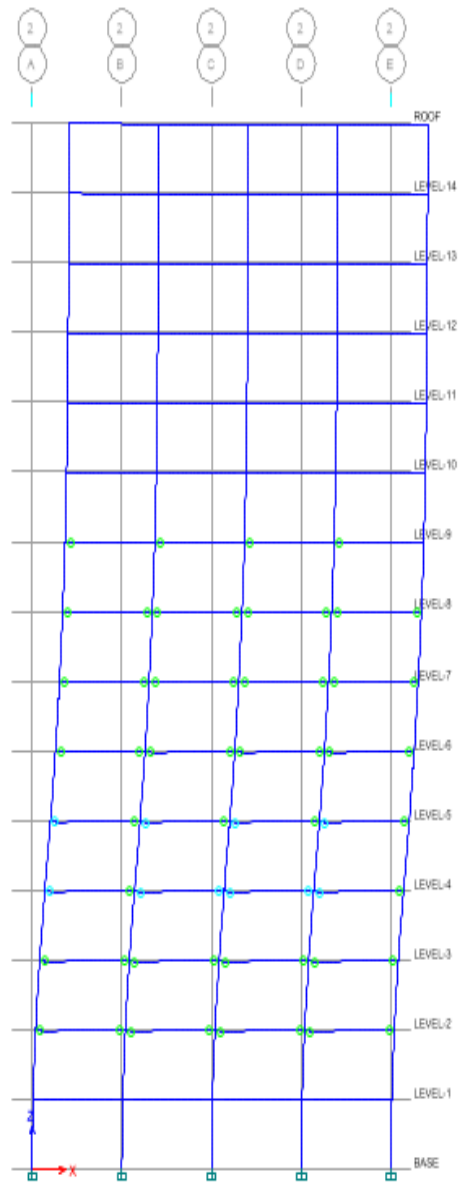
Figure 4.9: 2D view of plastic hinge formation at performance point for 15-storied RC Cracked section building
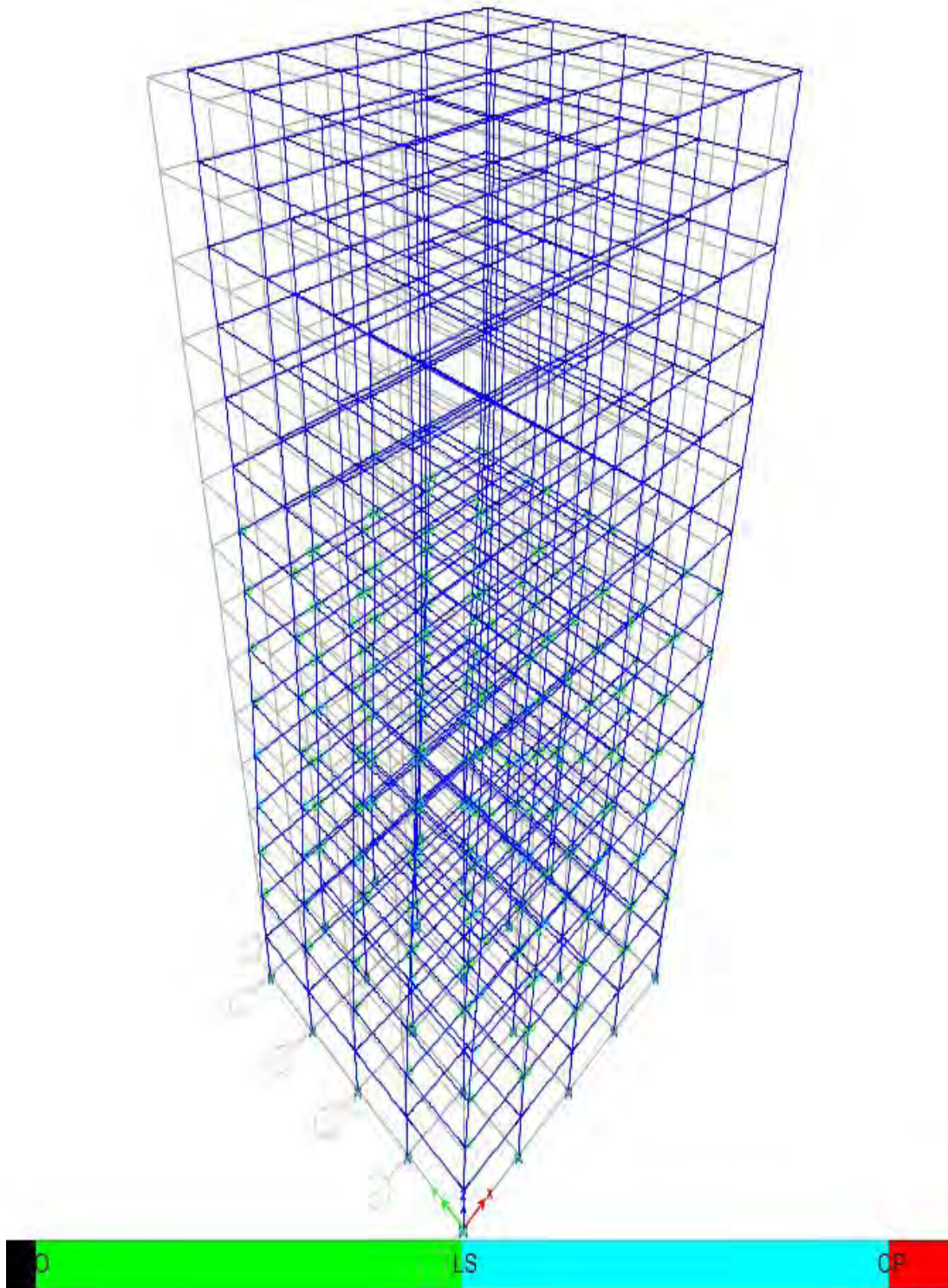
Figure 4.10: 3-D view of plastic hinge formation at performance point for 15-storied RC Cracked section building
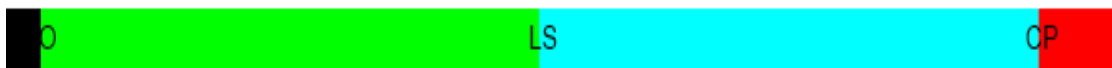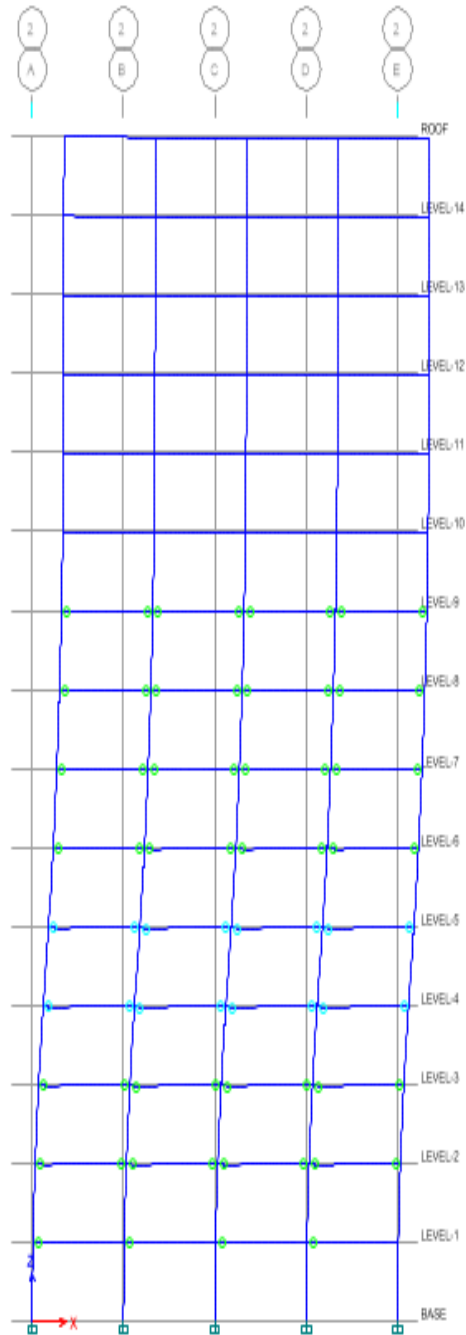
Figure 4.11: 2D View of Plastic hinge formation at performance point for 15-storied RC Gross section building

Figure 4.12: 3-D view of plastic hinge formation at performance point for 15-storied RC Gross section building

4.2.2 Performance of buildings under different level of earthquakes

Seismic performances of the considered building have been assessed by plotting the uncracked and cracked buildings in the same plot with three different level of

earthquakes. Figures 4.13 to 4.15 show the pushover curves considering cracked and uncracked properties of the buildings and plotted for 6-, 10-, and 15-storied, respectively.
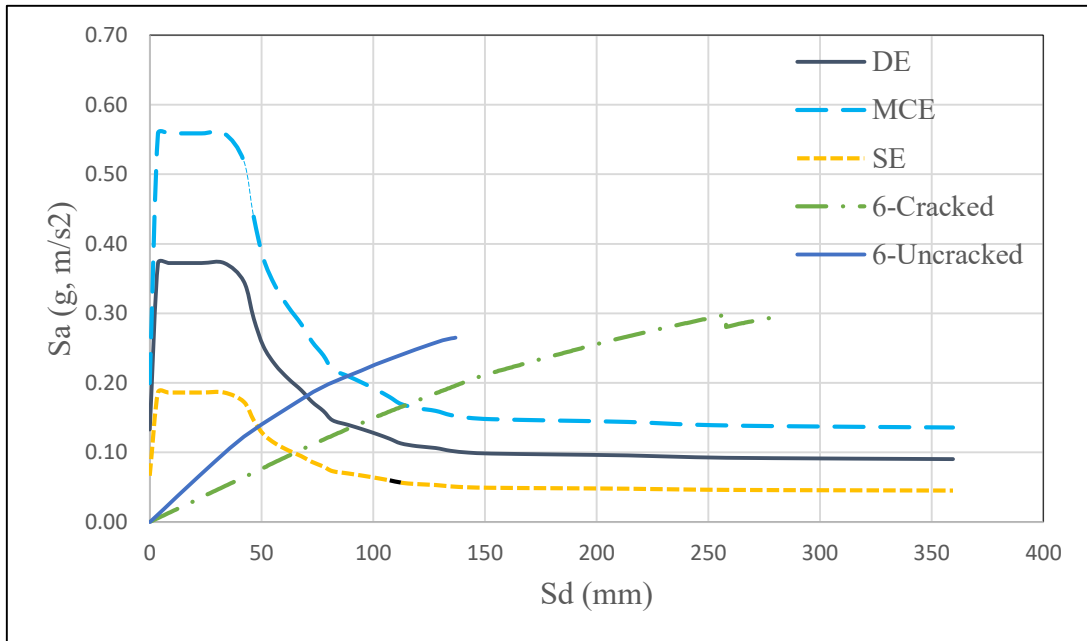
Figure 4.13: Comparison of seismic performance point of 6-storied RC buildings
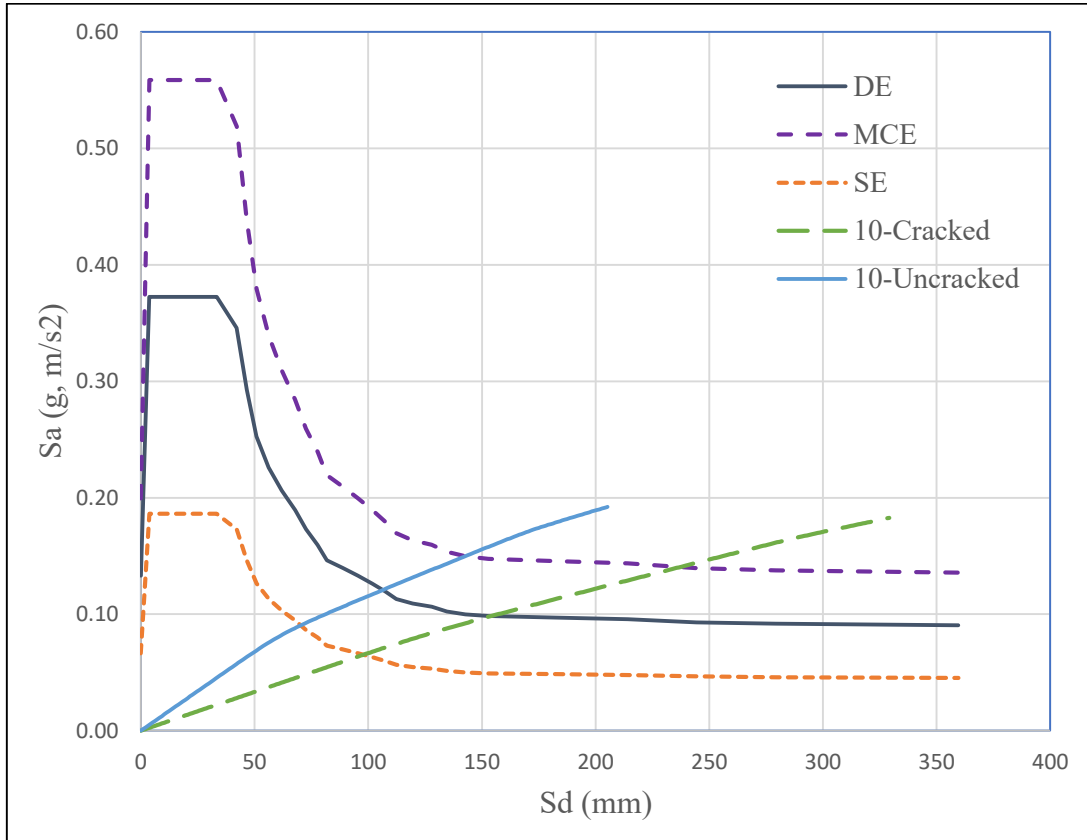
Figure 4.14: Comparison of seismic performance point of 10-storied RC buildings
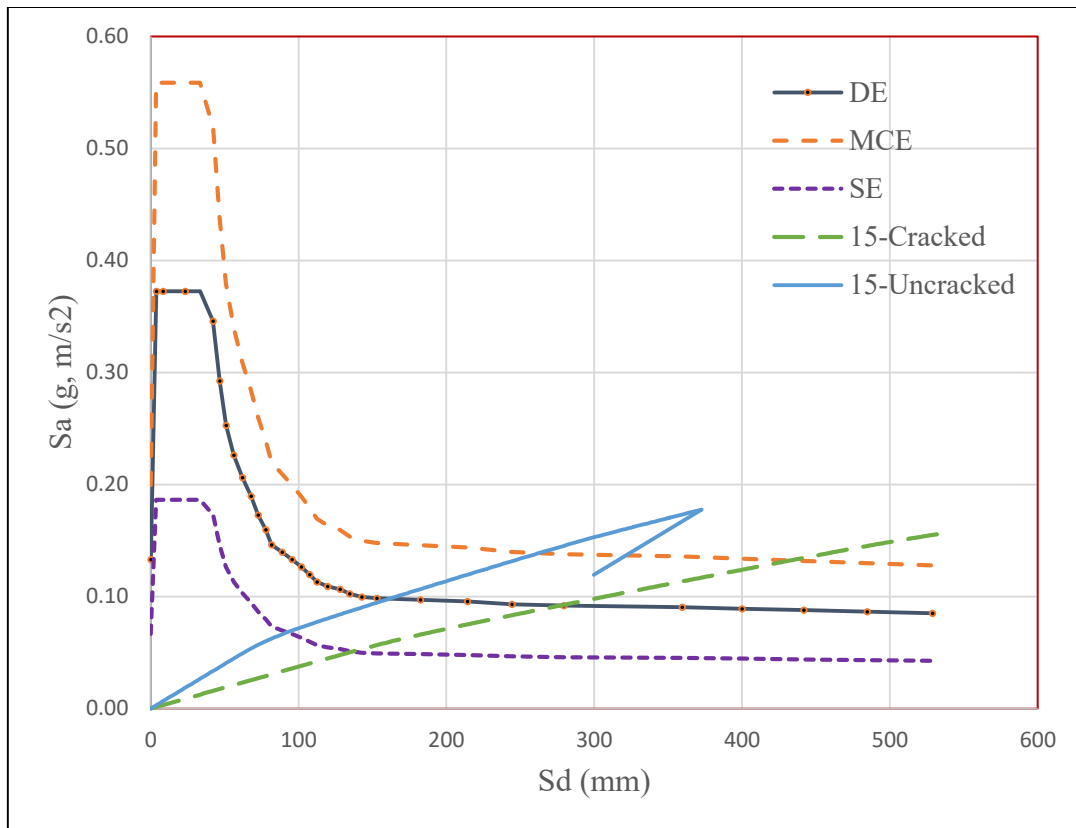
Figure 4.15: Comparison of seismic performance point of 15-storied RC buildings

From the above figures, it is observed that all these buildings satisfy the performance level requirements for all the three level of earthquakes such as Design Basis Earthquake (DE), Maximum Considered Earthquake (MCE) and Serviceability Earthquake (SE).

4.2.3 Base shear values of the buildings

Base shear values of the buildings considering cracked and uncracks sections have been shown in Figures 4.16 to 4.18 for 6-storied to 15-storied buildings, respectively. From the figures, it is shown that buildings with the gross section properties result in higher base shear in comparison to those of the cracked sections.
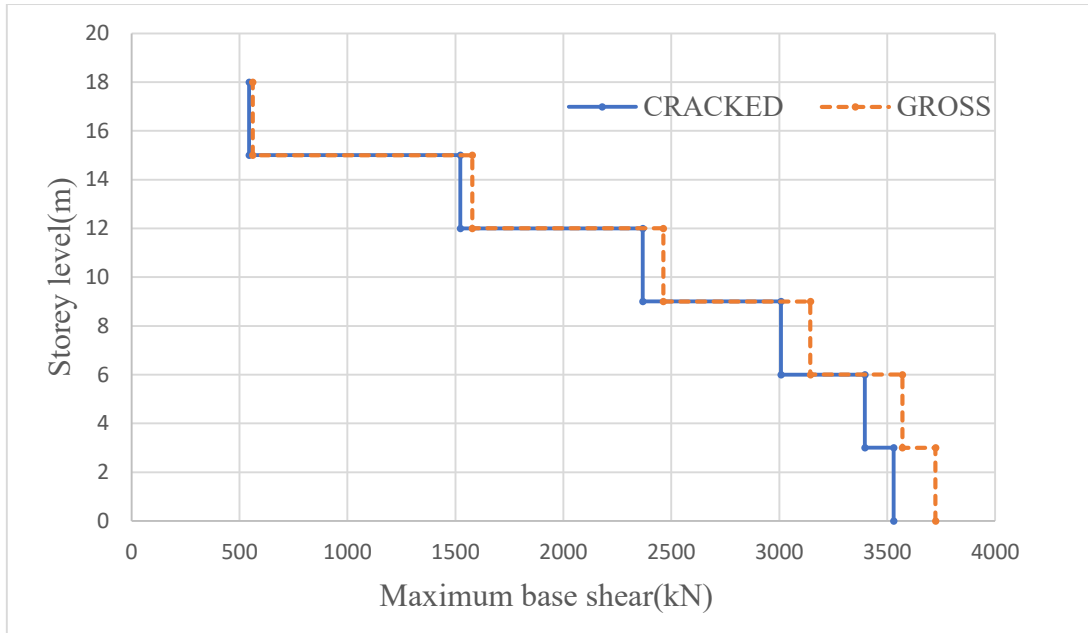
Figure 4.16: Comparison of base shear between Cracked and Gross sections for 6-storied RC building
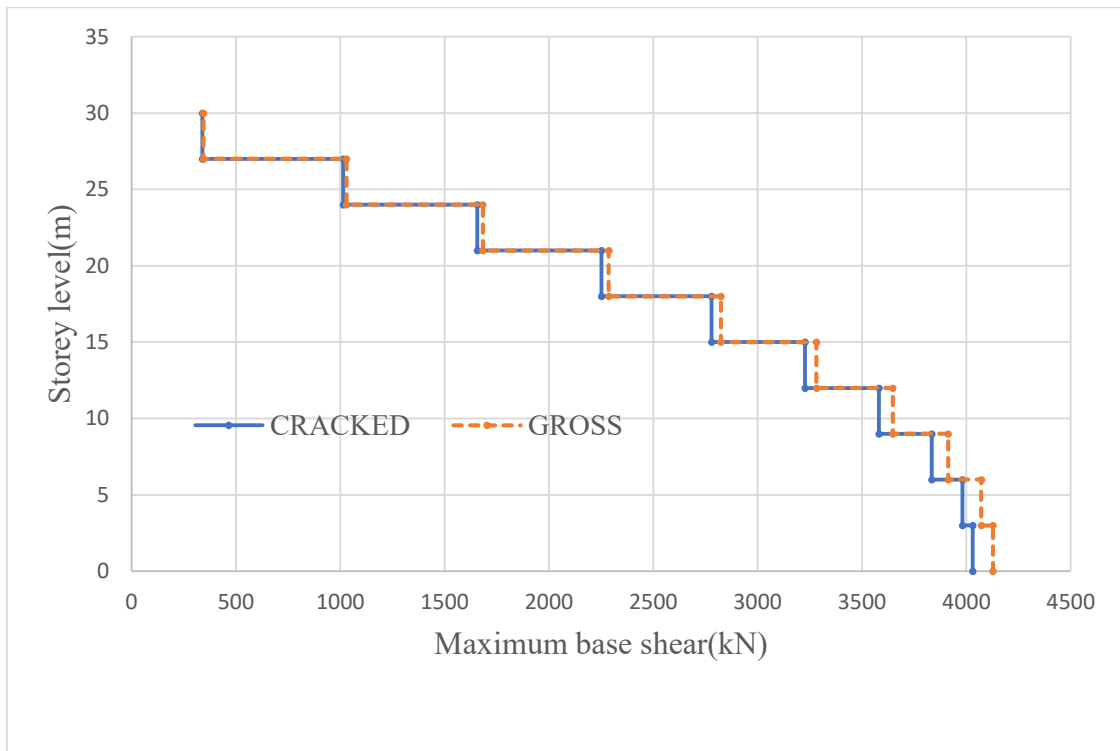
Figure 4.17: Comparison of base shear between Cracked and Gross sections for 10-storied RC building
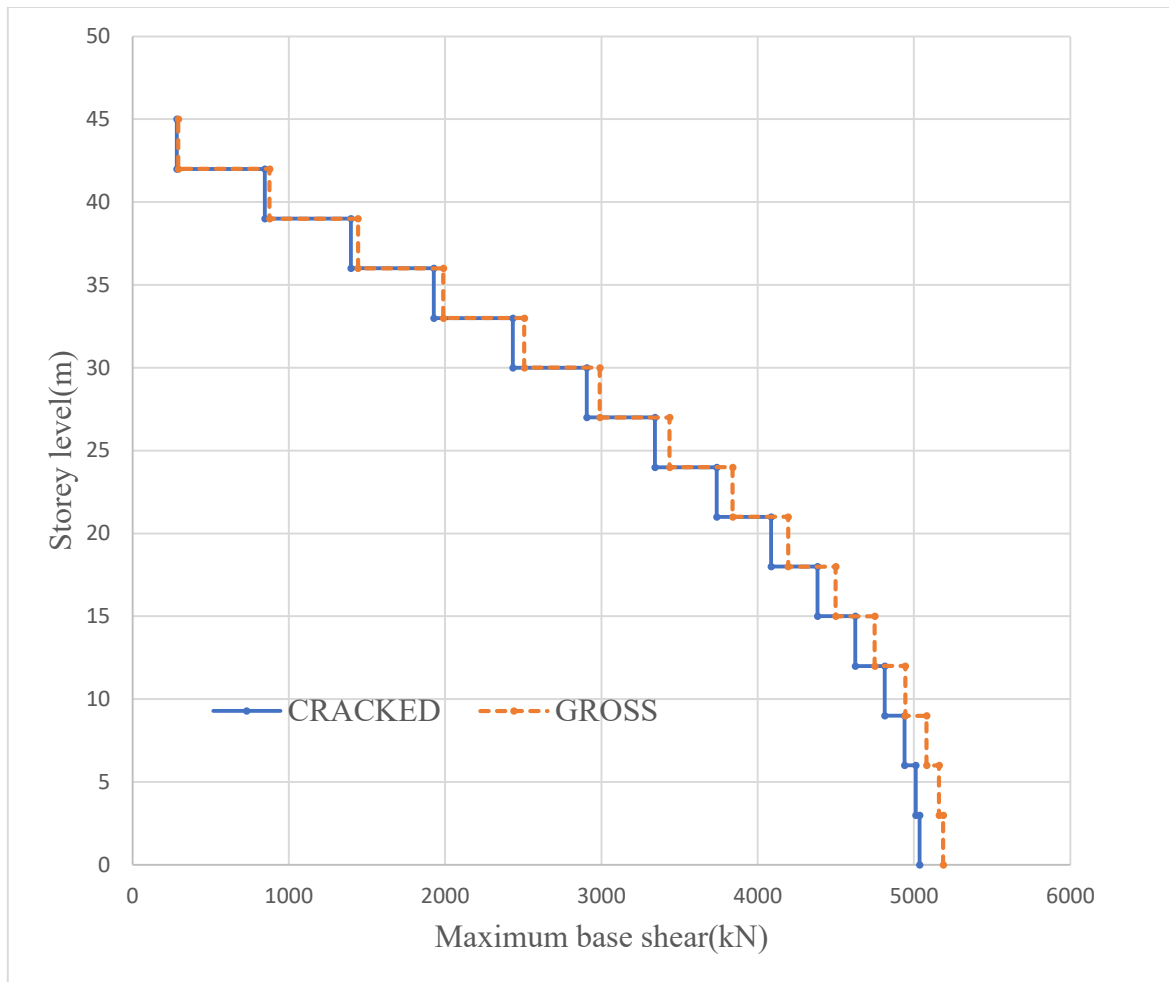
Figure 4.18: Comparison of base shear between Cracked and Gross sections for 15-storied RC building

4.2.4 Storey drift of the buildings

Figures 4.19 to 4.21 show the comparison of displacement of the buildings with gross and cracked section properties. Stiffness properties for structural elements of RC members under lateral loads are based on effective moment of inertia as per draft BNBC 2017 which are different for strength evaluation at factored load level. Figures 4.22 to 4.24 present the inter-storey drift ratios of 6, 10 and 15-storey RC frames designed with gross and cracked section properties. For the 6-, 10-, and 15-storey RC frame designed with gross section properties, the obtained drift at design load is well within the permissible inter-storey drift ratio of 0.4% due to higher stiffness of members. Whereas in case of similar RC frame analyzed and designed with cracked section properties, the inter-storey drift at design load is obtained higher than the RC frame building designed with gross section properties. It is to note that the RC frame analyzed and designed

based on cracked section property of beams and columns having higher percentages of reinforced steel as compared to similar members of RC frame designed using gross section property. Therefore 6-, 10-, and 15-storey RC frame designed using gross as well as cracked section properties of beams and columns do not satisfy the serviceability criteria of lateral deflection evaluated based on effective moment of inertia of beams and columns as per the provisions of revised standards BNBC-2017 (draft).This indicate that the buildings, which are designed based on gross section property using BNBC 1993 (2006) provisions could be unsafe from serviceability requirement as per BNBC-2017(draft).
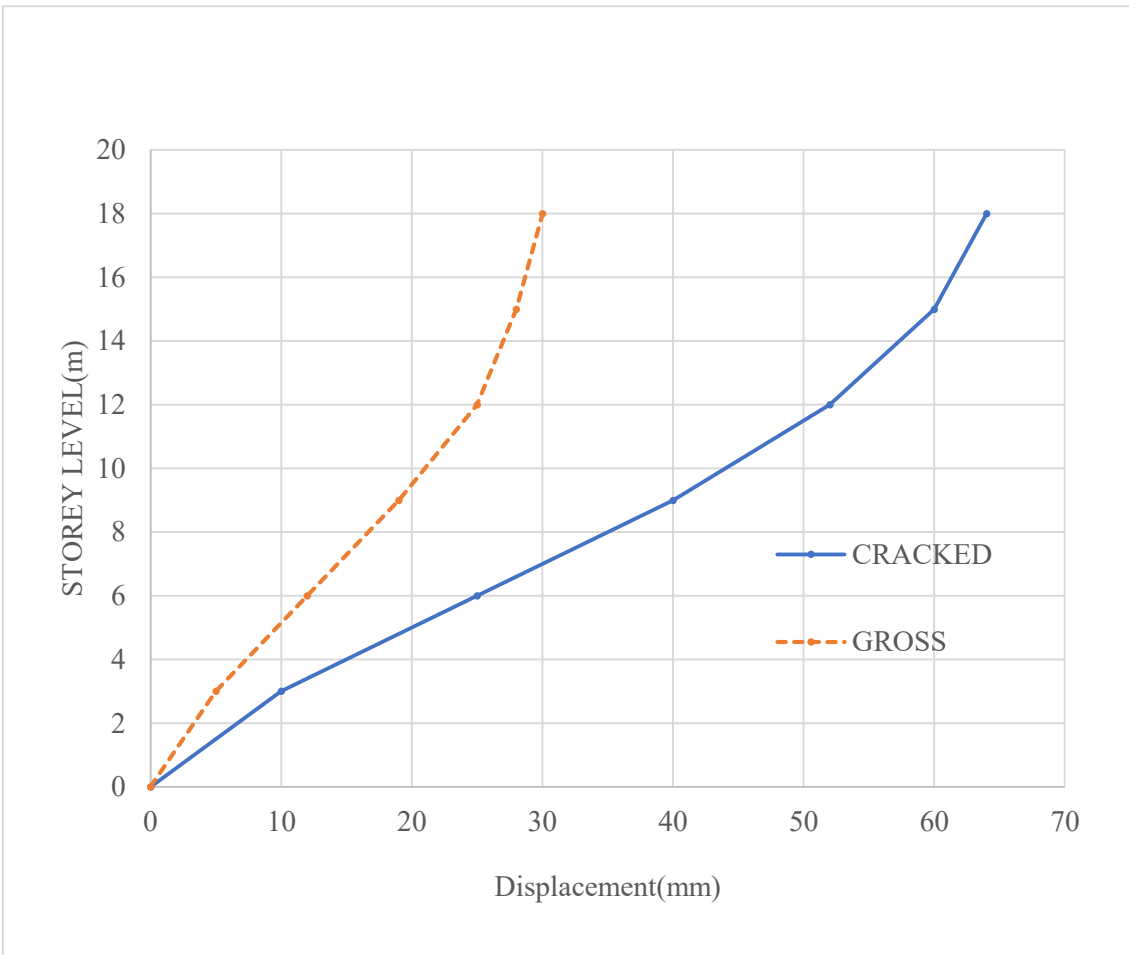
Figure 4.19: Comparison of displacement between Cracked and Gross sections for 6-storied buildings
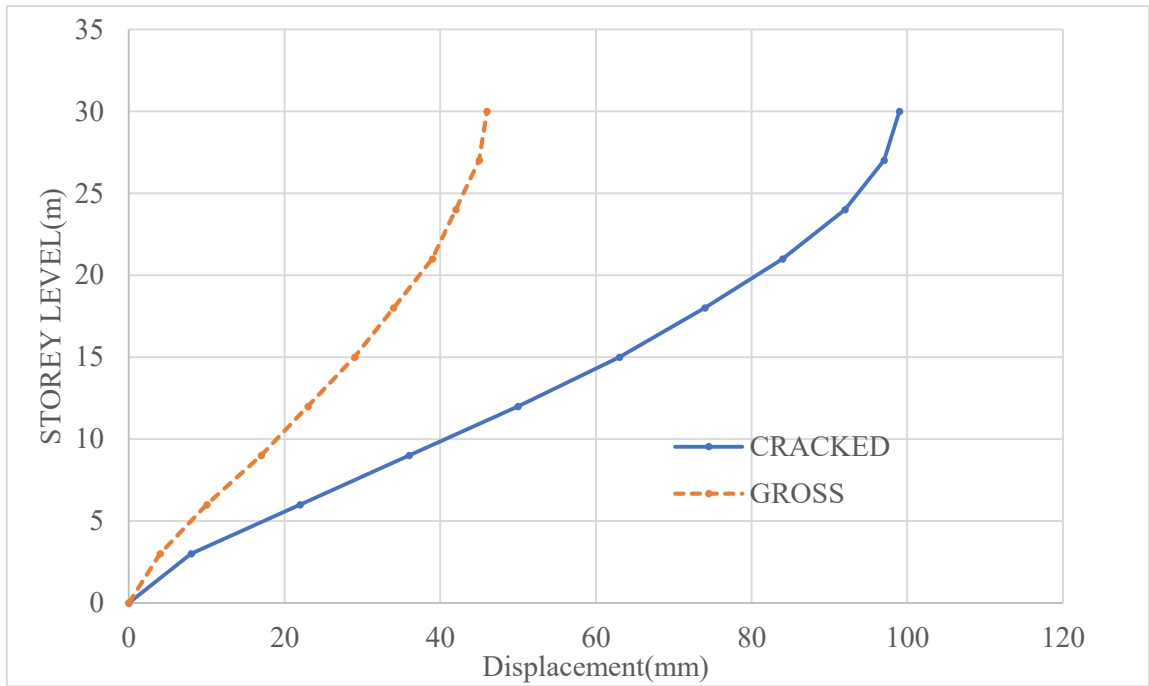
Figure 4.20: Comparison of displacement between Cracked and Gross sections for 10-storied buildings
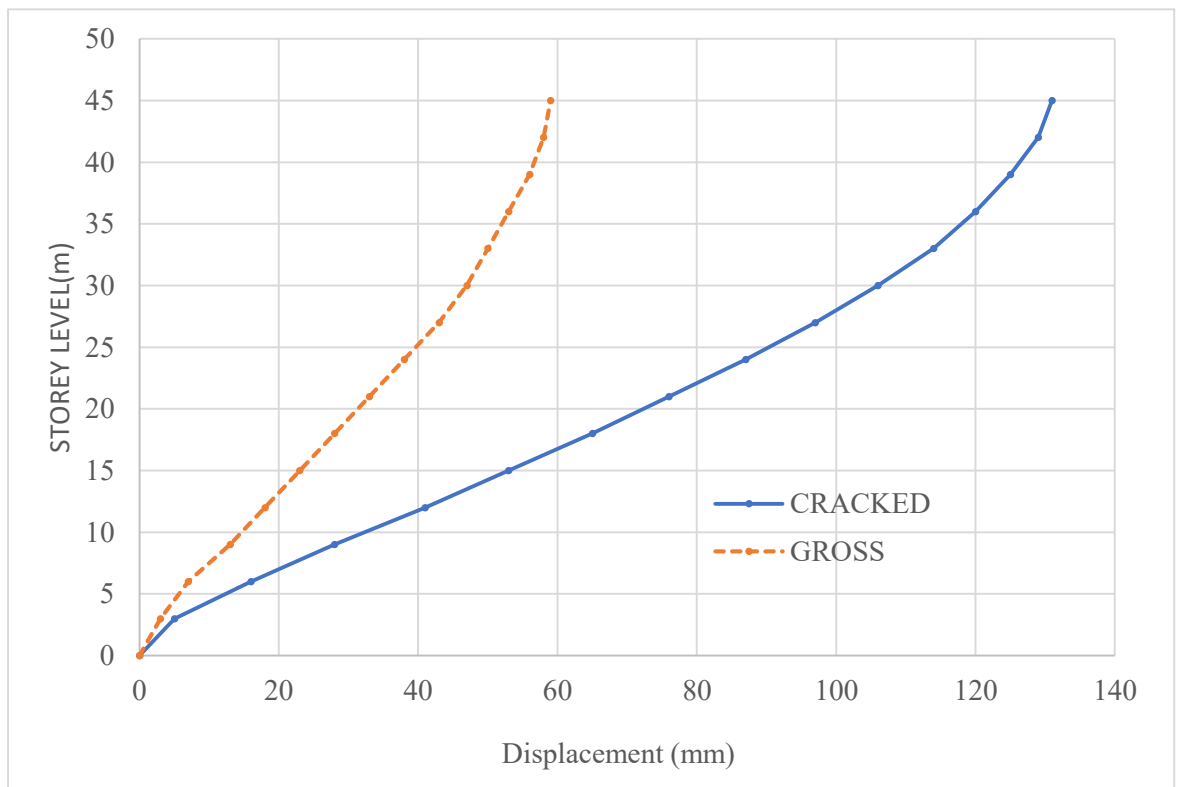
Figure 4.21: Comparison of displacement between Cracked and Gross sections for 15-storied buildings
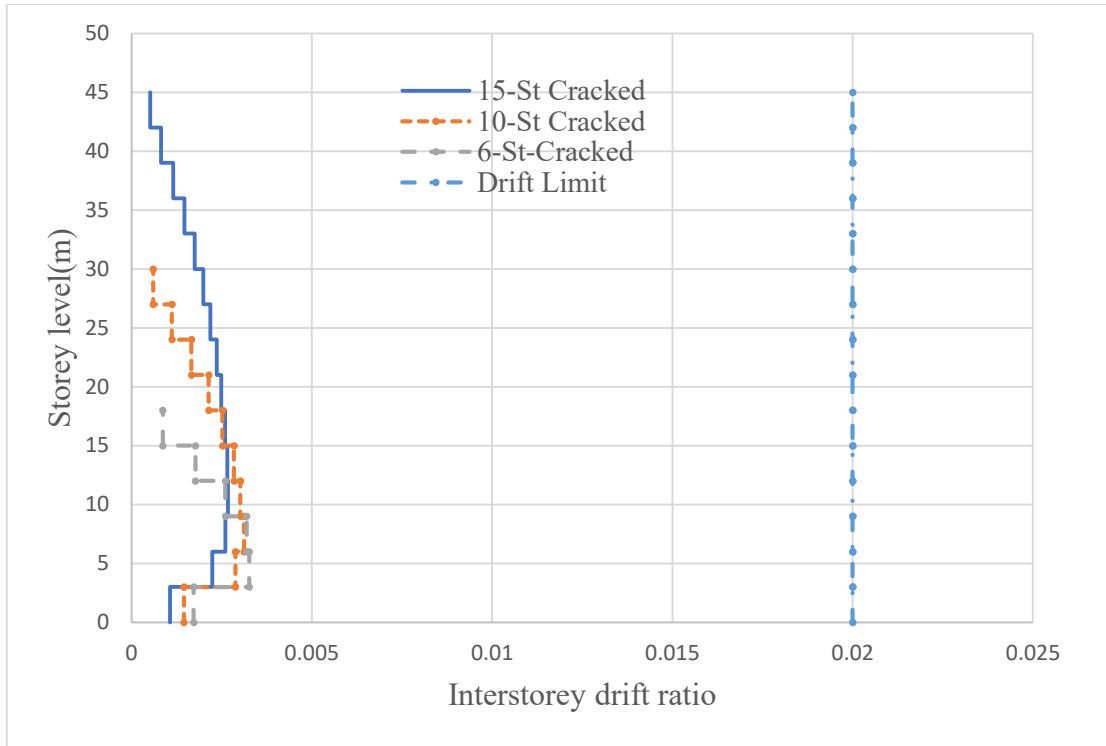
Figure 4.22: Comparison of drift ratios among the 6,10 and 15-storied Cracked sections buildings at Design Basis Earthquake
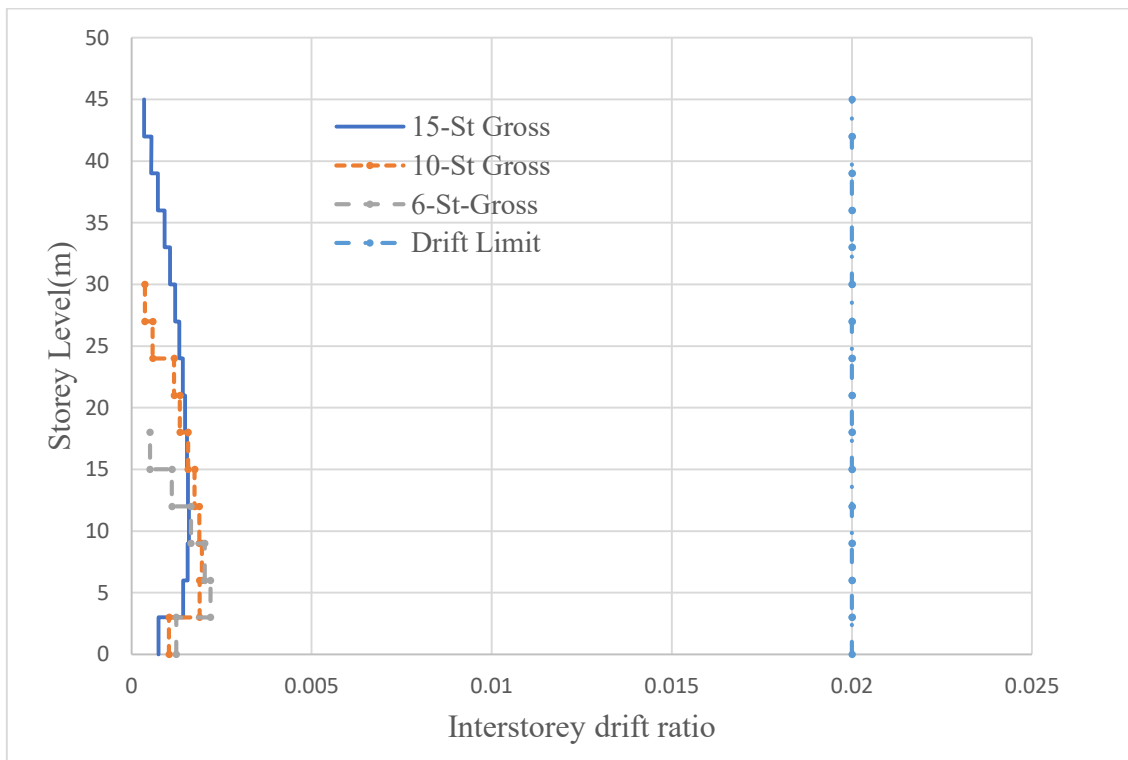
Figure 4.23: Comparison of drift ratios among the 6,10 and 15-storied Gross sections buildings at Design Basis Earthquake
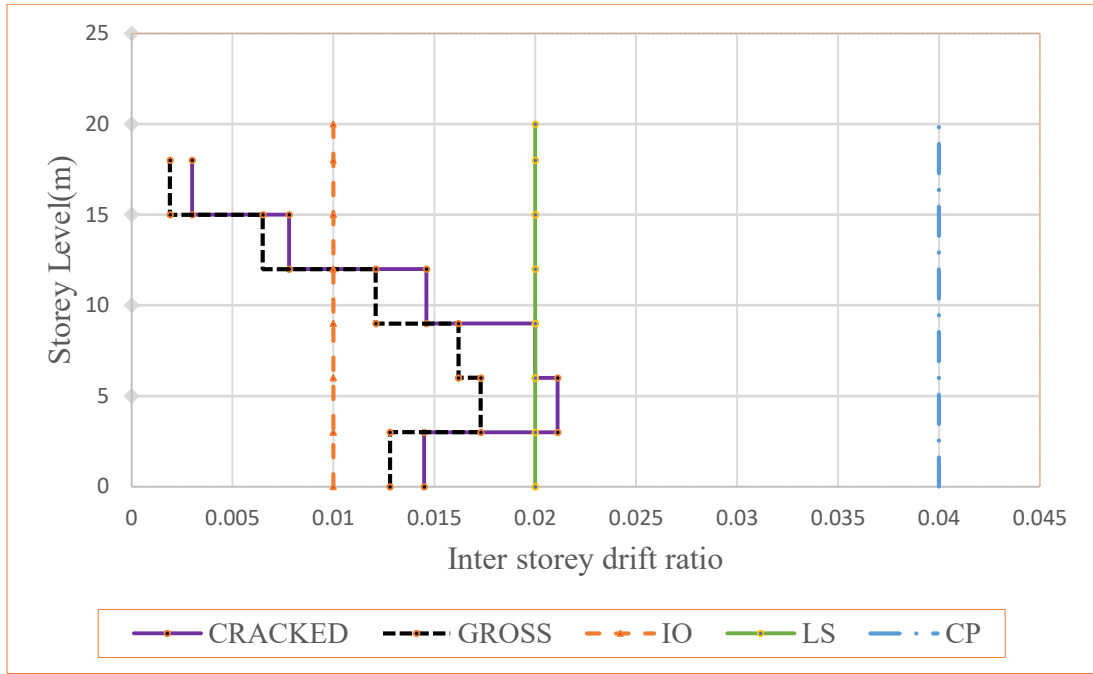
Figure 4.24: Comparison of Inter storey drift ratios between Cracked and Gross sections for 6-Storied RC building
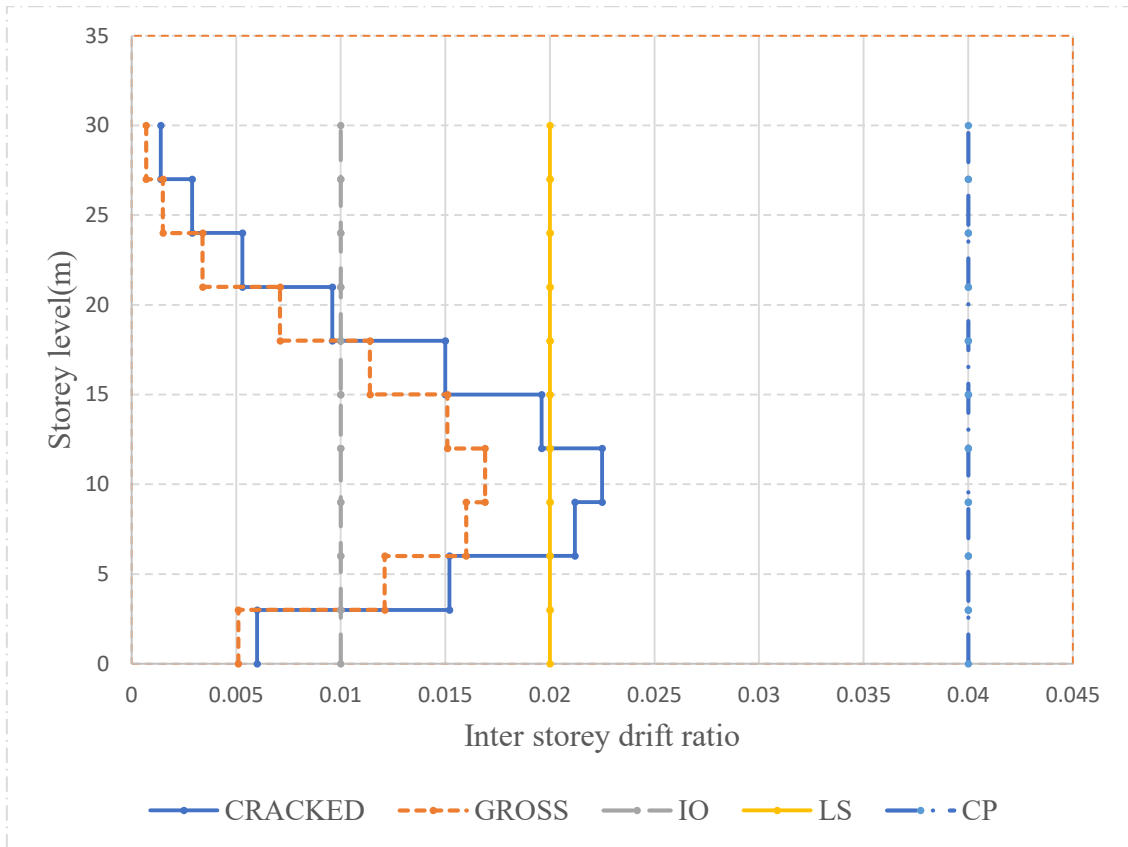
Figure 4.25: Comparison of Inter-storey drift ratios between Cracked and Gross sections for 10-Storied RC buildings
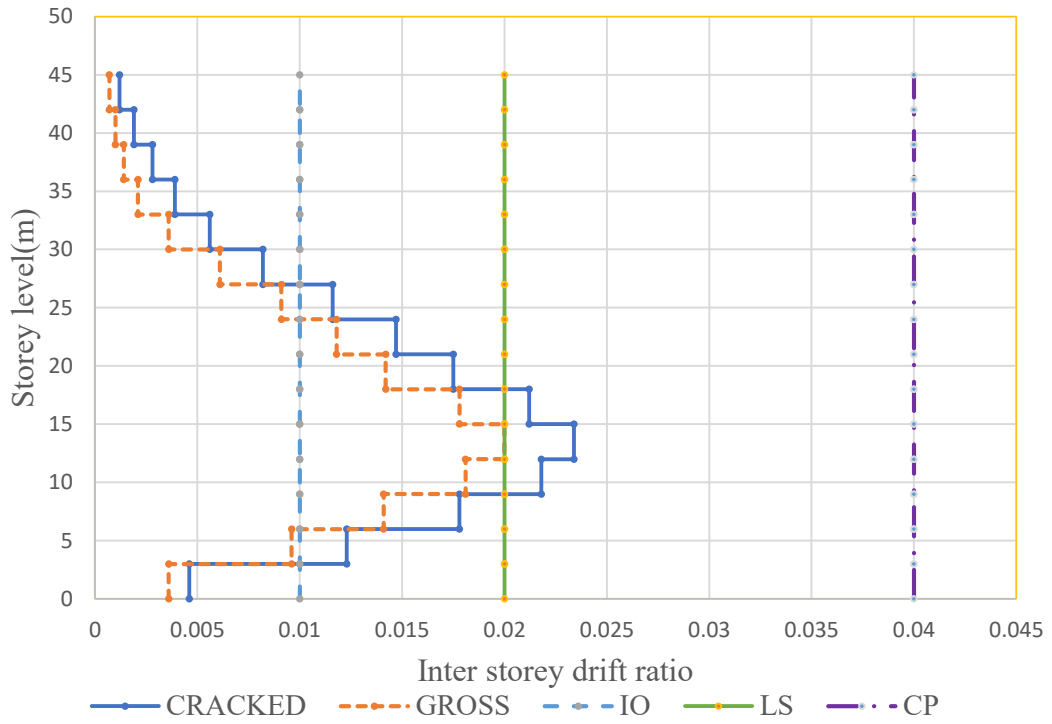
Figure 4.26: Comparison of Inter-storey drift ratios between Cracked and Gross sections for 15-Storied RC buildings
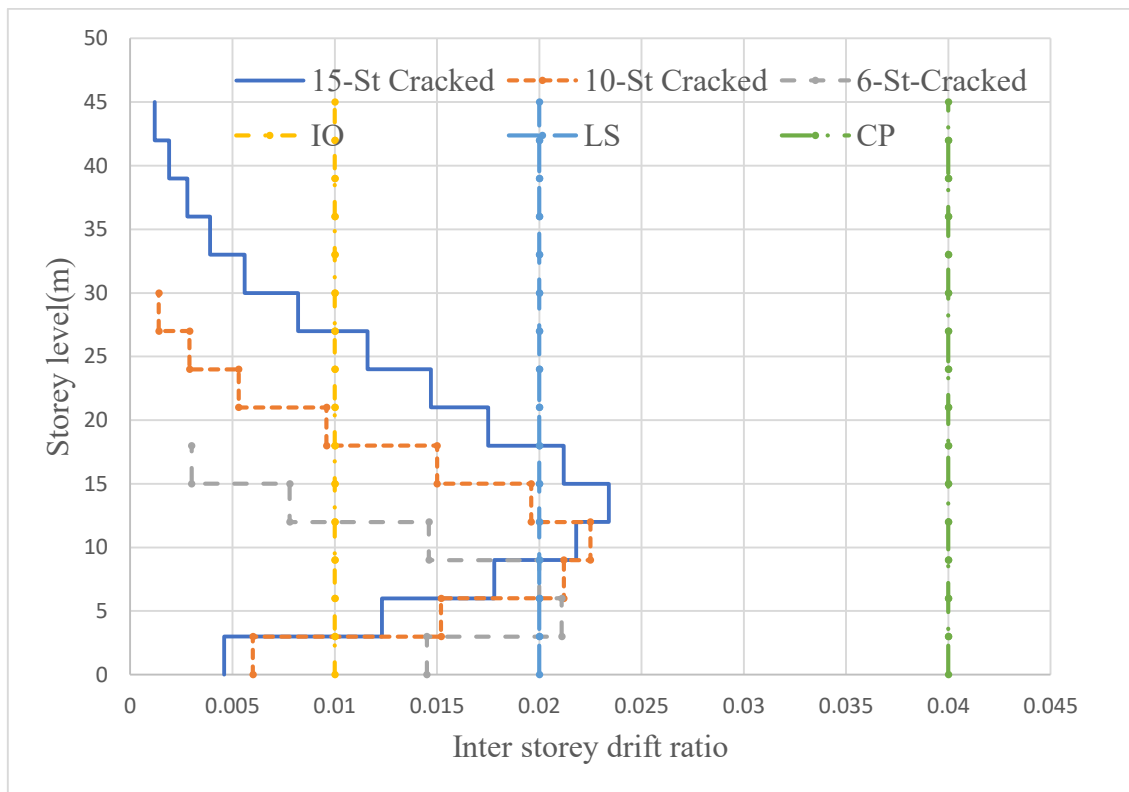
Figure 4.27: Comparison of drift ratio among 6,10,15-storied Cracked section buildings
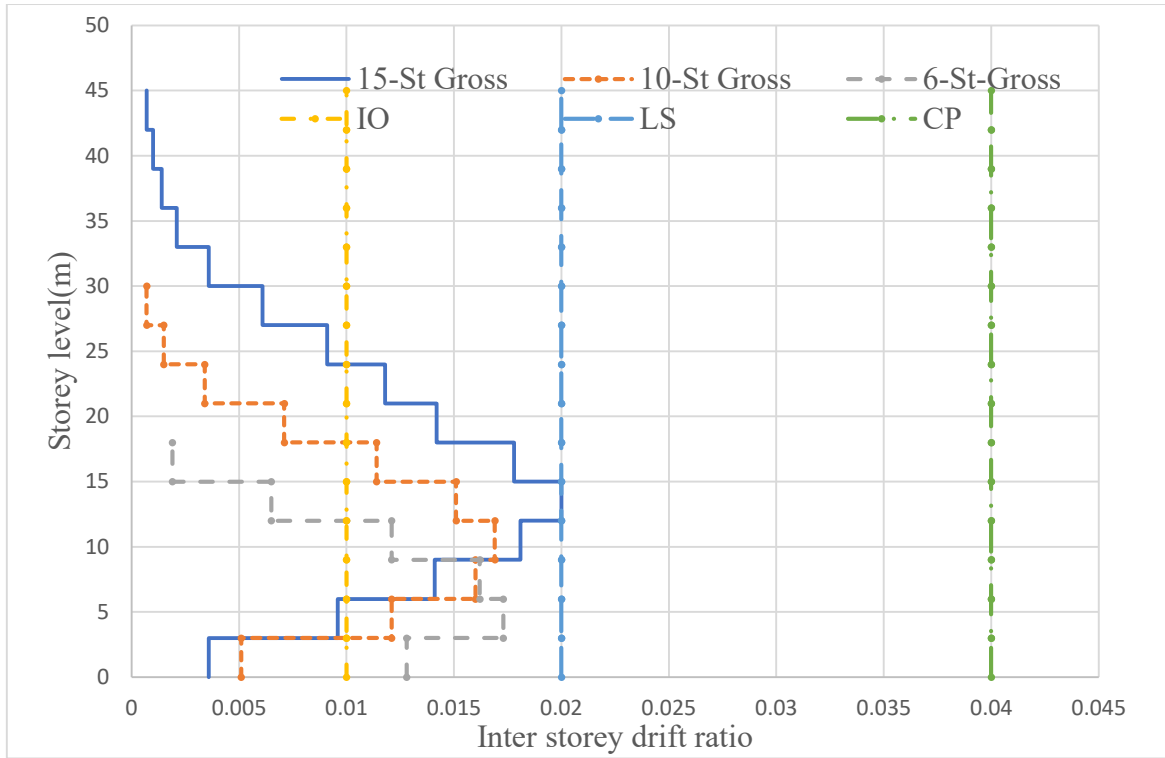
Figure 4.28: Comparison of drift ratio among 6,10,15-storied Gross section buildings
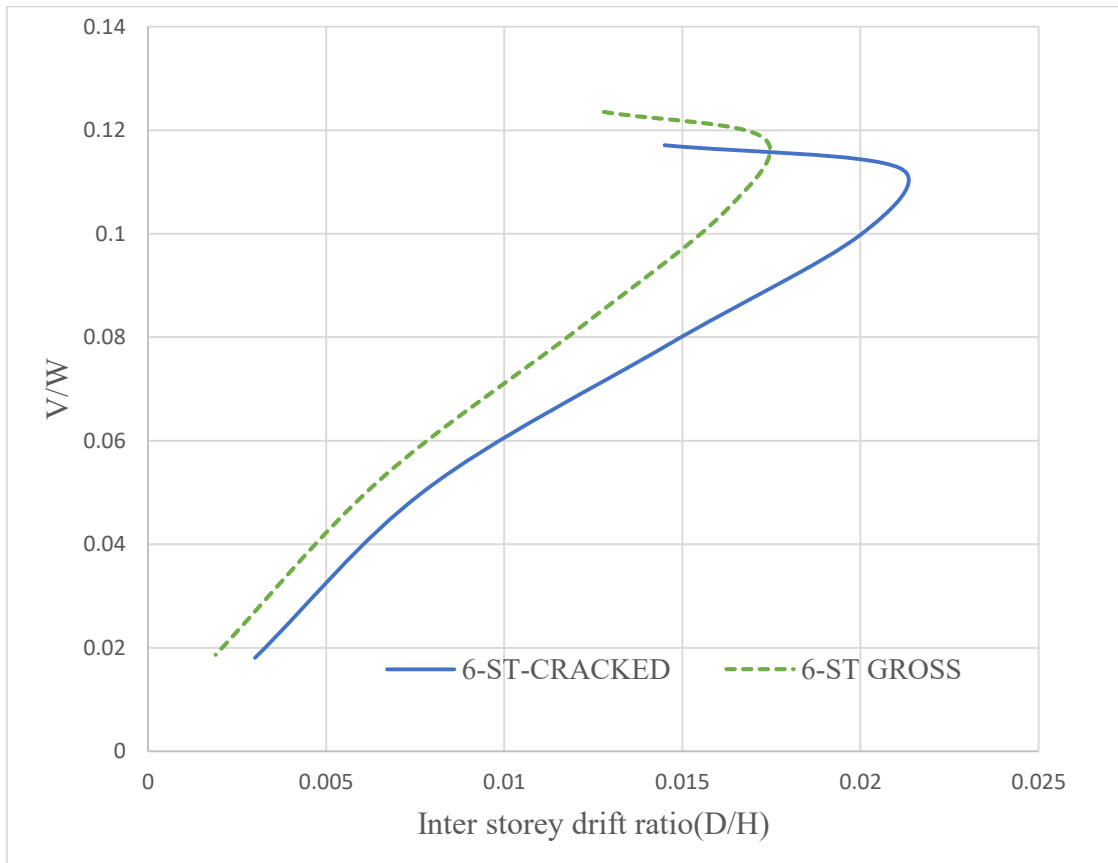
Figure 4.29: D/H vs. V/W curves for 6-storied Cracked and Gross section buildings
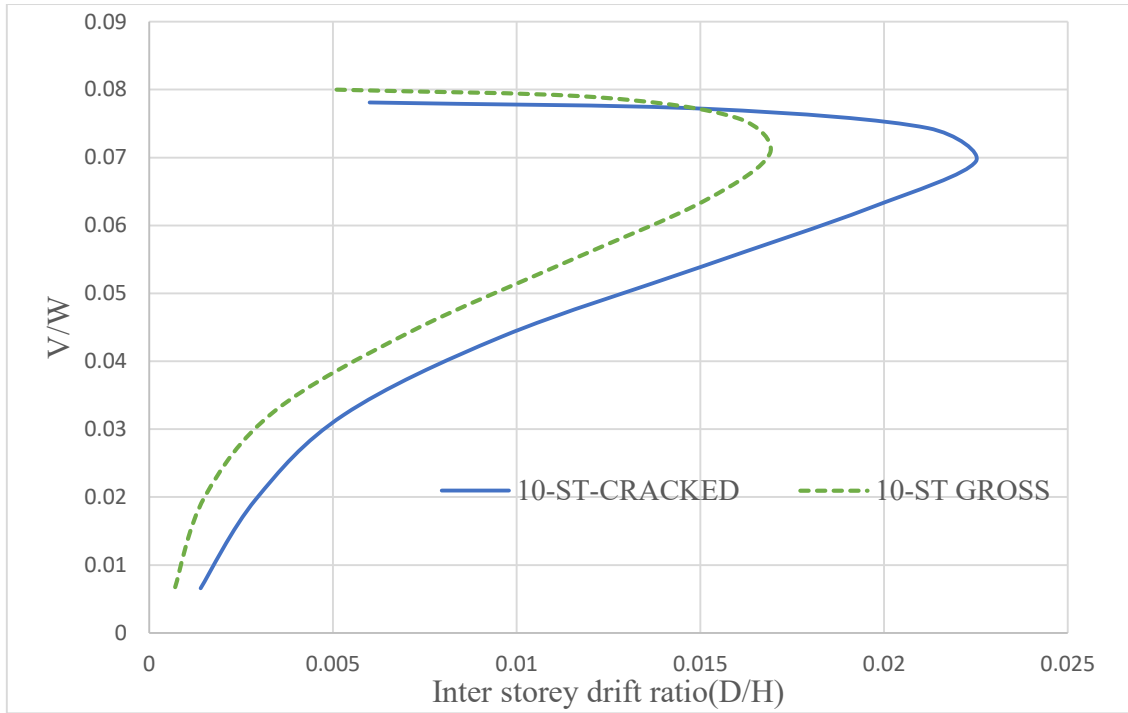
Figure 4.30: D/H vs. V/W curves for 15-storied Cracked and Gross section buildings
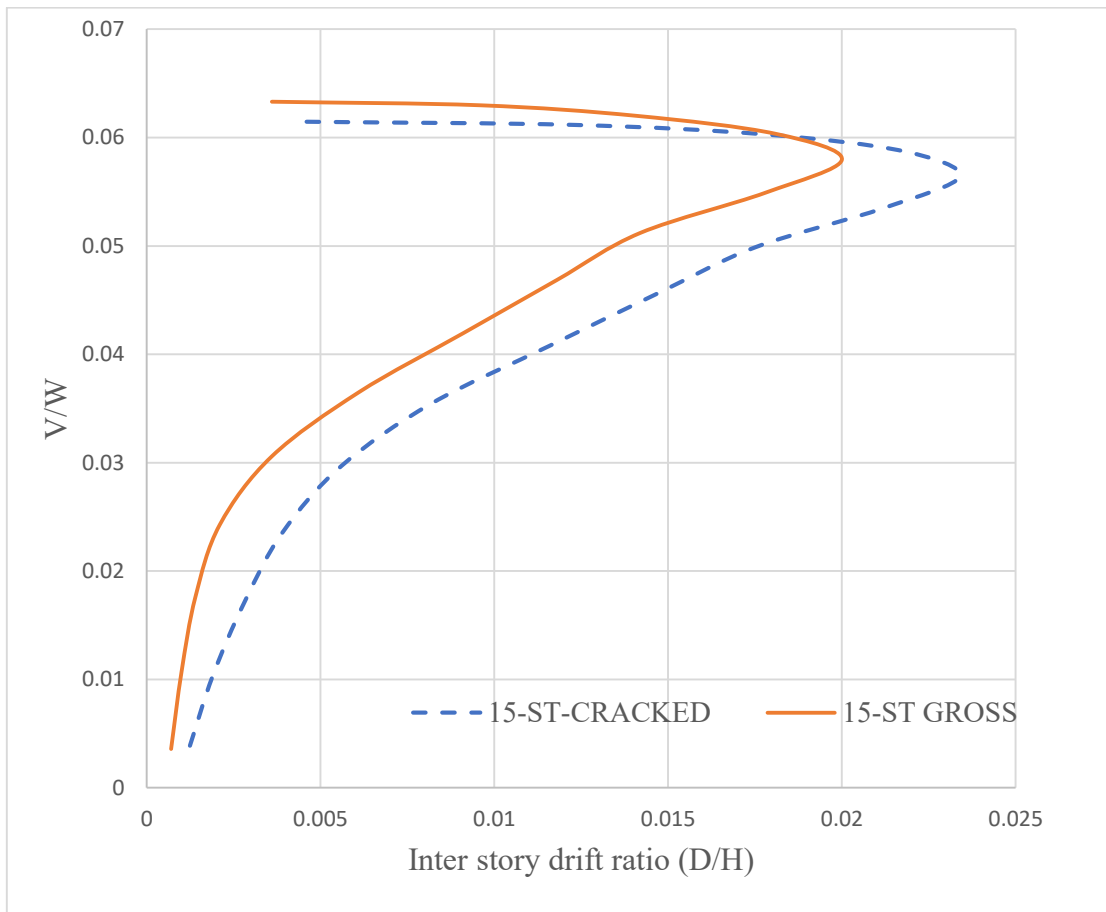
Figure 4.31: D/H vs. V/W curves for 15-storied Cracked and Gross section buildings

106
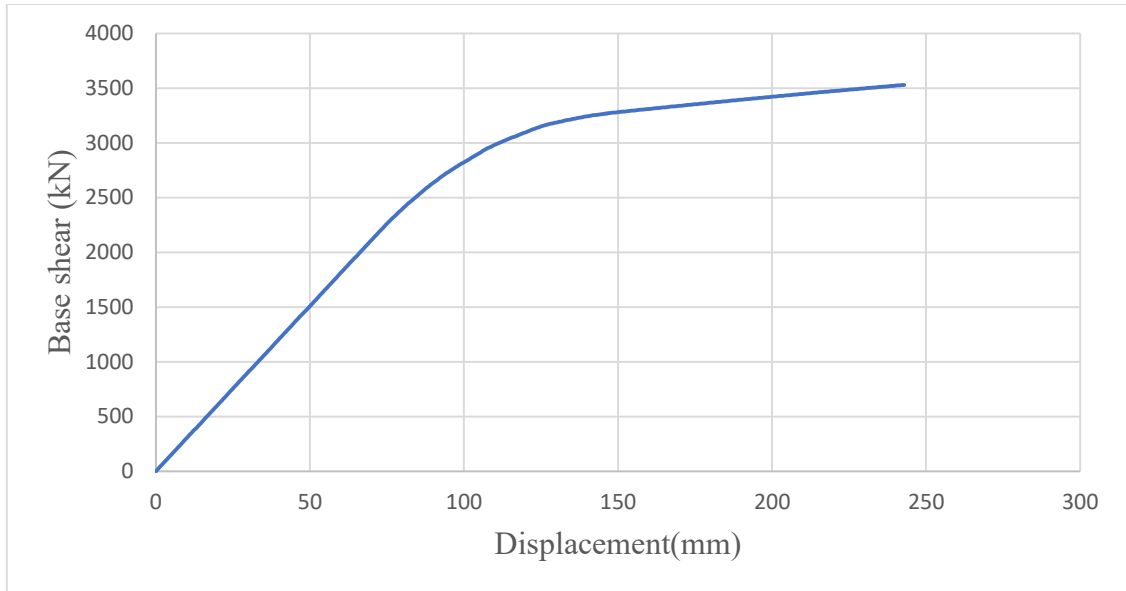
Figure 4.32: R value from Pushover curve for 6-storied Cracked section building

Δ_{max}=243 mm, V_e = 3530 kN, Δ_y=130 mm

R= 3.23
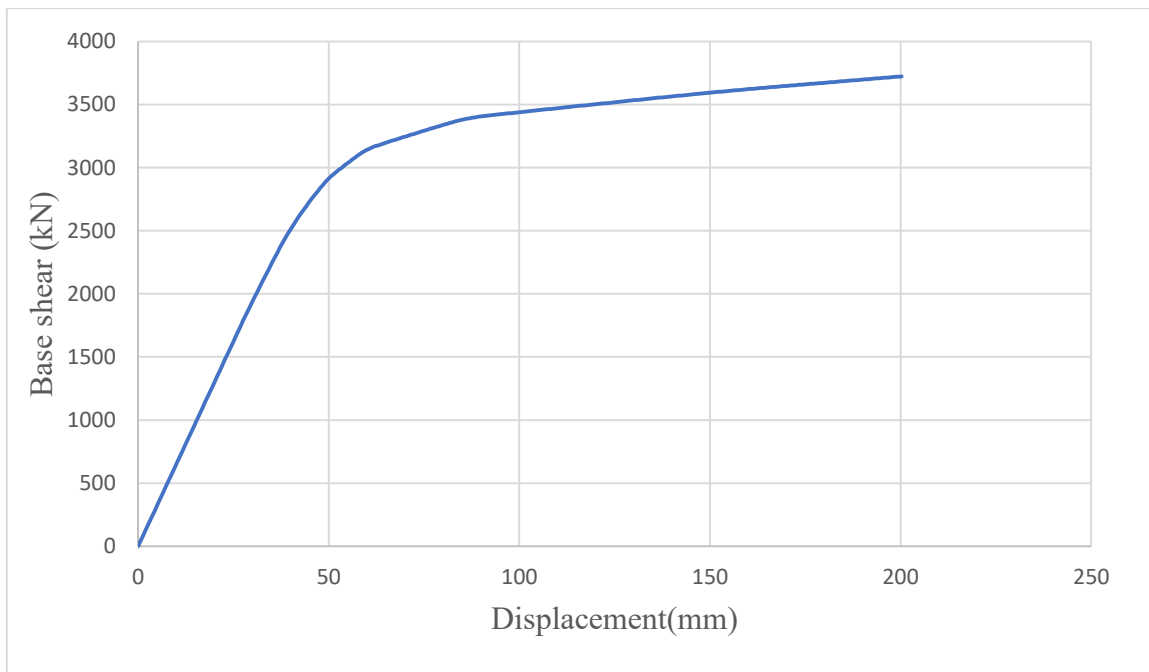
Figure 4.33: R value from Pushover curve for 6-storied Gross section building

Δ_{max}=201 mm, V_e = 3724 kN, Δ_y=65 mm

R= 5.64
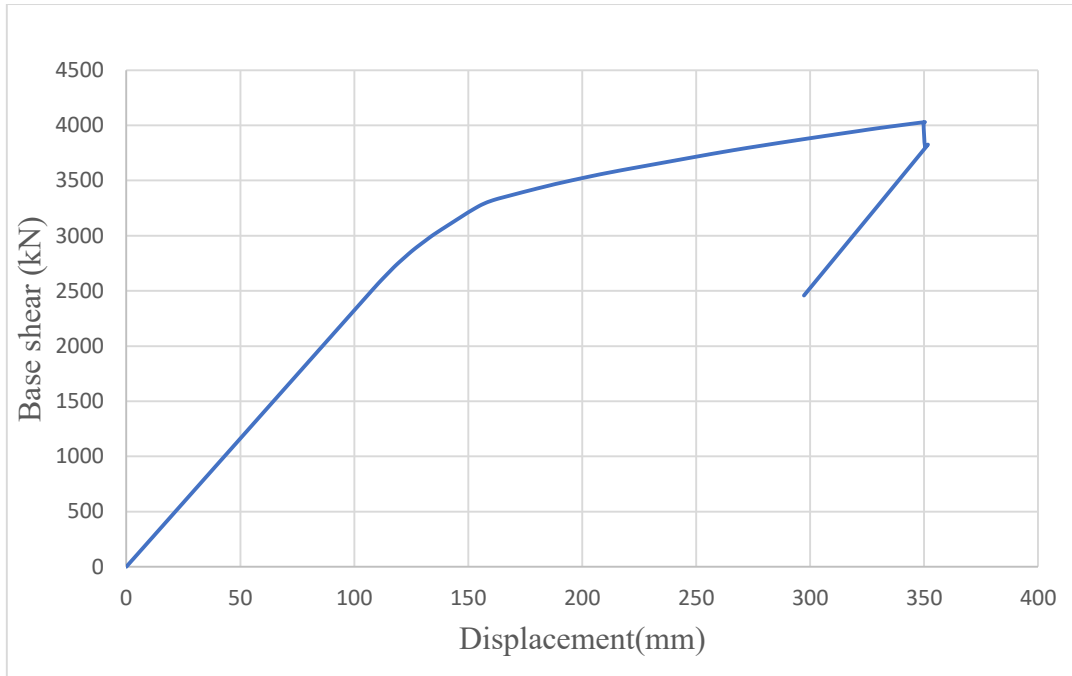
Figure 4.34: R value from Pushover curve for 10-storied Cracked section building

Δ_{max} =351 mm, V_e=4030 kN, Δ_y=210 mm

R= 2.92
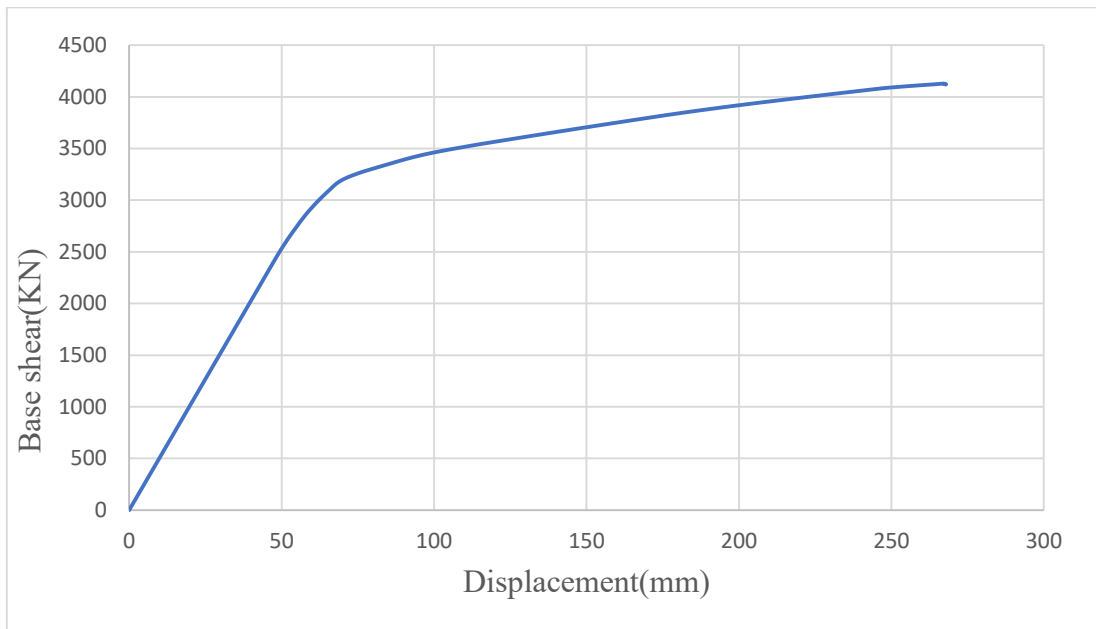
Figure 4.35: R value from Pushover curve for 10-storied Gross section building

Δ_{max}=268 mm, V_e= 4129 kN, Δ_y= 103 mm

R= 4.65
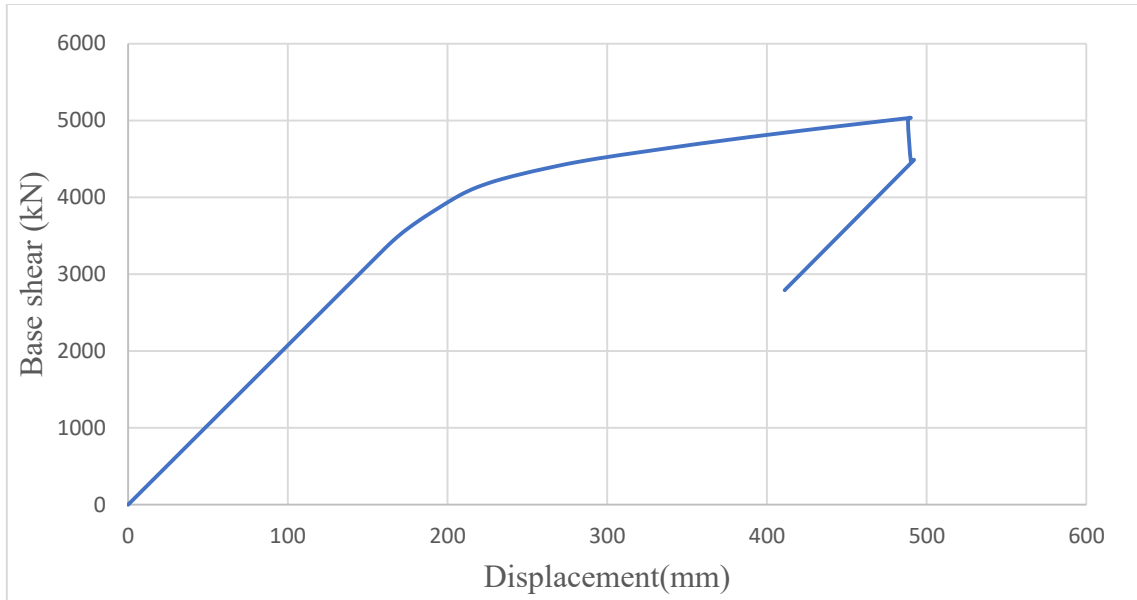
Figure 4.36: R value from Pushover curve for 15-storied Cracked section building

Δ_{max}= 491 mm, V_e=5036 kN, Δ_y= 277 mm

R = 3.41
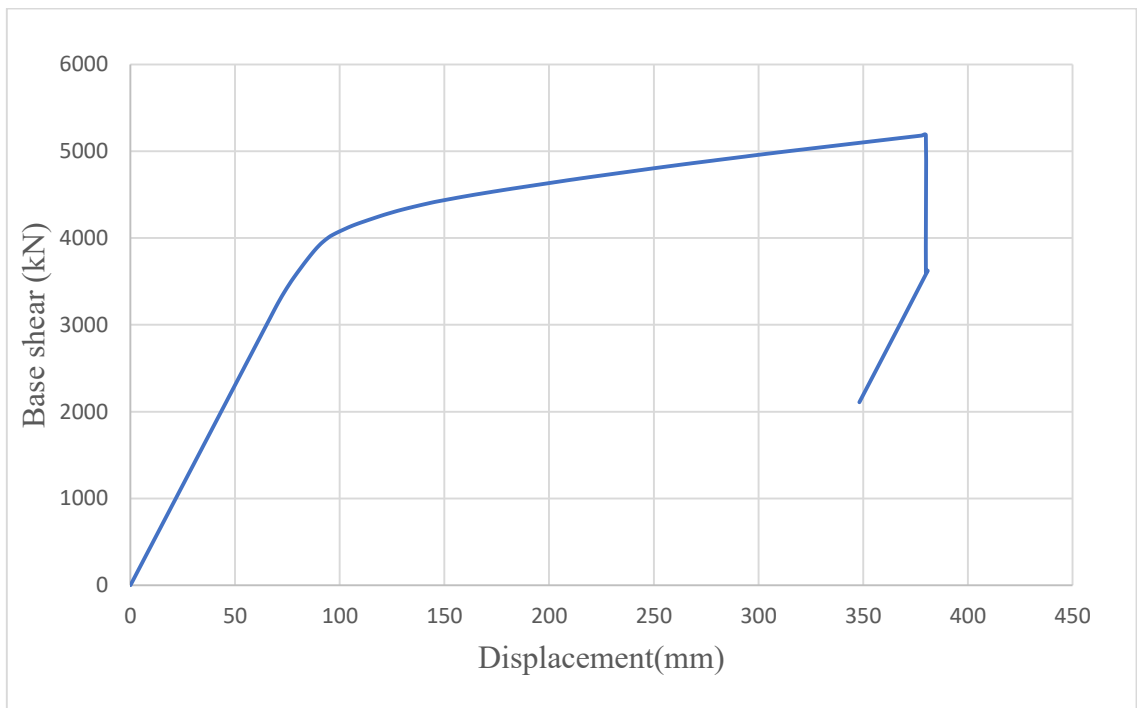
Figure 4.37: R value from Pushover curve for 15-storied Gross section building

Δ_{max}=380 mm, V_e=5187 kN, Δ_y=135 mm

R =5.57

Table 4.2 shows the comparison between the base shears obtained using draft BNBC 2017 and BNBC 2006. The base shear values as per BNBC 2006 is lower than those of the values as per draft BNBC 2017. However, this value is comparable at factored load level. Seismic load factor is used 1.4025 as per BNBC 2006 while this factor is 1 as per draft BNBC 2017.

Table 4.2: Comparison of elastic base shear between BNBC 2006 and BNBC 2017

Serial No	Description of the RC building	Elastic base shear [BNBC 2006]	Elastic base shear [BNBC 2017(draft)]
01	6-storied	1056 kN	2040 kN
02	10-storied	1453 kN	2311 kN
03	15 storied	1886 kN	2622 kN

4.2.5 Target displacements for the considered buildings

Analyses on the building models have been conducted to determine the target displacement. Table 4.3 present the target displacement requirements as per BNBC and also obtained results from numerical analyses. From the table, it is shown that all the building models satisfy the target displacement requirements.

Table 4.3: Target displacement requirements as per code and obtained results

Building	Building Type	Target displacement [BNBC 2017] (mm)	Target displacement [Analysis](mm)	Remarks
6-st	Cracked Section	57	90	OK
6-st	Gross Section	26	65	OK
10-st	Cracked Section	75	150	OK
10-st	Gross Section	46	110	OK
15-st	Cracked Section	116	280	OK
15-st	Gross Section	63	180	OK

4.3. Response reduction factor, R of the buildings

A comprehensive study has been conducted to determine the response reduction factor, R of the considered buildings. Both the cracked and gross section properties of the structural members of the buildings have been considered. In addition, analyses have been conducted on the three dimensional (3D) to assess the variation in R values. These factors have been generated from the pushover curves for the considered buildings. Table 4.4 shows the values of R for the 3D analyses.

Table 4.4: Seismic response factor for the considered building using 3D analyses

Storey No	Building Type	R-Value
6-Storey	Cracked Section	3.23
6-Storey	Gross Section	5.64
10-Storey	Cracked Section	2.92
10-Storey	Gross Section	4.65
15-Storey	Cracked Section	3.41
15-Storey	Gross Section	5.57

From the above tables, it is shown that buildings with gross section properties result higher values of response reduction factors than those of the cracked buildings. Figure 4.38 shows the R values obtained considering cracked and gross sections for 3D analyses. Figure 4.39 shows the comparison of R values considering gross, cracked and code provided. It is shown that from the figure, R values obtained considering cracked section is always lower than those of the gross section as well as code provided values.
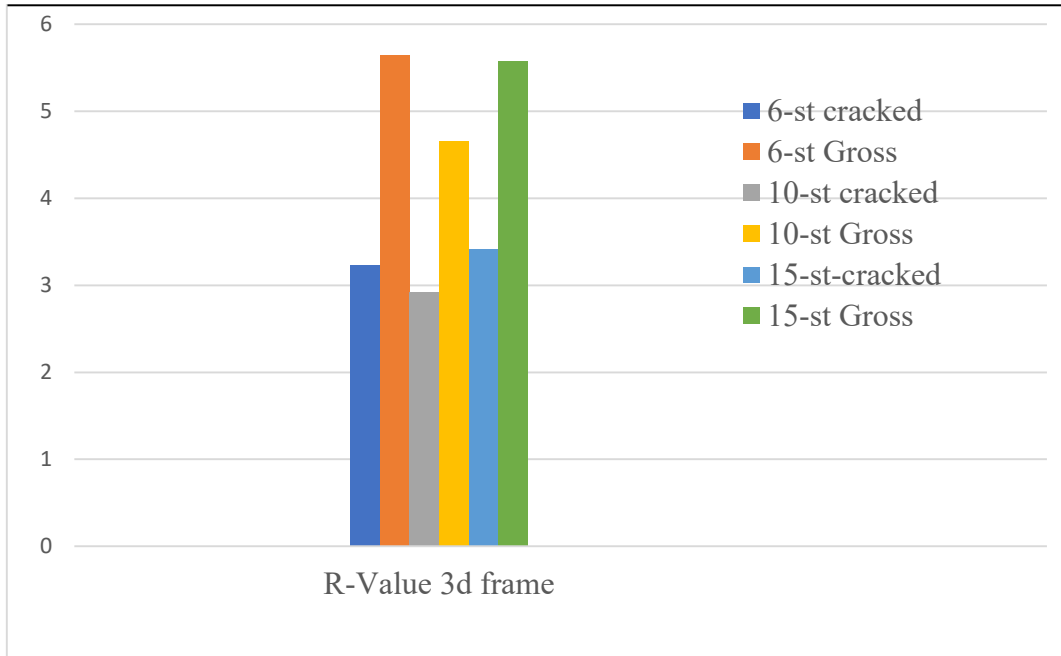
Figure 4.38: Comparison of seismic response factor R for 3D analyses
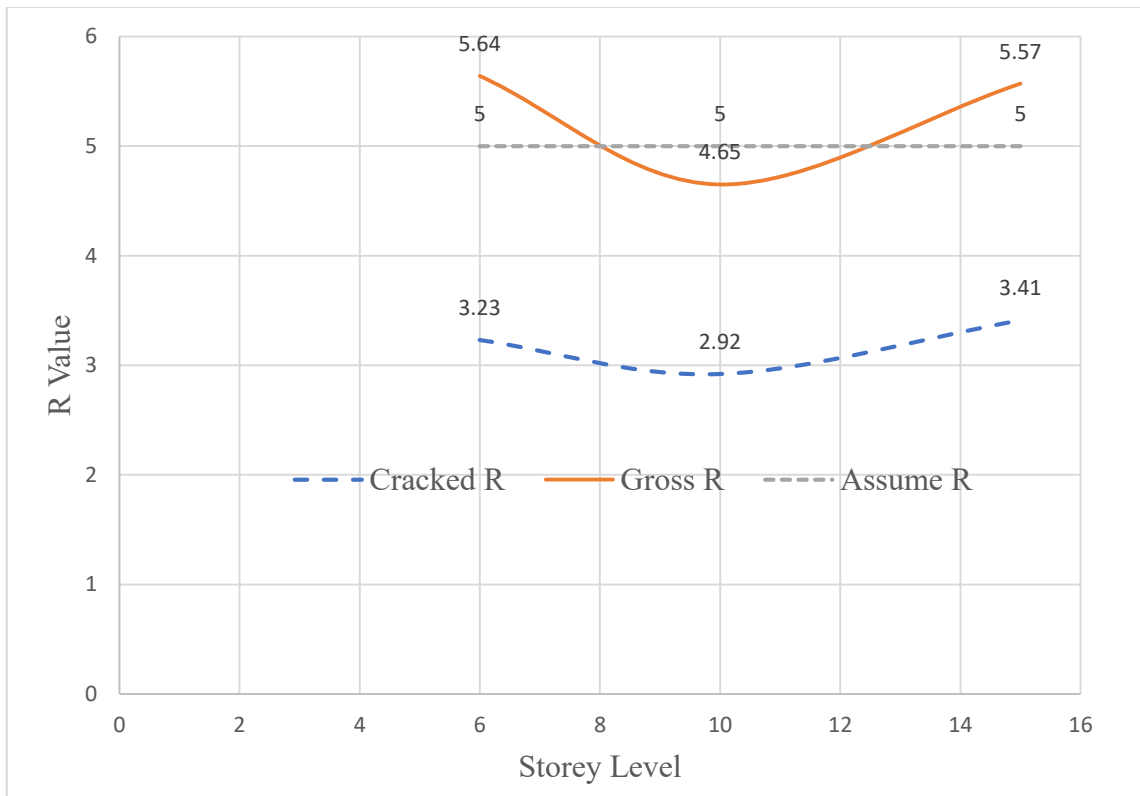
Figure 4.39: Comparison of R-value between Cracked and Gross section buildings

Chapter 5

CONCLUSIONS AND RECOMMENDATIONS

5.1 Introduction

A comparative seismic performance assessment of 6, 10, and 15-storey RC frame buildings analyzed and designed with gross section and cracked section properties. Equivalent static force method has been utilized to design the buildings as per BNBC 2017(draft). The seismic performances of the RC frames are evaluated using the nonlinear static pushover (NSP) analysis. The obtained results show that the drift at design loads for the RC frames designed with gross section is well within the prescribed limit. The inter-storey drift has been determined for 6-, 10-, and 15-storey RC frames designed with cracked and gross sections and compared with the drift limits provided by draft BNBC 2017. Since the design criteria significantly affect the seismic performance of the RC frames, the objective was also to assess the collapse level during the major earthquake events in all the RC frame buildings. The performance level of 6-, 10-, and 15-storey RC frames designed with cracked section and designed for force criteria corresponding to collapse prevention is evaluated for maximum considered earthquake (MCE).

The effect of reduction of flexural stiffness of RC sections during earthquake in terms of the lateral deformation of RC structures has been evaluated and is compared with the code provision. The effects of degradation of flexural stiffness on the inter-storey drift of RC frame has also been evaluated for the considered buildings. Response reduction factor R is determined for the buildings considering the gross and cracked stiffness properties. In addition, the buildings have been analyzed considering two dimensional and three dimensional to assess the variation of the results. Finally, the overall effect of cracked and gross sections of structural members of the buildings on the serviceability and strength parameters have been stated.

5.2 Conclusions from the present study

Based on results from numerical analyses, followings are the main conclusions of this research study:

(a) The results of the pushover analysis show that the inter-storey drift at the design

load of RC frames using gross section property is well within the prescribed limit of maximum permissible inter-storey drift. While the inter-storey drift of RC frame designed using cracked section properties of beams and columns is observed beyond the limit of maximum permissible inter-storey drift.

(b) The column reinforcement demand for the building with cracked section properties is higher than that of the gross section properties. The increase in reinforcement demand is higher for exterior and corner columns than those of the interior columns.

(c) The increase in column reinforcement demand with cracked section properties is higher for the building with 6-storied in comparison to 10 and 15-storied buildings. The corner column at the ground floor level of 6-storied cracked building demands an increase of 27.4% reinforcements while that of 10 and 15-storied demand 17.4% and 10.2%, respectively.

(d) The increase of reinforcement demand for beams of the buildings with cracked section properties is insignificant in comparison to that of the gross section properties,

(e) The seismic performance level of RC frame buildings for hazard level corresponding to design basis earthquake (DBE) and maximum considered earthquake (MCE) show that the performance level of 6-st RC frame building gross and cracked sections are found to be "IO" for DBE and MCE.

(f) Similarly, the performance level of 10-st RC frame buildings with gross and cracked sections are found "IO" for DBE. The performance level of 10-st RC frame buildings with gross and cracked sections are found "LS" for MCE.

(g) The performance level of 15-st RC frame buildings with gross and cracked sections are obtained "LS" for DBE. The performance level of 15-st RC frame buildings with gross section is found "LS" for MCE while that of 15-st with cracked section is found "CP" for MCE.

(h) Response reduction factors of the buildings with gross section properties result higher values than those of the cracked buildings. R values always fall below the design R for the cracked section buildings and it is obtained 3.23 for the 6-storied building,

(i) RC buildings with gross and cracked section properties satisfy the target displacement requirements as per the code.

5.3 Future Recommendations

This study mainly focused on seismic performance assessment of RC buildings with crack and gross section properties. Response reduction factor, R as per draft BNBC-2017 of frame buildings have been utilized to determine the earthquake effects on the buildings. A regular plan of 6, 10, 15-storied buildings are considered for seismic design category SDC C located in seismic zone-2 of Bangladesh. This work may be extended in future to include the following:

(a) Different seismic design category as well as different seismic zoning of Bangladesh can be considered for the design and analysis of the RC buildings with cracked and gross section properties.

(b) Variation of span length/bay dimensions for the building may be considered.

(c) Nonlinear behavior of RC cracked and gross section building frame system for vertical and plan irregularities can be studied to assess their performance under a seismic event.

(d) Different pushover analysis methods i.e. adaptive pushover, modal pushover may be studied.

(e) Nonlinear time history analysis for RC three-dimensional buildings may be carried out.

REFERENCES

ASCE/SEI 7-05. *Minimum Design Loads for Buildings and Other Structures*, American Society of Civil Engineers, Reston (VA), (2010).

Ahmed, M., Dad Khan, M. K., and Wamiq, M., "Effect of concrete cracking on the lateral response of RCC buildings," *Asian Journal of Civil Engineering*, Vol. 09, Issue No.1, 2008, pp. 25-34.

ASCE/SEI 41-13, *Seismic evaluation and retrofit of existing buildings*, American Society of Civil Engineers, Reston, VA, USA. (2014).

ACI 318-08, *Building Code Requirements for Structural Concrete*, American Concrete Institute, Farmington Hills, MI. USA.

ACI 318-11, *Building Code Requirements for Structural Concrete*, American Concrete Institute, Farmington Hills, MI. USA.

ACI 318-14, *Building Code Requirements for Structural Concrete, Michigan*. USA

ATC-3-06, "*Tentative Provisions for the Development of Seismic Regulations for Buildings*," Applied Technology Council, 555 Twin Dolphin Drive, Suite 550 Redwood City, CA 94065, 1978.

ATC 10, "An Investigation of the Correlation between Earthquake Ground Motion and Building Performance," ATC 10 Report, Applied Technology Council, Redwood City, California, 1982.

ATC-19, "*Structural Response Modification Factor*," Applied Technology Council, California, USA, 1995.

ATC-40, "*Seismic Evaluation and Retrofit of Concrete Buildings*," Applied Technology Council, California, USA, 1996.

ASCE 41, "*Seismic Evaluation and Retrofit of Existing Buildings*," American Society of Civil Engineers, Reston, VA, USA, 2013.

Ahmed, J. and Raza, S. A., "Seismic vulnerability of RC buildings by considering plan irregularities using pushover analysis," Global Journal for Research Analysis, Vol.3, Issue-9, Sept-2014, pp. 42-47.

Albanesi, T., Nuti, C., and Vanzi, I., "A simplified procedure to assess the seismic response of nonlinear structures," Earthquake Spectra, Vol.16, Issue No-4, 2000, pp. 715-734.

Albanesi, T., Biondi, S., and Petrangeli., "Pushover analysis: An energy based approach" Proceedings of the 12th European Conference on Earthquake Engineering, 2002, Elsevier Science Ltd, vol.3, Issue No-4, paper no. 605,ISSN:2456-6667.

Antoniou, S. and Pinho, R., "Development and verification of a displacement-based adaptive pushover procedure," Journal of Earthquake Engineering, Vol. 8, Issue No. 5, 2004, pp. 643-661.

Bangladesh National Building Code-1993, Housing and Building Research Institute (HBRI). Vol. 2, Part 6, Dhaka, Bangladesh, (2006).

Bangladesh National Building Code-2017, Housing and Building Research Institute (HBRI). Vol. 2, Part 6, Dhaka, Bangladesh (Draft BNBC-2017).

Bonet, J.L., Romero, M.L., and Miguel, P.F., "Effective flexural stiffness of slender reinforced concrete columns under axial forces and biaxial bending," *Engineering Structures* Vol. 33, 2011, pp. 881–893.

BSSC, "1997 Edition: NEHRP Recommended Provisions for Seismic Regulations for New Buildings and Other Structures, Part 1 - Provisions." Report No. FEMA-302, Federal Emergency Management Agency, Washington, D.C., 1998.

Bracci, J.M., Kunnath, S.K., and Reinhorn, A.M., "Seismic performance and retrofit evaluation for reinforced concrete structures" ASCE, Journal of Structural Engineering, Vol.123, 1997, pp. 3-10.

Cavdar, O., Cavdar, A., and Bayraktar, E., "Earthquake performance of reinforced-concrete shear-wall structure using nonlinear methods," Journal of Performance of Constructed Facilities, 2018, Vol.32, Issue No-1: Article-04017122.

Cimellaro, G.P., Giovine, T., and Lopez-Garcia, D., "Bidirectional pushover analysis of irregular structures," Journal of Structural Engineering, 2014, Vol.140, Issue No-9: Article- 04014059

Chopra A.K. and Goel R. K., "Evaluation of modal and FEMA pushover analysis: SAC buildings," *Earthquake Spectra*, Vol. 20, Issue No. 1, 2004, pp. 225-254.

Chopra A. K. and Goel R. K., "A modal pushover analysis procedure for estimating seismic demands for buildings," *Earthquake Engineering and Structural Dynamics*, Vol. 31, Issue No. 3, 2002, pp. 561–582.

Chopra, A.K. and Goel, R.K., "Evaluation of NSP to estimate seismic deformation: SDF systems," Journal of Structural Engineering, Vol. 126, Issue No-4, 2000, pp. 482-490.

Chopra, A.K., Goel, R.K., and Chintanapakdee, C., "Evaluation of a modified MPA procedure assuming higher modes as elastic to estimate seismic demands," Earthquake Spectra, Vol.20, 2004, pp.757-778.

Causevic. M., Frankovic, T., and Mahmutovic, N., "Effects of stiffness reduction on seismic capacity of buildings", *Gradevinar,* Vol. 6, 2012, pp. 463- 474.

Clough R. W., King. I. P., and Wilson E. L., "Structural analysis of multistory buildings," *Proceedings, American Society of Civil Engineers, Structural Division,* Vol. 90, Issue No. 3, 1964, pp. 19-34.

Coleman, J. and Spacone, E., "Localization issues in force-based frame elements," *Journal of Structural Engineering,* ASCE; Vol. 127, Issue No. 11, 2001, pp. 1257–1265.

Corley G.W., "Rotation Capacity of Reinforced Concrete Beams," *ASCE Journal of Structural Division*, Vol. 92, Issue No. 10, 1966, pp. 121–146.

CEN (Comité Européen de Normalisation) Techn. Comm. 250. *Eurocode 8: Design of Structures for Earthquake Resistance—Part 1: General Rules, Seismic Actions and Rules for Buildings (EN 1998-1:2004).* Brussels: CEN; (2004).

Computers and Structures Inc. (CSI), SAP2000 Three Dimensional Static and Dynamic Finite Element Analysis and Design of Structures, Berkeley, California, 2010.

Ceroni, F., Manfredi, G., and Maria, R. P., "A formulation of plastic hinge length in R.C. columns", Department of Engineering, University of Sannio. Department of Analysis and Structural Design, University of Naples Federico II. 17 May 2007.

Chan, C. and Wang, Q., "Nonlinear stiffness design optimization of tall reinforced concrete buildings under service loads," Structural Engineering journal, Vol. 132, Issue No. 6, 2006, pp. 978-990.

Chopra, A.K. and Goel, R. K., "Capacity-demand-diagram methods based on inelastic design spectrum," *Earthquake Spectra*, Vol.15, 1999, pp. 637-656.

Das, S. and Choudhury, S., "Influence of effective stiffness on the performance of RC frame buildings designed using displacement-based method and evaluation of column effective stiffness using ANN," *Engineering Structures*, Vol. 197, 2019, Article 109354.

Dolsek, M. and Fajfar, P., 'Simplified non-linear seismic analysis of infilled reinforced concrete frames," *Earthquake Engineering and Structural Dynamics*, Vol. 34, 2005, pp.49- 66.

Eurocode 4: Design of composite steel and concrete structures - Part 1-1: General rules and rules for buildings

ETABS 18 [Computer software]: *Computers and Structures, Inc.,* Berkeley, CA.

Elwood, K.J. and Eberhard, M.O., "Effective stiffness of reinforced concrete columns," ACI Structural Journal, Vol. 106, Issue No. 4, 2009, pp. 476–484.

Elnashai, A. S., "Advanced inelastic static (pushover) analysis for earthquake applications," Structural Engineering and Mechanics, Vol.12, Issue No-1,2001, pp. 51-69.

Elwood, K. J., "Update to ASCE/SEI 41 concrete provisions" Earthquake Spectra, Vol. 23, Issue No-3, 2007, pp. 493–523.

European Committee for Standardization. Eurocode 2: design of concrete structures—part 1: general rules and rules for buildings. EN 1992-1-1. December 2004.

Faella, G., "Evaluation of RC structures seismic response by means of nonlinear static pushover analyses", 11th World Conference on Earthquake Engineering, Acapulco, Mexico, 1996, Paper no. 1146.

Fajfar, P., "A nonlinear analysis method for performance-based seismic design," Earthquake Spectra, Vol.16, Issue No. 3, 2000, pp. 573-592.

Fajfar, P. and Fischinger, M., "N2 – A method for non-linear seismic analysis of regular structures." Proc. 9th World Conf. on Earthquake Engineering, Tokyo/Kyoto, Vol. 5, 1988, pp.111-116.

Fajfar, P. and Gaspersic, P., "The N2 method for the seismic damage analysis for RC buildings," Earthquake Engineering Structural Dynamics, Vol. 25, Issue No-1, 1996, pp. 23–67.

Fajfar, P., Gaspersic, P., and Drobnic, D., "A simplified nonlinear method for seismic damage analysis of structures," Proceedings Workshop on Seismic Design Methodologies for the Next Generation of Codes, Rotterdam, Balkema, June,1997, pp.183-194.

Freeman S.A., "Prediction of response of concrete buildings to severe earthquake motion," Douglas McHenry International Symposium on Concrete and Concrete Structures, SP-55, American Concrete Institute, Detroit, Michigan, 1978, pp. 589- 605

FEMA 273: "*NEHRP Guidelines for the Seismic Rehabilitation of Buildings*," Federal Emergency Management Agency, Washington, D.C. USA, 1997.

FEMA 356: "*Prestandard and Commentary for The Seismic Rehabilitation of Buildings*," Federal Emergency Management Agency, Washington, D.C. USA, 2000.

FEMA 440: "Improvement of Nonlinear Static Seismic Analysis Procedures," Federal Emergency Management Agency, Washington, D.C. USA. (2005).

Ferguson P. M., Breen J. E., and Jirsa J. O., "Reinforced concrete fundamentals," John Wiley and Sons. Canada, Chapter 22, 1988, pp. 683-684.

Foutch, D. A. and Wilcoski, J., "A rational approach for determining response modification factors for seismic design of buildings using current code provisions," *Earthquake Spectra,* Vol. 21, Issue No. 2, 2005, pp. 339–352.

Fajfar, P. and EERI, M., "A nonlinear analysis method for performance based seismic design," *Earthquake Spectra*, Vol. 16, Issue No. 3, 2000, pp. 573-592.

Fajfar, P. and Fischinger, M., "N2 – A method for non-linear seismic analysis of regular buildings," in *Proceedings of the 9th World Conference on Earthquake Engineering"* Tokyo, Kyoto, Maruzen, Tokyo, Vol. 5, 1988, pp. 111-116 .

Freeman, S.A., "The capacity spectrum method for determining the demand

displacement," ACI Spring Convention, 1994.

Gaspersic, P., Fajfar, P., and Fischinger, M., "An approximate method for seismic damage analysis of building," Proc. I0th world conference in earthquake engineering, Balkema, Rotterdam, 1992, pp. 3921-3926.

George, G. P. and Gregory, G. P., "Concrete Buildings in Seismic Regions," Taylor and Francis Group, LLC, 2014.

Goel, R.K. and Chopra A.K., "Role of higher- 'Mode' pushover analyses in seismic analysis of buildings," Earthquake Spectra, Vol. 21, Issue No-4, 2005, pp.1027-1041.

Gulkan, P. and Sozen, M.A., "Inelastic response of reinforced concrete structures to earthquake ground motions," *Journal of the American Concrete Institute*, Vol. 71, No. 12, 1974, pp. 604-610.

Gupta, B. and Kunnath, S. K., "Pushover analysis of isolated flexural reinforced concrete walls." Structural Engineering in the 21st Century, Proc. Structures Congress, New Orleans.1999, pp.410-414.

Gupta, B. and Kunnath, S. K., "Adaptive spectra-based pushover procedure for seismic evaluation of structures," Earthquake Spectra, Vol.16, Issue No-2, 2000, pp. 367–391.

Hakim, R.A., Alama, M.S., and Ashour, S.A., "Seismic assessment of RC building according to ATC40, FEMA356 and FEMA440", Arab J Sci Eng., Vol.39, 2014, pp.7691-7699.

Hete, S. P., Bhadke, S. K., and Khedikar, A., "Pushover analysis of existing RC frame structure: a state of the art review," International Research Journal of Engineering and Technology, Vol. 05, Issue-4, April-2018.

Inel, M. and Ozmen, H. B., "Effect of plastic hinge properties in nonlinear analysis of reinforced concrete buildings," *Engineering Structures*, Vol. 28, 2006, pp. 1494-1502.

Iwan, W. D., "Implications of near-fault ground motion for structural design" Proceedings of the US-Japan Workshop on Performance-Based Earthquake Engineering Methodology for RC Building Structures, PEER Center Report, UC Berkeley - 17-25, Maui, 1999, Hawai.

Jingjiang, S., Ono, T., Yangang, Z., and Wei, W., "Lateral load pattern in pushover analysis," Earthquake Engineering and Engineering Vibration, Vol. 2, Issue No.1, 2003, pp. 99-107.

Kalkan, E. and Kunnath, S.K., "Assessment of current nonlinear static procedures for seismic evaluation of buildings," Engineering Structures, Vol. 29, 2007, pp. 305-316.

Kaushik, H. B. and Mane, A. L., "Effect of cracked section on lateral response of RC structures," *In 14th European conference on earthquake engineering, Ohrid,* Vol. 1, 2010.

Kwon, J. and Ghannoum, W. M., "Assessment of international standard provisions on stiffness of reinforced concrete moment frame and shear wall buildings," *Engineering Structures*, Vol. 128, 2016, pp. 149-160.

Kilar, V. and Fajfar, P., "Simple push-over analysis of asymmetric buildings," Earthquake Engineering and Structural Dynamics, Vol. 26, Issue No-2, 1997, pp. 233-49.

Khuntia, M. and Ghosh, S. K., "Flexural stiffness of reinforced concrete columns and beams: analytical approach," *ACI Structural Journal*, Vol. 101, Issue No. 3, May-June 2004, pp. 351-363.

Khuntia, M. and Ghosh, S. K., "Flexural stiffness of reinforced concrete columns and beams: experimental verification," *ACI Structural Journal*, Vol. 101, Issue No. 3, May-June 2004, pp. 364-374.

Kalkan, E. and Chopra, A.K., "Modal-pushover-based ground motion scaling procedure," *Journal of Structural Engineering* Special Issue, Vol.137, Issue No.3,2010.

Kunnath, S. K., "Identification of modal combinations for nonlinear static analysis of building structures," Computer-Aided Civil and Infrastructure Engineering, Vol.19, 2004, pp. 246-259.

Kunnath, S. K., Valles, M.R.E., and Reinhorn, A.M., "Evaluation of seismic damageability of a typical RC building in mid-west united states", 11th World Conference on Earthquake Engineering, Acapulco, Mexico.1996.

Lew, H.S. and Kunnath, S.K., "Evaluation of nonlinear static procedures for seismic design of buildings", Presented at the 33rd Joint Meeting of the UJNR Panel on Wind and Seismic Effects, 2001, pp. 1-17.

Liu, J., Zhang, Y. and Luo, P., "Flexural stiffness reduction factor of reinforced concrete column with equal L shaped section", The Twelfth COTA International Conference of Transportation Professionals, 2012, pp. 3187-3193.

Los Angeles Tall Buildings Structural Design Council, "An alternative procedure for seismic analysis and design of tall buildings located in the los angeles region." 2014 edition with 2015 supplements.

Mahaney, J.A., Paret, T.F., Kehoe, B.E., and Freeman, S.A., "The capacity spectrum method for evaluating structural response during the loma prieta earthquake" in "Earthquake hazard reduction in the central and eastern united states: A Time for examination and action", Proceedings of 1993 National Earthquake Conference, Earthquake Engineering Research Institute, Oakland, CA, U.S.A.,1993, pp. 501-510.

Makarios, T. K., "Optimum definition of equivalent non-linear SDF system in pushover procedure of multistory RC frames," Engineering Structures, Vol. 27, No. 5, 2004, pp. 814- 825.

Matsumori, T., Otani, S., Shiohara, H., and Kabeyasawa, T., "Earthquake member deformation demands in reinforced concrete frame structures", Proceedings of the US-Japan Workshop on Performance-Based Earthquake Engineering Methodology for R/C Building Structures, PEER Center Report,1999, UC Berkeley pp. 79-94, Maui, Hawaii.

Memari, A.M., Rafiee, S., Motlagh, A.Y., and Scanlon, A., "Comparative evaluation of seismic assessment methodologies applied to a 32-story reinforced concrete office building," JSEE, 2001, Vol. 3, Issue No. 1, pp. 31-43.

Mondal, S. S., *Remedial measures for reduction of seismic vulnerability in buildings with soft ground storey*, MSc Engg Thesis, BUET, 2009.

Moghadam, A. S., "A pushover procedure for tall buildings," 12th European Conference on Earthquake Engineering, Paper No. 395.

Mithaiwala, M., E., Patil, A. A., and Khadake, N. V., "A Review on Effect on Different set of stiffness modifiers varying through height of structure on analysis of multi-storey

R.C.C structure," International Research Journal of Engineering and Technology, Vol.07, Issue. No 08, Aug. 2020.

Moehle, J. P., "Performance-based seismic design of tall buildings in the U.S." The 14th World Conference on Earthquake Engineering, October 12-17, 2008, Beijing, China.

Madas, P., *Advanced Modeling of Composite Frames Subjected to Earthquake Loading.* Ph. D. thesis, Imperial College, University of London, London, 1993.

Moehle, J.P., Hooper, J.D., and Lubke, C.D., "Seismic design of reinforced concrete special moment frames," A Guide for Practicing Engineers, NEHRP Seismic Design Technical Brief No. 1, NIST GCR 8-917-1,2008.

Mwafy, A. and Elnashai, A.S., "Static pushover versus dynamic collapse analysis of RC buildings", Journal of Engineering Structures, Vol. 23, No. 5, 2001, pp. 407-424.

Mwafy, A. and Elnashai, A.S., "Calibration of force reduction factors of RC buildings," Journal of Earthquake Engineering, Vol. 6, No, 2, 2002, pp. 239-273.

"National Building Code of India 2016 (NBC-2016)" IS SP 7-NBC Bureau of Indian Standards (BIS)

"National Building Code of Canada 2015" The Structural Commentaries (User's Guide – NBC 2015: Part 4 of Division B)

Nilson, A.H., Darwin, D., and Dolan, C.W. *Design of concrete structure.* Thirteenth edition, Mc Graw Hill, New York, USA, 2003.

Nilson, A.H., and Chmn., "A report on finite element analysis of reinforced concrete structures," ASCE Task Committee, American Society of Civil Engineers, New York, pp-545, 1982.

Newmark, N.M., and Hall, W.J., "Earthquake spectra and design," Earthquake Engineering Research Institute, Berkeley, CA, 1982.

New Zealand Standard NZS 3101.Part 2. 2.2006 *Code of practice for the design of concrete structures*, New Zealand Standards Association, Wellington, New Zealand.

Oguz, S., *Evaluation of pushover analysis procedures for frame structures*, MSc thesis, Graduate School of Natural and Applied Sciences, Middle East Technical University, 2005.

Papanikolaou, V.K. and Elnashai, A.S., "Evaluation of conventional and adaptive pushover analysis i: methodology," Journal of Earthquake Engineering, Vol. 9, Issue No. 6, 2005, pp.923-941.

Peter, K. and Badoux, M., "Application of the capacity spectrum method to RC buildings with bearing walls" Proceedings of the 12th World Conference on Earthquake Engineering Auckland, CD-ROM, 2000, Paper 0609, New Zealand Society for Earthquake Engineering.

Paulay, T. and Priestley, M. J. N. *Seismic design of reinforced concrete and masonry buildings. John Wiley and Sons*, Inc., 1992.

Paulay, T., "A re-definition of the stiffness of RC elements and its implication in seismic design," Structural Engineering International, Vol.11, Issue No-1, Feb.2001, pp. 36-41.

Prajapati, S. K., and Amin, J. A., "Seismic assessment of RC frame building designed using gross and cracked section as per Indian standards," *Asian Journal of Civil Engineering*, Vol. 20, Issue 6, Sep. 2019, pp. 821-836.

Pique, J. R., and Burgos, M., "Effective rigidity of reinforced concrete elements in seismic analysis and design," *The 14th World Conference on Earthquake Engineering,* October12-17, 2008, Beijing, China

Priestley, M.J.N., Calvi, G. M.., and Kowalsky, M.J. *Displacement based design of structures*. IUSS Press; 1st Edition, 2007.

Rahman, M.M., *Pushover analysis of 2-D frames with stiffness irregularity in vertical direction,* MSc Engg. Thesis, BUET, 2008.

Requena, M. and Ayala, A.V., "Evaluation of a simplified method for determination of the nonlinear seismic response of RC frames," 12th World Conference on Earthquake Engineering, New Zealand, 2000, Paper 2109.

Rosenblueth, E. and Herrera, I., "On a kind of hysteretic damping," *Journal of Engineering Mechanics Division*, ASCE, Vol. 90, 1964, pp. 37-48,

Saiidi, M. and Sozen, M.A., "Simple and complex models for nonlinear seismic response of reinforced concrete structures," Civil Engineering Studies, 1979, Report No 465, Univ. of Illinois, Urbana, Illinois.

Saiidi, M. and Sozen, M.A., "Simple nonlinear seismic analysis of RC structures," Journal of the Structural Division, 1981, Vol. 107, ST5, ASCE, 937-952.

Satyarno, I., Carr, A.J., and Restrepo, J., "Refined pushover analysis for the assessment of older reinforced concrete buildings," NZSEE Technology Conference, 1998, Wairakei, New Zealand, pp.75-82.

Sharifi, S. and Toopchi-Nezhad, H., "Seismic response modification factor of RC-frame structures based on limit state design," *International Journal of Civil Engineering*, Vol. 16, Issue no. 9, 2018. pp. 1185-1200.

Smith B.S. and Coull A. *Tall building structure analysis and design*. John Wiley and Sons. Inc, 1991.

Shuraim, A. and Charif, A., "Performance of pushover procedure in evaluating the seismic adequacy of reinforced concrete frames" Research Gate, Jan.2007.

Tang, T. O. and Su, R. K. L., "Shear and flexural stiffnesses of reinforced concrete shear walls subjected to cyclic loading," The Open Construction and Building Technology Journal, Vol. 8, Issue No-1, 2014, pp. 104-121.

Tjhin, T., Aschheim, M., and Hernandez, M. E., "Observations on the reliability of alternative multiple-mode pushover analysis methods" Journal of Structural Engineering. ASCE, 2006, Vol. 132, Issue No-3, pp. 471-477.

Themelis, S., *Pushover Analysis for Seismic Assessment and Design of Structures*, Ph.D. Thesis, Heriot-Watt University, 2008.

Tso, W.K. and Moghadam, A.S., "Seismic response of asymmetrical buildings using pushover analysis", Seismic Design Methodologies for the Next Generation of Codes edited by Fajfar P. and Krawinkler, H., Balkema, 1997, pp. 311-322.

Tripathy, R. and Sarkar, P., "Pushover analysis of RC setback building frames," International Journal of Civil Engineering (IJCE), Vol.1, Issue 1 Aug 2012, pp. 79-101.

TBEC 2018 *Turkish Building Earthquake Code*: Specifications for building design under earthquake effects. Ankara, Turkey.

Vidovic, D., Grandic, D., and Sculac, P., "Effective stiffness for structural analysis of buildings in earthquake", 4th international conference civil engineering - science and practice, (2012), Zabljak, pp. 811-818.

Wong, J., Sommer, A., Briggs, K., and Ergin, C., "Effective stiffness for modeling reinforced concrete structures," Article of Structural Analysis, Jan-2017.

Wu, J.P., and Hanson, R.D., "Study of inelastic response spectra with high damping," J. Struct. Div. ASCE, Vol.115, Issue-6, 1989, pp. 1412-1431.

Yang, P. and Wang, Y., "A study on improvement of pushover analysis" Proceedings of the 12th World Conference on Earthquake Engineering Auckland, 2000, Paper 1940, New Zealand Society for Earthquake Engineering.

Yu, W-W. and Winter, G., "Instantaneous and Long-term Deflections of Reinforced concrete beams under working loads," ACI Journal Proceedings, Vol. 57, Issue No. 7, 1960, pp. 29-50.

Ýnel, M., Tjhin, T., and Aschheim, A.M., "The significance of lateral load pattern in pushover analysis", Istanbul Fifth National Conference on Earthquake Engineering, Paper No: AE-009, Istanbul, Turkey. 2003.

Zhao, X., Wu, Y., Leung, A. Y., and Lam, H. F., "Plastic hinge length in reinforced concrete flexural members," Procedia Engineering, Vol. 14, 2011, pp. 1266-1274.

Appendix A

Table A1: Damage Control and Building Performance Levels (FEMA-356)

	Target Building Performance Levels			
	Collapse Prevention Level (5-E)	Life Safety Level (3-C)	Immediate Occupancy Level (1-B)	Operational Level (1-A)
Overall Damage	Severe	Moderate	Light	Very Light
General	Little residual stiffness and strength, but load-bearing columns and walls function. Large permanent drifts. Some exits blocked. Infills and unbraced parapets failed or at incipient failure. Building is near collapse.	Some residual strength and stiffness left in all stories. Gravity-load-bearing elements function. No out-of-plane failure of walls or tipping of parapets. Some permanent drift. Damage to partitions. Building may be beyond economical repair.	No permanent drift. Structure substantially retains original strength and stiffness. Minor cracking of facades, partitions, and ceilings as well as structural elements. Elevators can be restarted. Fire protection operable.	No permanent drift. Structure substantially retains original strength and stiffness. Minor cracking of facades, partitions, and ceilings as well as structural elements. All systems important to normal operation are functional.
Nonstructural components	Extensive damage.	Falling hazards mitigated but many architectural, mechanical, and electrical systems are damaged.	Equipment and contents are generally secure, but may not operate due to mechanical failure or lack of utilities.	Negligible damage occurs. Power and other utilities are available, possibly from standby sources.
Comparison with performance intended for buildings designed under the *NEHRP Provisions,* for the Design Earthquake	Significantly more damage and greater risk.	Somewhat more damage and slightly higher risk.	Less damage and lower risk.	Much less damage and lower risk.

Table A2: Structural Performance Levels and Damage–Vertical Elements (FEMA-356)

Elements	Type	Structural Performance Levels		
		Collapse Prevention S-5	Life Safety S-3	Immediate Occupancy S-1
Concrete Frames	Primary	Extensive cracking and hinge formation in ductile elements. Limited cracking and/or splice failure in some nonductile columns. Severe damage in short columns.	Extensive damage to beams. Spalling of cover and shear cracking (<1/8" width) for ductile columns. Minor spalling in nonductile columns. Joint cracks <1/8" wide.	Minor hairline cracking. Limited yielding possible at a few locations. No crushing (strains below 0.003).
	Secondary	Extensive spalling in columns (limited shortening) and beams. Severe joint damage. Some reinforcing buckled.	Extensive cracking and hinge formation in ductile elements. Limited cracking and/or splice failure in some nonductile columns. Severe damage in short columns.	Minor spalling in a few places in ductile columns and beams. Flexural cracking in beams and columns. Shear cracking in joints <1/16" width.
	Drift	4% transient or permanent	2% transient; 1% permanent	1% transient; negligible permanent

Table A3: Structural Performance Levels and Damage–Horizontal Elements (FEMA-356)

	Structural Performance Levels		
Element	**Collapse Prevention S-5**	**Life Safety S-3**	**Immediate Occupancy S-1**
Metal Deck Diaphragms	Large distortion with buckling of some units and tearing of many welds and seam attachments.	Some localized failure of welded connections of deck to framing and between panels. Minor local buckling of deck.	Connections between deck units and framing intact. Minor distortions.
Wood Diaphragms	Large permanent distortion with partial withdrawal of nails and extensive splitting of elements.	Some splitting at connections. Loosening of sheathing. Observable withdrawal of fasteners. Splitting of framing and sheathing.	No observable loosening or withdrawal of fasteners. No splitting of sheathing or framing.
Concrete Diaphragms	Extensive crushing and observable offset across many cracks.	Extensive cracking (<1/4" width). Local crushing and spalling.	Distributed hairline cracking. Some minor cracks of larger size (<1/8" width).
Precast Diaphragms	Connections between units fail. Units shift relative to each other. Crushing and spalling at joints.	Extensive cracking (<1/4" width). Local crushing and spalling.	Some minor cracking along joints.

Appendix B

Table B4.1: Seismic Performance point for 6-st cracked RC frame building

Capacity Curve Coordinates (Part 1 of 2, continued)

Step	Monitored Displ mm	Base Force kN	A-B	B-C	C-D	D-E	>E	A-IO	IO-LS	LS-CP
87	63.642	2041.8027	780	0	0	0	0	780	0	0
88	64.374	2065.2717	780	0	0	0	0	780	0	0
89	65.105	2088.7407	780	0	0	0	0	780	0	0
90	65.837	2112.2097	780	0	0	0	0	780	0	0
91	66.568	2135.6787	780	0	0	0	0	780	0	0
92	67.3	2159.1477	780	0	0	0	0	780	0	0
93	68.031	2182.6167	780	0	0	0	0	780	0	0
94	68.763	2206.0857	780	0	0	0	0	780	0	0
95	69.494	2229.5547	780	0	0	0	0	780	0	0
96	70.226	2253.0237	780	0	0	0	0	780	0	0
97	70.957	2276.4927	780	0	0	0	0	780	0	0
98	71.689	2299.9616	780	0	0	0	0	780	0	0
99	72.42	2323.4306	780	0	0	0	0	780	0	0
100	73.152	2346.8996	780	0	0	0	0	780	0	0
101	73.884	2370.3686	780	0	0	0	0	780	0	0
102	74.615	2393.8376	780	0	0	0	0	780	0	0
103	75.347	2417.3066	777	3	0	0	0	780	0	0
104	76.078	2440.678	777	3	0	0	0	780	0	0
105	76.81	2464.0494	777	3	0	0	0	780	0	0
106	77.541	2487.4207	777	3	0	0	0	780	0	0
107	78.273	2510.7921	772	8	0	0	0	780	0	0
108	79.004	2534.0029	772	8	0	0	0	780	0	0
109	79.736	2557.2138	772	8	0	0	0	780	0	0
110	80.467	2580.4246	772	8	0	0	0	780	0	0
111	81.199	2603.6354	771	9	0	0	0	780	0	0
112	81.93	2626.8158	766	14	0	0	0	780	0	0
113	82.662	2649.8406	763	17	0	0	0	780	0	0
114	83.393	2672.7705	761	19	0	0	0	780	0	0
115	84.125	2695.6374	761	19	0	0	0	780	0	0
116	84.856	2718.5043	761	19	0	0	0	780	0	0
117	85.588	2741.3713	761	19	0	0	0	780	0	0
118	86.319	2764.2382	761	19	0	0	0	780	0	0
119	87.051	2787.1051	757	23	0	0	0	780	0	0
120	87.782	2809.815	750	30	0	0	0	780	0	0
121	88.514	2832.3454	746	34	0	0	0	780	0	0
122	89.245	2854.7467	743	37	0	0	0	780	0	0
123	89.977	2877.0723	743	37	0	0	0	780	0	0

Step	Monitored Displ mm	Base Force kN	A-B	B-C	C-D	D-E	>E	A-IO	IO-LS	LS-CP
131	95.829	3054.7597	722	58	0	0	0	780	0	0
132	96.561	3076.582	717	63	0	0	0	780	0	0
133	97.292	3098.2661	717	63	0	0	0	780	0	0
134	98.024	3119.9502	717	63	0	0	0	780	0	0
135	98.755	3141.6343	717	63	0	0	0	780	0	0
136	99.487	3163.3184	714	66	0	0	0	780	0	0
137	100.218	3184.9443	714	66	0	0	0	780	0	0
138	100.95	3206.5702	710	70	0	0	0	780	0	0
139	101.681	3228.0639	710	70	0	0	0	780	0	0
140	102.413	3249.5575	710	70	0	0	0	780	0	0
141	103.144	3271.0511	708	72	0	0	0	780	0	0
142	103.876	3292.4784	708	72	0	0	0	780	0	0
143	104.607	3313.9058	708	72	0	0	0	780	0	0
144	105.339	3335.3332	708	72	0	0	0	780	0	0
145	106.07	3356.7605	708	72	0	0	0	780	0	0
146	106.802	3378.1879	708	72	0	0	0	780	0	0
147	107.533	3399.6153	708	72	0	0	0	780	0	0
148	108.265	3421.0426	702	78	0	0	0	780	0	0
149	108.996	3442.3308	701	79	0	0	0	780	0	0
150	109.728	3463.5891	693	87	0	0	0	780	0	0
151	110.46	3484.6125	691	89	0	0	0	780	0	0
152	111.191	3505.5673	691	89	0	0	0	780	0	0
153	111.923	3526.522	687	93	0	0	0	780	0	0
154	112.654	3547.3351	687	93	0	0	0	780	0	0
155	113.386	3568.1482	685	95	0	0	0	780	0	0
156	114.117	3588.886	685	95	0	0	0	780	0	0
157	114.849	3609.6239	682	98	0	0	0	780	0	0
158	115.58	3630.2963	676	104	0	0	0	780	0	0
159	116.312	3650.8639	676	104	0	0	0	780	0	0
160	117.043	3671.4314	676	104	0	0	0	780	0	0
161	117.775	3691.999	672	108	0	0	0	780	0	0
162	118.506	3712.4793	667	113	0	0	0	780	0	0
163	119.238	3732.8459	662	118	0	0	0	780	0	0
164	119.969	3753.11	662	118	0	0	0	780	0	0

Capacity Curve Coordinates (Part 1 of 2, continued)

Step	Monitored Displ mm	Base Force kN	A-B	B-C	C-D	D-E	>E	A-IO	IO-LS	LS-CP
175	128.016	3974.6364	642	138	0	0	0	780	0	0
176	128.748	3994.4053	642	138	0	0	0	780	0	0
177	129.479	4014.1743	642	138	0	0	0	780	0	0
178	130.211	4033.9432	636	144	0	0	0	780	0	0
179	130.942	4053.5328	636	144	0	0	0	780	0	0
180	131.674	4073.1224	636	144	0	0	0	780	0	0
181	132.405	4092.712	636	144	0	0	0	780	0	0
182	133.137	4112.3015	634	146	0	0	0	780	0	0
183	133.868	4131.8284	634	146	0	0	0	780	0	0
184	134.6	4151.3552	634	146	0	0	0	780	0	0
185	135.331	4170.882	634	146	0	0	0	780	0	0
186	136.063	4190.4089	634	146	0	0	0	780	0	0
187	136.794	4209.9357	630	150	0	0	0	780	0	0
188	137.526	4229.3739	630	150	0	0	0	780	0	0
189	138.257	4248.812	630	150	0	0	0	780	0	0
190	138.989	4268.2502	630	150	0	0	0	780	0	0
191	139.72	4287.6884	630	150	0	0	0	780	0	0
192	140.452	4307.1266	630	150	0	0	0	780	0	0
193	141.183	4326.5647	630	150	0	0	0	780	0	0
194	141.915	4346.0029	628	152	0	0	0	780	0	0
195	142.646	4365.3971	628	152	0	0	0	780	0	0
196	143.378	4384.7914	628	152	0	0	0	780	0	0
197	144.109	4404.1856	628	152	0	0	0	780	0	0
198	144.841	4423.5799	628	152	0	0	0	780	0	0
199	145.572	4442.9741	628	152	0	0	0	780	0	0
200	146.304	4462.3684	628	152	0	0	0	780	0	0
201	147.036	4481.7626	628	152	0	0	0	780	0	0
202	147.767	4501.1568	626	154	0	0	0	780	0	0
203	148.499	4520.443	626	154	0	0	0	780	0	0
204	149.23	4539.7292	624	156	0	0	0	780	0	0
205	149.962	4558.9035	624	156	0	0	0	780	0	0
206	150.693	4578.0778	622	158	0	0	0	780	0	0
207	151.425	4597.1321	622	158	0	0	0	780	0	0
208	152.156	4616.1863	622	158	0	0	0	780	0	0

Table B.2: Seismic Performance point for 6-st Uncracked RC frame building

Capacity Curve Coordinates (Part 1 of 2)

Step	Monitored Displ mm	Base Force kN	A-B	B-C	C-D	D-E	>E	A-IO	IO-LS	LS-CP
0	0	0	780	0	0	0	0	780	0	0
1	0.732	47.3221	780	0	0	0	0	780	0	0
2	1.463	94.6443	780	0	0	0	0	780	0	0
3	2.195	141.9664	780	0	0	0	0	780	0	0
4	2.926	189.2886	780	0	0	0	0	780	0	0
5	3.658	236.6107	780	0	0	0	0	780	0	0
6	4.389	283.9329	780	0	0	0	0	780	0	0
7	5.121	331.255	780	0	0	0	0	780	0	0
8	5.852	378.5772	780	0	0	0	0	780	0	0
9	6.584	425.8993	780	0	0	0	0	780	0	0
10	7.315	473.2215	780	0	0	0	0	780	0	0
11	8.047	520.5436	780	0	0	0	0	780	0	0
12	8.778	567.8658	780	0	0	0	0	780	0	0
13	9.51	615.1879	780	0	0	0	0	780	0	0
14	10.241	662.5101	780	0	0	0	0	780	0	0
15	10.973	709.8322	780	0	0	0	0	780	0	0
16	11.704	757.1543	780	0	0	0	0	780	0	0
17	12.436	804.4765	780	0	0	0	0	780	0	0
18	13.167	851.7986	780	0	0	0	0	780	0	0
19	13.899	899.1208	780	0	0	0	0	780	0	0
20	14.63	946.4429	780	0	0	0	0	780	0	0
21	15.362	993.7651	780	0	0	0	0	780	0	0
22	16.093	1041.0872	780	0	0	0	0	780	0	0
23	16.825	1088.4094	780	0	0	0	0	780	0	0
24	17.556	1135.7315	780	0	0	0	0	780	0	0
25	18.288	1183.0537	780	0	0	0	0	780	0	0
26	19.02	1230.3758	780	0	0	0	0	780	0	0
27	19.751	1277.698	780	0	0	0	0	780	0	0
28	20.483	1325.0201	780	0	0	0	0	780	0	0
29	21.214	1372.3423	780	0	0	0	0	780	0	0
30	21.946	1419.6644	780	0	0	0	0	780	0	0
31	22.677	1466.9866	780	0	0	0	0	780	0	0
32	23.409	1514.3087	780	0	0	0	0	780	0	0
33	24.14	1561.6308	780	0	0	0	0	780	0	0
34	24.872	1608.953	780	0	0	0	0	780	0	0
35	25.603	1656.2751	780	0	0	0	0	780	0	0

Capacity Curve Coordinates (Part 1 of 2, continued)

Step	Monitored Displ mm	Base Force kN	A-B	B-C	C-D	D-E	>E	A-IO	IO-LS	LS-CP
87	68.396	3997.2375	618	162	0	0	0	780	0	0
88	69.128	4029.1503	618	162	0	0	0	780	0	0
89	69.86	4061.063	616	164	0	0	0	780	0	0
90	70.591	4092.8546	616	164	0	0	0	780	0	0
91	71.323	4124.6461	616	164	0	0	0	780	0	0
92	72.054	4156.4377	616	164	0	0	0	780	0	0
93	72.786	4188.2292	616	164	0	0	0	780	0	0
94	73.517	4220.0208	616	164	0	0	0	780	0	0
95	74.249	4251.8123	616	164	0	0	0	780	0	0
96	74.98	4283.6039	616	164	0	0	0	780	0	0
97	75.712	4315.3955	616	164	0	0	0	780	0	0
98	76.443	4347.187	616	164	0	0	0	780	0	0
99	77.175	4378.9786	616	164	0	0	0	780	0	0
100	77.906	4410.7701	616	164	0	0	0	780	0	0
101	78.638	4442.5617	612	168	0	0	0	780	0	0
102	79.369	4474.0551	612	168	0	0	0	780	0	0
103	80.101	4505.5486	612	168	0	0	0	780	0	0
104	80.832	4537.0421	610	170	0	0	0	780	0	0
105	81.564	4568.372	610	170	0	0	0	780	0	0
106	82.295	4599.702	610	170	0	0	0	780	0	0
107	83.027	4631.0319	610	170	0	0	0	780	0	0
108	83.758	4662.3619	610	170	0	0	0	780	0	0
109	84.49	4693.6918	609	171	0	0	0	780	0	0
110	85.221	4724.9218	596	184	0	0	0	780	0	0
111	85.953	4754.7884	596	184	0	0	0	780	0	0
112	86.684	4784.655	594	186	0	0	0	780	0	0
113	87.416	4814.2209	594	186	0	0	0	780	0	0
114	88.148	4843.7868	591	189	0	0	0	780	0	0
115	88.879	4873.0473	584	196	0	0	0	780	0	0
116	89.611	4901.3052	582	198	0	0	0	780	0	0
117	90.342	4929.2861	580	200	0	0	0	780	0	0
118	91.074	4956.3647	573	207	0	0	0	780	0	0
119	91.805	4978.3545	573	207	0	0	0	780	0	0
120	92.537	5000.5185	571	209	0	0	0	780	0	0

134

Step	Monitored Displ mm	Base Force kN	A-B	B-C	C-D	D-E	>E	A-IO	IO-LS	LS-CP
131	100.583	5238.2145	565	215	0	0	0	779	0	0
132	101.315	5259.6994	565	215	0	0	0	779	0	0
133	102.046	5280.9103	565	215	0	0	0	779	0	0
134	102.778	5302.2158	565	215	0	0	0	779	0	0
135	103.509	5323.7006	565	215	0	0	0	779	0	0
136	104.241	5344.9139	565	215	0	0	0	778	0	0
137	104.972	5366.3985	565	215	0	0	0	778	0	0
138	105.704	5387.607	562	218	0	0	0	778	0	0
139	106.436	5409.0502	562	218	0	0	0	778	0	0
140	107.167	5430.1558	559	221	0	0	0	778	0	0
141	107.899	5451.559	556	224	0	0	0	778	0	0
142	108.63	5472.6179	556	224	0	0	0	778	0	0
143	109.362	5493.9778	556	224	0	0	0	778	0	0
144	110.093	5515.0586	556	224	0	0	0	778	0	0
145	110.825	5536.4183	556	224	0	0	0	778	0	0
146	111.556	5557.4965	556	224	0	0	0	778	0	0
147	112.288	5578.8562	556	224	0	0	0	778	0	0
148	113.019	5599.9174	556	224	0	0	0	778	0	0
149	113.751	5621.2769	556	224	0	0	0	778	0	0
150	114.482	5642.3563	556	224	0	0	0	776	2	0
151	115.214	5663.7157	556	224	0	0	0	775	3	0
152	115.945	5684.7773	556	224	0	0	0	775	3	0
153	116.677	5706.1365	556	224	0	0	0	775	3	0
154	117.408	5727.1985	556	224	0	0	0	767	11	0
155	118.14	5748.448	552	228	0	0	0	767	11	0
156	118.871	5769.2508	550	230	0	0	0	767	11	0
157	119.603	5789.9327	549	231	0	0	0	763	15	0
158	120.334	5810.7219	546	234	0	0	0	757	20	0
159	121.066	5830.9328	544	236	0	0	0	757	20	0
160	121.797	5851.0989	538	242	0	0	0	757	20	0
161	122.529	5871.0546	538	242	0	0	0	757	20	0
162	123.26	5890.685	538	242	0	0	0	757	20	0
163	123.992	5910.5549	538	242	0	0	0	757	20	0
164	124.724	5930.1697	534	246	0	0	0	757	20	0

Table B 4.3: Seismic Performance point for 10-st cracked RC frame building

Capacity Curve Coordinates (Part 1 of 2, continued)

Step	Monitored Displ mm	Base Force kN	A-B	B-C	C-D	D-E	>E	A-IO	IO-LS	LS-CP
87	106.07	2632.7353	1300	0	0	0	0	1300	0	0
88	107.29	2662.9966	1300	0	0	0	0	1300	0	0
89	108.509	2693.258	1300	0	0	0	0	1300	0	0
90	109.728	2723.5193	1300	0	0	0	0	1300	0	0
91	110.947	2753.7806	1300	0	0	0	0	1300	0	0
92	112.166	2784.0419	1300	0	0	0	0	1300	0	0
93	113.386	2814.3033	1297	3	0	0	0	1300	0	0
94	114.605	2844.4758	1297	3	0	0	0	1300	0	0
95	115.824	2874.6483	1294	6	0	0	0	1300	0	0
96	117.043	2904.7241	1288	12	0	0	0	1300	0	0
97	118.262	2934.6202	1288	12	0	0	0	1300	0	0
98	119.482	2964.5163	1282	18	0	0	0	1300	0	0
99	120.701	2994.2318	1282	18	0	0	0	1300	0	0
100	121.92	3023.9474	1274	26	0	0	0	1300	0	0
101	123.139	3053.39	1271	29	0	0	0	1300	0	0
102	124.358	3082.7384	1265	35	0	0	0	1300	0	0
103	125.578	3111.8949	1263	37	0	0	0	1300	0	0
104	126.797	3140.9632	1260	40	0	0	0	1300	0	0
105	128.016	3169.9357	1260	40	0	0	0	1300	0	0
106	129.235	3198.9082	1253	47	0	0	0	1300	0	0
107	130.454	3227.6359	1249	51	0	0	0	1300	0	0
108	131.674	3256.2694	1238	62	0	0	0	1300	0	0
109	132.893	3284.5168	1238	62	0	0	0	1300	0	0
110	134.112	3312.7643	1236	64	0	0	0	1300	0	0
111	135.331	3340.9262	1226	74	0	0	0	1300	0	0
112	136.55	3368.8077	1222	78	0	0	0	1300	0	0
113	137.77	3396.5592	1220	80	0	0	0	1300	0	0
114	138.989	3424.2539	1217	83	0	0	0	1300	0	0
115	140.208	3451.8645	1217	83	0	0	0	1300	0	0
116	141.427	3479.4751	1210	90	0	0	0	1300	0	0
117	142.646	3506.8555	1207	93	0	0	0	1300	0	0
118	143.866	3534.1723	1204	96	0	0	0	1300	0	0
119	145.085	3561.425	1202	98	0	0	0	1300	0	0
120	146.304	3588.5971	1202	98	0	0	>E	1300	0	0
121	147.523	3615.7691	1202	98	0	0	0	1300	0	0
122	148.742	3642.9411	1202	98	0	0	0	1300	0	0
123	149.962	3670.1131	1202	98	0	0	0	1300	0	0
124	151.181	3697.2853	1202	98	0	0	0	1300	0	0

Step	Monitored Displ mm	Base Force kN	A-B	B-C	C-D	D-E	>E	A-IO	IO-LS	LS-CP
131	159.715	3882.2016	1134	166	0	0	0	1300	0	0
132	160.934	3907.3411	1132	168	0	0	0	1300	0	0
133	162.154	3932.3993	1129	171	0	0	0	1300	0	0
134	163.373	3957.3589	1128	172	0	0	0	1300	0	0
135	164.592	3982.3021	1124	176	0	0	0	1300	0	0
136	165.811	4007.1484	1120	180	0	0	0	1300	0	0
137	167.03	4031.8975	1118	182	0	0	0	1300	0	0
138	168.25	4056.5965	1118	182	0	0	0	1300	0	0
139	169.469	4081.2955	1114	186	0	0	0	1300	0	0
140	170.688	4105.8446	1112	188	0	0	0	1300	0	0
141	171.907	4130.3172	1112	188	0	0	0	1300	0	0
142	173.126	4154.7898	1112	188	0	0	0	1300	0	0
143	174.346	4179.2624	1112	188	0	0	0	1300	0	0
144	175.565	4203.735	1108	192	0	0	0	1300	0	0
145	176.784	4228.0877	1108	192	0	0	0	1300	0	0
146	178.003	4252.4404	1108	192	0	0	0	1300	0	0
147	179.222	4276.7931	1108	192	0	0	0	1300	0	0
148	180.442	4301.1458	1108	192	0	0	0	1300	0	0
149	181.661	4325.4986	1108	192	0	0	0	1300	0	0
150	182.88	4349.8513	1092	208	0	0	0	1300	0	0
151	184.099	4373.8854	1088	212	0	0	0	1300	0	0
152	185.318	4397.8262	1080	220	0	0	0	1300	0	0
153	186.538	4421.6017	1078	222	0	0	0	1300	0	0
154	187.757	4445.3266	1075	225	0	0	0	1300	0	0
155	188.976	4468.9982	1073	227	0	0	0	1300	0	0
156	190.195	4492.6227	1073	227	0	0	0	1300	0	0
157	191.414	4516.2472	1073	227	0	0	0	1300	0	0
158	192.634	4539.8717	1069	231	0	0	0	1300	0	0
159	193.853	4563.3747	1069	231	0	0	0	1300	0	0
160	195.072	4586.8777	1064	236	0	0	0	1300	0	0
161	196.291	4610.2662	1064	236	0	0	0	1300	0	0
162	197.51	4633.6548	1062	238	0	0	0	1300	0	0
163	198.73	4656.9967	1062	238	0	0	0	1300	0	0
164	199.949	4680.3386	1062	238	0	0	0	1300	0	0
165	201.168	4703.6805	1062	238	0	0	0	1300	0	0
166	202.387	4727.0224	1057	243	0	0	0	1300	0	0
167	203.606	4750.2662	1054	246	0	0	0	1300	0	0

Capacity Curve Coordinates (Part 1 of 2, continued)

Step	Monitored Displ mm	Base Force kN	A-B	B-C	C-D	D-E	>E	A-IO	IO-LS	LS-CP
263	320.65	6940.3004	992	308	0	0	0	1298	2	0
264	321.869	6962.6228	992	308	0	0	0	1298	2	0
265	323.088	6984.9451	992	308	0	0	0	1298	2	0
266	324.307	7007.2674	992	308	0	0	0	1298	2	0
267	325.526	7029.5898	992	308	0	0	0	1296	4	0
268	326.746	7051.9121	992	308	0	0	0	1296	4	0
269	327.965	7074.2344	992	308	0	0	0	1296	4	0
270	329.184	7096.5568	990	310	0	0	0	1296	4	0
271	330.403	7118.7529	982	318	0	0	0	1296	4	0
272	331.622	7140.2696	980	320	0	0	0	1296	4	0
273	332.842	7161.7779	980	320	0	0	0	1292	8	0
274	334.061	7183.2528	978	322	0	0	0	1292	8	0
275	335.28	7204.6724	978	322	0	0	0	1292	8	0
276	336.499	7226.1892	977	323	0	0	0	1288	12	0
277	337.718	7247.5947	975	325	0	0	0	1288	12	0
278	338.938	7268.8512	973	327	0	0	0	1286	14	0
279	340.157	7289.8285	972	328	0	0	0	1286	14	0
280	341.376	7310.6812	970	330	0	0	0	1286	14	0
281	341.681	7315.7869	970	330	0	0	0	1286	14	0
282	342.9	7336.1981	970	330	0	0	0	1284	16	0
283	344.576	7364.0033	970	330	0	0	0	1284	16	0
284	345.948	7386.7729	970	330	0	0	0	1284	16	0
285	347.167	7407.0623	966	334	0	0	0	1284	16	0
286	348.539	7429.6765	962	338	0	0	0	1284	16	0
287	349.91	7451.9956	960	340	0	0	0	1284	16	0
288	351.358	7475.4274	956	344	0	0	0	1284	16	0
289	352.654	7495.6339	956	344	0	0	0	1284	16	0
290	353.873	7514.6422	955	345	0	0	0	1283	16	0
291	355.168	7534.4518	955	345	0	0	0	1281	18	0
292	356.387	7553.1413	953	347	0	0	0	1281	18	0
293	357.683	7573.0701	953	347	0	0	0	1281	18	0
294	358.902	7591.7559	953	347	0	0	0	1281	18	0
295	360.121	7610.4296	953	347	0	0	0	1279	20	0
296	361.34	7629.1109	953	347	0	0	0	1279	20	0
297	362.56	7647.7794	953	347	0	0	0	1279	20	0
298	363.779	7666.4523	953	347	0	0	0	1279	20	0
299	364.998	7685.127	953	347	0	0	0	1271	28	0

Table B4.4: Seismic Performance point for 10-st Uncracked RC frame building

Capacity Curve Coordinates (Part 1 of 2)

Step	Monitored Displ mm	Base Force kN	A-B	B-C	C-D	D-E	>E	A-IO	IO-LS	LS-CP
0	0	0	1300	0	0	0	0	1300	0	0
1	1.219	62.5436	1300	0	0	0	0	1300	0	0
2	2.438	125.0873	1300	0	0	0	0	1300	0	0
3	3.658	187.6309	1300	0	0	0	0	1300	0	0
4	4.877	250.1745	1300	0	0	0	0	1300	0	0
5	6.096	312.7181	1300	0	0	0	0	1300	0	0
6	7.315	375.2618	1300	0	0	0	0	1300	0	0
7	8.534	437.8054	1300	0	0	0	0	1300	0	0
8	9.754	500.349	1300	0	0	0	0	1300	0	0
9	10.973	562.8926	1300	0	0	0	0	1300	0	0
10	12.192	625.4363	1300	0	0	0	0	1300	0	0
11	13.411	687.9799	1300	0	0	0	0	1300	0	0
12	14.63	750.5235	1300	0	0	0	0	1300	0	0
13	15.85	813.0671	1300	0	0	0	0	1300	0	0
14	17.069	875.6108	1300	0	0	0	0	1300	0	0
15	18.288	938.1544	1300	0	0	0	0	1300	0	0
16	19.507	1000.698	1300	0	0	0	0	1300	0	0
17	20.726	1063.2416	1300	0	0	0	0	1300	0	0
18	21.946	1125.7853	1300	0	0	0	0	1300	0	0
19	23.165	1188.3289	1300	0	0	0	0	1300	0	0
20	24.384	1250.8725	1300	0	0	0	0	1300	0	0
21	25.603	1313.4161	1300	0	0	0	0	1300	0	0
22	26.822	1375.9598	1300	0	0	0	0	1300	0	0
23	28.042	1438.5034	1300	0	0	0	0	1300	0	0
24	29.261	1501.047	1300	0	0	0	0	1300	0	0
25	30.48	1563.5906	1300	0	0	0	0	1300	0	0
26	31.699	1626.1343	1300	0	0	0	0	1300	0	0
27	32.918	1688.6779	1300	0	0	0	0	1300	0	0
28	34.138	1751.2215	1300	0	0	0	0	1300	0	0
29	35.357	1813.7651	1300	0	0	0	0	1300	0	0
30	36.576	1876.3088	1300	0	0	0	0	1300	0	0
31	37.795	1938.8524	1300	0	0	0	0	1300	0	0
32	39.014	2001.396	1300	0	0	0	0	1300	0	0
33	40.234	2063.9396	1300	0	0	0	0	1300	0	0
34	41.453	2126.4833	1300	0	0	0	0	1300	0	0
35	42.672	2189.0269	1300	0	0	0	0	1300	0	0
36	43.891	2251.5705	1300	0	0	0	0	1300	0	0
37	45.11	2314.1141	1300	0	0	0	0	1300	0	0
38	46.33	2376.6578	1300	0	0	0	0	1300	0	0
39	47.549	2439.2014	1300	0	0	0	0	1300	0	0
40	48.768	2501.745	1300	0	0	0	0	1300	0	0
41	49.987	2564.2886	1299	1	0	0	0	1300	0	0
42	50.783	2605.048	1297	3	0	0	0	1300	0	0

Capacity Curve Coordinates (Part 1 of 2, continued)

Step	Monitored Displ mm	Base Force kN	A-B	B-C	C-D	D-E	>E	A-IO	IO-LS	LS-CP
87	116.873	5117.1313	1042	258	0	0	0	1300	0	0
88	118.092	5154.8188	1042	258	0	0	0	1300	0	0
89	119.311	5192.5062	1042	258	0	0	0	1300	0	0
90	120.53	5230.1936	1040	260	0	0	0	1300	0	0
91	121.75	5267.8131	1034	266	0	0	0	1300	0	0
92	122.969	5305.1799	1034	266	0	0	0	1300	0	0
93	124.188	5342.5468	1034	266	0	0	0	1300	0	0
94	125.407	5379.9136	1032	268	0	0	0	1300	0	0
95	126.626	5417.1825	1030	270	0	0	0	1300	0	0
96	127.846	5454.3483	1030	270	0	0	0	1300	0	0
97	129.065	5491.5141	1030	270	0	0	0	1300	0	0
98	130.284	5528.6799	1030	270	0	0	0	1300	0	0
99	131.503	5565.8458	1030	270	0	0	0	1300	0	0
100	132.722	5603.0116	1030	270	0	0	0	1300	0	0
101	133.942	5640.1774	1027	273	0	0	0	1300	0	0
102	135.161	5677.2215	1024	276	0	0	0	1300	0	0
103	136.38	5714.1971	1024	276	0	0	0	1300	0	0
104	137.599	5751.1727	1024	276	0	0	0	1300	0	0
105	138.818	5788.1483	1024	276	0	0	0	1300	0	0
106	140.038	5825.1238	1019	281	0	0	0	1300	0	0
107	141.257	5861.9377	1019	281	0	0	0	1300	0	0
108	142.476	5898.7516	1019	281	0	0	0	1300	0	0
109	143.695	5935.5655	1019	281	0	0	0	1300	0	0
110	144.914	5972.3794	1019	281	0	0	0	1300	0	0
111	146.134	6009.1933	1016	284	0	0	0	1300	0	0
112	147.353	6045.8828	1016	284	0	0	0	1300	0	0
113	148.572	6082.5722	1013	287	0	0	0	1300	0	0
114	149.791	6119.2278	1013	287	0	0	0	1300	0	0
115	151.01	6155.8834	1011	289	0	0	0	1300	0	0
116	152.23	6192.4848	1006	294	0	0	0	1300	0	0
117	153.449	6228.9549	1006	294	0	0	0	1300	0	0
118	154.668	6265.425	1006	294	0	0	0	1300	0	0
119	155.887	6301.8951	1006	294	0	0	0	1300	0	0
120	157.106	6338.3651	1006	294	0	0	0	1300	0	0
121	158.326	6374.8352	1006	294	0	0	0	1300	0	0
122	159.545	6411.3053	1002	298	0	0	0	1300	0	0
123	160.764	6447.6942	1002	298	0	0	0	1300	0	0
124	161.983	6484.0831	1002	298	0	0	0	1300	0	0
125	163.202	6520.472	1002	298	0	0	0	1300	0	0
126	164.422	6556.8609	1002	298	0	0	0	1300	0	0
127	165.641	6593.2497	997	303	0	0	0	1300	0	0
128	166.86	6629.5419	997	303	0	0	0	1300	0	0
129	168.079	6665.834	997	303	0	0	0	1300	0	0
130	169.298	6702.1261	997	303	0	0	0	1300	0	0

140

Step	Monitored Displ mm	Base Force kN	A-B	B-C	C-D	D-E	>E	A-IO	IO-LS	LS-CP
131	170.518	6738.4182	997	303	0	0	0	1300	0	0
132	171.737	6774.7103	994	306	0	0	0	1300	0	0
133	172.956	6810.9439	994	306	0	0	0	1300	0	0
134	174.175	6847.1775	994	306	0	0	0	1300	0	0
135	175.394	6883.4111	992	308	0	0	0	1300	0	0
136	176.614	6919.5492	992	308	0	0	0	1300	0	0
137	177.833	6955.6873	992	308	0	0	0	1300	0	0
138	179.052	6991.8254	992	308	0	0	0	1300	0	0
139	180.271	7027.9635	992	308	0	0	0	1300	0	0
140	181.49	7064.1016	990	310	0	0	0	1300	0	0
141	182.71	7100.1552	985	315	0	0	0	1300	0	0
142	183.929	7136.0417	980	320	0	0	0	1300	0	0
143	185.148	7171.7506	978	322	0	0	0	1300	0	0
144	186.367	7207.3982	973	327	0	0	0	1300	0	0
145	187.586	7242.7008	971	329	0	0	0	1300	0	0
146	188.806	7277.954	971	329	0	0	0	1300	0	0
147	190.025	7313.2073	969	331	0	0	0	1300	0	0
148	191.244	7348.3928	969	331	0	0	0	1300	0	0
149	192.463	7383.5699	969	331	0	0	0	1300	0	0
150	193.682	7418.7387	969	331	0	0	0	1300	0	0
151	194.902	7453.8585	962	338	0	0	0	1298	2	0
152	196.121	7488.3162	957	343	0	0	0	1298	2	0
153	197.34	7522.0705	954	346	0	0	0	1298	2	0
154	198.559	7555.2445	954	346	0	0	0	1298	2	0
155	199.778	7588.4183	950	350	0	0	0	1298	2	0
156	200.998	7620.9585	943	357	0	0	0	1296	4	0
157	202.217	7652.9684	940	360	0	0	0	1296	4	0
158	203.436	7684.3775	938	362	0	0	0	1296	4	0
159	204.655	7715.9088	934	366	0	0	0	1296	4	0
160	206.179	7754.5421	928	372	0	0	0	1296	4	0
161	207.551	7787.7413	924	376	0	0	0	1294	6	0
162	208.77	7816.0646	924	376	0	0	0	1292	8	0
163	209.989	7844.2452	924	376	0	0	0	1288	12	0
164	211.208	7872.4677	924	376	0	0	0	1288	12	0
165	212.428	7900.8758	924	376	0	0	0	1286	14	0
166	213.799	7932.5544	922	378	0	0	0	1286	14	0
167	215.018	7960.7656	919	381	0	0	0	1284	16	0
168	216.238	7988.9688	919	381	0	0	0	1283	16	0
169	217.457	8017.3784	916	384	0	0	0	1281	18	0
170	218.676	8045.6381	912	388	0	0	0	1281	18	0
171	219.895	8073.6948	912	388	0	0	0	1280	18	0
172	221.114	8101.6133	909	391	0	0	0	1278	20	0
173	222.41	8131.0127	906	394	0	0	0	1273	24	0
174	223.781	8162.0561	902	398	0	0	0	1271	26	0

Table B4.5: Seismic Performance point for 15-st cracked RC frame building

Step	Monitored Displ mm	Base Force kN	A-B	B-C	C-D	D-E	>E	A-IO	IO-LS	LS-CP
43	78.638	1744.077	1950	0	0	0	0	1950	0	0
44	80.467	1784.637	1950	0	0	0	0	1950	0	0
45	82.296	1825.1969	1950	0	0	0	0	1950	0	0
46	84.125	1865.7568	1950	0	0	0	0	1950	0	0
47	85.954	1906.3168	1950	0	0	0	0	1950	0	0
48	87.782	1946.8767	1950	0	0	0	0	1950	0	0
49	89.611	1987.4366	1950	0	0	0	0	1950	0	0
50	91.44	2027.9965	1950	0	0	0	0	1950	0	0
51	93.269	2068.5565	1950	0	0	0	0	1950	0	0
52	95.098	2109.1164	1950	0	0	0	0	1950	0	0
53	96.926	2149.6763	1950	0	0	0	0	1950	0	0
54	98.755	2190.2363	1950	0	0	0	0	1950	0	0
55	100.584	2230.7962	1950	0	0	0	0	1950	0	0
56	102.413	2271.3561	1950	0	0	0	0	1950	0	0
57	104.242	2311.9161	1950	0	0	0	0	1950	0	0
58	106.07	2352.476	1950	0	0	0	0	1950	0	0
59	107.899	2393.0359	1950	0	0	0	0	1950	0	0
60	109.728	2433.5959	1950	0	0	0	0	1950	0	0
61	111.557	2474.1558	1950	0	0	0	0	1950	0	0
62	113.386	2514.7157	1950	0	0	0	0	1950	0	0
63	115.214	2555.2756	1950	0	0	0	0	1950	0	0
64	117.043	2595.8356	1950	0	0	0	0	1950	0	0
65	118.872	2636.3955	1950	0	0	0	0	1950	0	0
66	120.701	2676.9554	1950	0	0	0	0	1950	0	0
67	122.53	2717.5154	1950	0	0	0	0	1950	0	0
68	124.358	2758.0753	1950	0	0	0	0	1950	0	0
69	126.187	2798.6352	1950	0	0	0	0	1950	0	0
70	128.016	2839.1952	1950	0	0	0	0	1950	0	0
71	129.845	2879.7551	1950	0	0	0	0	1950	0	0
72	131.674	2920.315	1950	0	0	0	0	1950	0	0
73	133.502	2960.875	1950	0	0	0	0	1950	0	0
74	135.331	3001.4349	1950	0	0	0	0	1950	0	0
75	137.16	3041.9948	1950	0	0	0	0	1950	0	0
76	138.989	3082.5547	1950	0	0	0	0	1950	0	0
77	140.818	3123.1147	1950	0	0	0	0	1950	0	0
78	142.646	3163.6746	1950	0	0	0	0	1950	0	0
79	144.475	3204.2345	1950	0	0	0	0	1950	0	0
80	146.304	3244.7945	1950	0	0	0	0	1950	0	0
81	148.133	3285.3544	1950	0	0	0	0	1950	0	0
82	149.962	3325.9143	1941	9	0	0	0	1950	0	0
83	151.79	3366.1613	1940	10	0	0	0	1950	0	0
84	153.619	3406.3739	1929	21	0	0	0	1950	0	0
85	155.448	3446.2144	1926	24	0	0	0	1950	0	0

Step	Monitored Displ mm	Base Force kN	A-B	B-C	C-D	D-E	>E	A-IO	IO-LS	LS-CP
175	320.04	6332.8064	1550	400	0	0	0	1950	0	0
176	321.869	6361.4637	1550	400	0	0	0	1950	0	0
177	323.698	6390.1211	1550	400	0	0	0	1950	0	0
178	325.526	6418.7784	1549	401	0	0	0	1950	0	0
179	327.355	6447.4215	1547	403	0	0	0	1950	0	0
180	329.184	6476.0358	1547	403	0	0	0	1950	0	0
181	331.013	6504.65	1547	403	0	0	0	1950	0	0
182	332.842	6533.2643	1546	404	0	0	0	1950	0	0
183	334.67	6561.8692	1546	404	0	0	0	1950	0	0
184	336.499	6590.4741	1544	406	0	0	0	1950	0	0
185	338.328	6619.0601	1544	406	0	0	0	1950	0	0
186	340.157	6647.6462	1544	406	0	0	0	1950	0	0
187	341.986	6676.2322	1544	406	0	0	0	1950	0	0
188	343.814	6704.8182	1544	406	0	0	0	1950	0	0
189	345.643	6733.4043	1544	406	0	0	0	1950	0	0
190	347.472	6761.9903	1544	406	0	0	0	1950	0	0
191	349.301	6790.5764	1544	406	0	0	0	1950	0	0
192	351.13	6819.1624	1541	409	0	0	0	1950	0	0
193	352.958	6847.7171	1541	409	0	0	0	1950	0	0
194	354.787	6876.2718	1541	409	0	0	0	1950	0	0
195	356.616	6904.8266	1541	409	0	0	0	1950	0	0
196	358.445	6933.3813	1538	412	0	0	0	1950	0	0
197	360.274	6961.8936	1538	412	0	0	0	1950	0	0
198	362.102	6990.406	1538	412	0	0	0	1950	0	0
199	363.931	7018.9183	1535	415	0	0	0	1950	0	0
200	365.76	7047.3892	1533	417	0	0	0	1950	0	0
201	367.589	7075.8492	1531	419	0	0	0	1950	0	0
202	369.418	7104.2817	1527	423	0	0	0	1950	0	0
203	371.246	7132.6628	1524	426	0	0	0	1950	0	0
204	373.075	7161.0271	1522	428	0	0	0	1950	0	0
205	374.904	7189.3757	1522	428	0	0	0	1950	0	0
206	376.733	7217.7244	1522	428	0	0	0	1950	0	0
207	378.562	7246.073	1517	433	0	0	0	1950	0	0
208	380.39	7274.3586	1514	436	0	0	0	1950	0	0
209	382.219	7302.6063	1514	436	0	0	0	1950	0	0
210	384.048	7330.854	1514	436	0	0	0	1950	0	0
211	385.877	7359.1017	1508	442	0	0	0	1950	0	0
212	387.706	7387.3004	1504	446	0	0	0	1950	0	0
213	389.534	7415.4475	1502	448	0	0	0	1950	0	0
214	391.363	7443.5597	1502	448	0	0	0	1950	0	0
215	393.192	7471.6719	1502	448	0	0	0	1950	0	0
216	395.021	7499.7842	1495	455	0	0	0	1950	0	0
217	396.85	7527.839	1494	456	0	0	0	1950	0	0
218	398.678	7555.888	1492	458	0	0	0	1948	2	0

Step	Monitored Displ mm	Base Force kN	A-B	B-C	C-D	D-E	>E	A-IO	IO-LS	LS-CP
307	561.442	10014.5532	1416	534	0	0	0	1771	179	0
308	563.27	10040.6957	1415	535	0	0	0	1771	179	0
309	565.099	10066.8297	1415	535	0	0	0	1768	182	0
310	566.928	10092.9636	1413	537	0	0	0	1752	198	0
311	568.757	10119.0811	1410	540	0	0	0	1750	200	0
312	570.586	10144.7593	1408	542	0	0	0	1750	200	0
313	572.414	10170.4289	1408	542	0	0	0	1748	200	0
314	574.243	10196.0865	1406	544	0	0	0	1738	210	0
315	576.072	10221.5056	1406	544	0	0	0	1738	210	0
316	577.901	10246.9276	1404	546	0	0	0	1736	212	0
317	579.73	10272.0301	1404	546	0	0	0	1736	212	0
318	581.558	10296.9871	1401	549	0	0	0	1736	212	0
319	583.387	10321.541	1399	551	0	0	0	1729	219	0
320	585.216	10346.0814	1399	551	0	0	0	1729	219	0
321	587.045	10370.5822	1397	553	0	0	0	1725	223	0
322	588.874	10395.0334	1395	555	0	0	0	1723	225	0
323	590.702	10419.3712	1395	555	0	0	0	1721	227	0
324	592.531	10443.6096	1392	558	0	0	0	1721	227	0
325	594.36	10467.7627	1390	560	0	0	0	1721	227	0
326	594.817	10473.6995	1390	560	0	0	0	1721	227	0
327	597.675	10510.9764	1388	562	0	0	0	1713	235	0
328	599.504	10534.7869	1388	562	0	0	0	1708	240	0
329	601.332	10558.574	1386	564	0	0	0	1707	241	0
330	603.161	10582.4478	1386	564	0	0	0	1707	241	0
331	604.99	10606.2761	1386	564	0	0	0	1707	241	0
332	606.819	10630.0285	1386	564	0	0	0	1702	246	0
333	608.648	10653.8333	1386	564	0	0	0	1697	251	0
334	611.848	10695.2732	1382	568	0	0	0	1697	251	0
335	613.677	10719.1392	1382	568	0	0	0	1697	251	0
336	615.963	10748.6244	1382	568	0	0	0	1697	249	2
337	617.792	10772.5092	1382	568	0	0	0	1697	249	2
338	620.992	10813.903	1382	568	0	0	0	1697	249	2
339	622.821	10837.7838	1382	568	0	0	0	1694	252	2
340	626.021	10879.1369	1382	568	0	0	0	1687	259	2
341	627.85	10903.0055	1377	573	0	0	0	1687	259	2
342	631.05	10944.2091	1372	578	0	0	0	1687	259	2
343	632.879	10967.9387	1372	578	0	0	0	1684	262	2
344	636.08	11009.0691	1367	583	0	0	0	1678	268	2
345	637.908	11032.5192	1367	583	0	0	0	1675	271	2
346	638.668	11042.2766	1367	581	2	0	0	1673	273	2
347	494.313	7831.4772	1367	581	0	1	1	1673	273	0

144

Table B4.6: Seismic Performance point for 15-st Uncracked RC frame building

Step	Monitored Displ mm	Base Force kN	A-B	B-C	C-D	D-E	>E	A-IO	IO-LS	LS-CP
0	0	0	1950	0	0	0	0	1950	0	0
1	1.829	86.1579	1950	0	0	0	0	1950	0	0
2	3.658	172.3158	1950	0	0	0	0	1950	0	0
3	5.486	258.4737	1950	0	0	0	0	1950	0	0
4	7.315	344.6316	1950	0	0	0	0	1950	0	0
5	9.144	430.7895	1950	0	0	0	0	1950	0	0
6	10.973	516.9475	1950	0	0	0	0	1950	0	0
7	12.802	603.1054	1950	0	0	0	0	1950	0	0
8	14.63	689.2633	1950	0	0	0	0	1950	0	0
9	16.459	775.4212	1950	0	0	0	0	1950	0	0
10	18.288	861.5791	1950	0	0	0	0	1950	0	0
11	20.117	947.737	1950	0	0	0	0	1950	0	0
12	21.946	1033.8949	1950	0	0	0	0	1950	0	0
13	23.774	1120.0528	1950	0	0	0	0	1950	0	0
14	25.603	1206.2107	1950	0	0	0	0	1950	0	0
15	27.432	1292.3686	1950	0	0	0	0	1950	0	0
16	29.261	1378.5266	1950	0	0	0	0	1950	0	0
17	31.09	1464.6845	1950	0	0	0	0	1950	0	0
18	32.918	1550.8424	1950	0	0	0	0	1950	0	0
19	34.747	1637.0003	1950	0	0	0	0	1950	0	0
20	36.576	1723.1582	1950	0	0	0	0	1950	0	0
21	38.405	1809.3161	1950	0	0	0	0	1950	0	0
22	40.234	1895.474	1950	0	0	0	0	1950	0	0
23	42.062	1981.6319	1950	0	0	0	0	1950	0	0
24	43.891	2067.7898	1950	0	0	0	0	1950	0	0
25	45.72	2153.9477	1950	0	0	0	0	1950	0	0
26	47.549	2240.1057	1950	0	0	0	0	1950	0	0
27	49.378	2326.2636	1950	0	0	0	0	1950	0	0
28	51.206	2412.4215	1950	0	0	0	0	1950	0	0
29	53.035	2498.5794	1950	0	0	0	0	1950	0	0
30	54.864	2584.7373	1950	0	0	0	0	1950	0	0
31	56.693	2670.8952	1950	0	0	0	0	1950	0	0
32	58.522	2757.0531	1950	0	0	0	0	1950	0	0
33	60.35	2843.211	1950	0	0	0	0	1950	0	0
34	62.179	2929.3689	1950	0	0	0	0	1950	0	0
35	64.008	3015.5268	1950	0	0	0	0	1950	0	0
36	65.837	3101.6847	1950	0	0	0	0	1950	0	0
37	67.666	3187.8427	1950	0	0	0	0	1950	0	0
38	69.494	3274.0006	1950	0	0	0	0	1950	0	0
39	71.107	3349.9609	1939	11	0	0	0	1950	0	0

Step	Monitored Displ mm	Base Force kN	A-B	B-C	C-D	D-E	>E	A-IO	IO-LS	LS-CP
87	179.361	6593.474	1536	414	0	0	0	1950	0	0
88	181.19	6638.7563	1533	417	0	0	0	1950	0	0
89	183.018	6683.983	1530	420	0	0	0	1950	0	0
90	184.847	6729.1355	1528	422	0	0	0	1950	0	0
91	186.676	6774.2226	1522	428	0	0	0	1950	0	0
92	188.505	6819.2018	1520	430	0	0	0	1950	0	0
93	190.334	6864.113	1518	432	0	0	0	1950	0	0
94	192.162	6908.9959	1512	438	0	0	0	1950	0	0
95	193.991	6953.7618	1507	443	0	0	0	1950	0	0
96	195.82	6998.4049	1502	448	0	0	0	1950	0	0
97	197.649	7042.8465	1500	450	0	0	0	1950	0	0
98	199.478	7087.1922	1498	452	0	0	0	1950	0	0
99	201.306	7131.4807	1498	452	0	0	0	1950	0	0
100	203.135	7175.7692	1496	454	0	0	0	1950	0	0
101	204.964	7219.9804	1496	454	0	0	0	1950	0	0
102	206.793	7264.1516	1494	456	0	0	0	1950	0	0
103	208.622	7308.2392	1494	456	0	0	0	1950	0	0
104	210.45	7352.3269	1494	456	0	0	0	1950	0	0
105	212.279	7396.4145	1492	458	0	0	0	1950	0	0
106	214.108	7440.4313	1492	458	0	0	0	1950	0	0
107	215.937	7484.4482	1490	460	0	0	0	1950	0	0
108	217.766	7528.3871	1490	460	0	0	0	1950	0	0
109	219.594	7572.326	1489	461	0	0	0	1950	0	0
110	221.423	7616.2338	1489	461	0	0	0	1950	0	0
111	223.252	7660.1415	1487	463	0	0	0	1950	0	0
112	225.081	7703.9854	1487	463	0	0	0	1950	0	0
113	226.91	7747.8292	1487	463	0	0	0	1950	0	0
114	228.738	7791.6731	1487	463	0	0	0	1950	0	0
115	230.567	7835.5169	1487	463	0	0	0	1950	0	0
116	232.396	7879.3608	1487	463	0	0	0	1950	0	0
117	234.225	7923.2046	1487	463	0	0	0	1950	0	0
118	236.054	7967.0485	1487	463	0	0	0	1950	0	0
119	237.882	8010.8924	1487	463	0	0	0	1950	0	0
120	239.711	8054.7362	1487	463	0	0	0	1950	0	0
121	241.54	8098.5801	1484	466	0	0	0	1950	0	0
122	243.369	8142.354	1484	466	0	0	0	1946	4	0
123	245.198	8186.1279	1484	466	0	0	0	1946	4	0
124	247.026	8229.9019	1484	466	0	0	0	1942	8	0
125	248.855	8273.6758	1481	469	0	0	0	1942	8	0
126	250.684	8317.3694	1481	469	0	0	0	1942	8	0
127	252.513	8361.063	1481	469	0	0	0	1942	8	0

Step	Monitored Displ mm	Base Force kN	A-B	B-C	C-D	D-E	>E	A-IO	IO-LS	LS-CP
175	340.295	10408.0158	1415	535	0	0	0	1752	198	0
176	342.124	10448.6673	1415	535	0	0	0	1748	202	0
177	343.953	10489.3175	1415	535	0	0	0	1748	202	0
178	345.782	10529.9673	1415	535	0	0	0	1745	205	0
179	347.61	10570.6168	1415	535	0	0	0	1736	214	0
180	349.439	10611.2481	1408	542	0	0	0	1733	217	0
181	351.268	10651.0575	1406	544	0	0	0	1728	222	0
182	353.097	10690.8433	1406	544	0	0	0	1725	225	0
183	354.926	10730.6223	1401	549	0	0	0	1718	232	0
184	356.754	10769.937	1401	549	0	0	0	1718	232	0
185	358.583	10809.0226	1397	553	0	0	0	1718	232	0
186	360.412	10847.5292	1397	553	0	0	0	1718	232	0
187	362.241	10886.0323	1395	555	0	0	0	1718	232	0
188	364.07	10923.7632	1395	555	0	0	0	1714	236	0
189	365.898	10961.4987	1395	555	0	0	0	1710	240	0
190	368.184	11008.1972	1392	558	0	0	0	1708	242	0
191	370.013	11045.2029	1392	558	0	0	0	1706	244	0
192	372.071	11086.6203	1392	558	0	0	0	1706	244	0
193	373.899	11123.3745	1392	558	0	0	0	1704	246	0
194	375.728	11160.1902	1390	560	0	0	0	1695	255	0
195	377.557	11197.0196	1388	562	0	0	0	1684	266	0
196	379.386	11233.7716	1388	562	0	0	0	1681	269	0
197	382.129	11288.911	1385	565	0	0	0	1668	282	0
198	384.415	11334.7609	1385	565	0	0	0	1667	283	0
199	386.244	11371.546	1383	567	0	0	0	1667	283	0
200	388.301	11412.8514	1383	567	0	0	0	1667	283	0
201	390.359	11454.1593	1381	569	0	0	0	1662	288	0
202	392.416	11495.4026	1381	569	0	0	0	1658	292	0
203	394.473	11536.6125	1381	569	0	0	0	1658	292	0
204	396.531	11577.8055	1381	569	0	0	0	1652	298	0
205	399.274	11632.7862	1381	569	0	0	0	1649	301	0
206	401.56	11678.5676	1381	569	0	0	0	1646	304	0
207	403.389	11715.2077	1381	569	0	0	0	1644	306	0
208	405.218	11751.7709	1381	569	0	0	0	1637	313	0
209	407.046	11788.5303	1380	570	0	0	0	1630	320	0
210	408.875	11825.0539	1379	571	0	0	0	1628	322	0
211	410.704	11861.7696	1379	571	0	0	0	1628	322	0
212	413.904	11925.8325	1379	571	0	0	0	1623	327	0
213	415.733	11962.4208	1379	571	0	0	0	1623	327	0
214	417.562	11999.1288	1379	571	0	0	0	1620	330	0
215	419.848	12044.7581	1379	571	0	0	0	1620	330	0
216	421.677	12081.49	1379	571	0	0	0	1618	328	2